CONTROL SYSTEMS DESIGN FOR LINEAR DYNAMIC SYSTEMS USING SIMPLE MODELS: SOME CASE STUDIES

PART I: The single-input/single-output case

by

A. Chotai and D.H. Owens

Department of Control Engineering,
University of Sheffield,
Mappin Street, Sheffield S1 3JD.

Research Report No. 247

November 1983

This work is supported by SERC under grant GR/B/23250

1. INTRODUCTION

Closed-loop control system designs are frequently based on the use of a simplified model either because the available model is regarded as being too complex for design work or because an accurate plant model is not available. An approximate model can be of arbitrary dynamic complexity. However, it is desirable that the model is of low order with the consequent benefits of reduced computational requirements and the possibility of achieving simple designs to form the basis for further refinement and understanding.

The purpose of this report is to make a numerical study of a number of single-input/single-output systems using recent results developed by the authors (Owens and Chotai, 1983) with the objectives of

(i) assessing the validity of 'standard' first and second order differential-delay plant models for design,

(ii) assessing the conservatism of the approach and the effect of the choice of model by plotting

(a) the predicted and actual stability regions in parameter plane,

(b) confidence bands on the systems frequency response and

(iii) assessing the success of the technique in predicting standard Ziegler-Nichols design conditions despite the modelling errors,

(iv) noting the improvement made possible by the use of the Smith Predictor scheme.

For this report the standard models used for approximate plant dynamics are taken to be

(i) First order model: $G_A(s) = \frac{a}{1+Ts}$ (1.1)

(ii) First order model with delay: $G_A(s) = \frac{ae^{-s\tau}}{1+Ts}$ (1.2)

(iii) Second order model: $G_A(s) = \frac{a}{s^2+bs+c}$ (1.3)

(iv) Second order model with delay: $G_A(s) = \dfrac{ae^{-s\tau}}{s^2+bs+c}$ (1.4)

where the choice of the parameters a,b,c,T and τ are undertaken by simple graphical operations on plant step data.

The controller considered is taken to be of the P+I form

$$K(s) = k_1 + k_{2/s} \tag{1.5}$$

with performance objectives that

(a) the closed-loop system is asymptotically stable, with typical transient characteristics, such as $\leq$ 10% overshoot and response speed increased by 2-3 times.

(b) asymptotic tracking of step input.

(c) the attainment of standard damping characteristics.

Numerous examples, varying from a third order to 9th order are studied using both time-domain and frequency-domain techniques introduced by Owens and Chotai (1983). The basic ideas are outlined in section 2.

2. BACKGROUND THEORY

2.1 Problem: The problem considered here is the design of the proper, rational forward path controller K in Fig. 2.1 for the stable plant G in the presence of the proper, rational measurement dynamics F. All elements are assumed to be continuous and linear and it is assumed that the detailed dynamics of the plant G are unknow, but that the response Y(t) of the plant from zero initial conditions to a unit step input at t = o is available.

Given the data Y(t), an approximate model G_A of the real plant G is constructed by analytical or graphical curve fitting to the transient data Y(t) or by model reduction. The (stable) response $Y_A(t)$ of G_A from zero initial conditions to a unit step input at t = o can be obtained by simulation. The control system K can now be designed, by any means at the designers disposal, to ensure the required stability and transient performance from the approximating feedback system of Fig. 2.2. The problem considered is how the modelling error

$$E(t) = Y(t) - Y_A(t) \tag{2.1}$$

can be used to ensure the simultaneous stability and acceptable performance of the real systems Fig. 2.1.

2.2 Frequency-domain stability response (see [1])

If K stabilises the model $G_A(s)$, it will also stabilise the real plant G(s) if:

(a) the composite system GKF is both controllabe and observable, and

(b) $$\lambda_o \triangleq \sup_{s \epsilon D} \gamma(s) < 1 \tag{2.2}$$

where $\gamma(s)$ is any conveinent real valued function satisfying

$$\gamma(s) \geq \left|(1+G_A(s)K(s)F(s))^{-1}K(s)F(s)\right|\Delta(s) \tag{2.3}$$

for all $s \epsilon D$

$\Delta(s)$ is any available function satisfying

$$\Delta(s) \geq \left|G(s) - G_A(s)\right| \text{ for all } s \epsilon D \tag{2.4}$$

and D is the usual Nyquist contour in the complex plane.

The result given above has a useful grahpical interpretation similar to that of the inverse Nyquist array technique [2-5] as follows:

Expression (2.2) can be replaced by the two conditions:

(i) The inequality

$$\underset{\substack{\text{Re } s \geq o \\ |s| \to \infty}}{\text{Lim sup}} \left|\frac{K(s)F(s)}{1+G_A(s)K(s)F(s)}\right| \Delta(s) < 1 \tag{2.5}$$

is satisfied and

(ii) the 'confidence band' generated by plotting the inverse Nyquist locus of $G_A(s)K(s)f(s)$ for $s = i\omega$, $\omega \geq o$ with superimposed 'confidence circle' at each point of radius

$$r(i\omega) \triangleq \left|G_A^{-1}(i\omega)\right| \Delta(i\omega) \tag{2.6}$$

does not contain or touch the (-1,0) point of the complex plane.

2.3 Choice of $\Delta(s)$

There are many choices of $\Delta(s)$, the detail and complexity of $\Delta(s)$ reflecting the degree of plant information that is to be used in design. In this report we will assume that only the plant step response $Y(t)$ is available and that information about the modelling error, $(E(t))$, integrated modelling error $(Z(t))$, and derivative of modelling error $(\dot{E}(t))$ can be obtained.

It can be shown [1] that

$$|G(s) - G_A(s)| \leq N_\infty(E) \text{ for all Re } s \geq o \tag{2.7}$$

where, for every function f, $N_\infty(f)$ is the norm of f defined by the total variation

$$N_T(f) \triangleq \sup \left(f(o^+) + \sum_{n=1}^{n^*(T)} |f(t_n) - f(t_{n-1})| + |f(T) - f(t_n^*)| \right) \tag{2.8}$$

where $o = t_o < t_1 < t_2 \ldots$ are the local maxima and minima of f and $n^*(T)$ is the largest integer satisfying $t_n \leq T$.

Also, [6],

$$|G(s) - G_A(s)| \leq E(\infty) + |s| N_\infty(Z) \text{ for all Re } s \geq o \tag{2.9}$$

where Z is an integrated modelling error defined by

$$Z(t) \triangleq \int_o^t (E(t') - E(\infty))dt' \tag{2.10}$$

If the derivative $\dot{E} = dE/dt$ is continuous on $[o, +\infty)$ then we can also deduce that

$$|G(s) - G_A(s)| \leq |s|^{-1} N_\infty(\dot{E}) \text{ for all Re } s \geq o \tag{2.11}$$

For our purpose, the best choice of $\Delta(s)$ is obtained by combining (2.7) (2.9) and (2.11) and setting

$$\Delta(s) = \min(N_\infty(E), E(\infty) + |s| N_\infty(Z), |s|^{-1} N_\infty(\dot{E})) \tag{2.12}$$

2.4 Time-domain stability result (see [1])

Suppose that the controller K stabilises the model $G_A(s)$ and that the response $W_A(t)$ of the systems $(1 + KFG_A)^{-1}KF$ from zero initial conditions to the demand input E(t) has been computed. Then the controller K will

stabilise the real plant G if:

(a) the composite system GKF is controllable and observable, and

(b) the following inequality holds:

$$N_\infty(W_A) < 1 \tag{2.13}$$

2.5 Output Performance Assessment (see [1])

The output feedback response $y(t)$ of the real system Fig. 2.1 from the zero initial conditions to the unit step demand satisfies the bound

$$|y(t)-y^{(1)}(t)| \leq \varepsilon(t) \triangleq \frac{N_t(W_A)}{1 - N_t(W_A)} \max_{o\leq t'\leq t} |\eta(t')| \tag{2.14}$$

where

$$y^{(1)}(t) = y_A(t) + \eta(t) \quad , \; t \geq o \tag{2.15}$$

$y_A(t)$ is the response of the approximate systems, (Fig. 2.2) from the zero initial conditions to the unit step demand, and $\eta(t)$ is the response of the system $(1+ KFG_A)^{-1}K\ (1 - FH)$ to the error $E(t)$ and H is given by

$$H = (1 + G_A KF)^{-1} G_A K \tag{2.16}$$

2.6 Input Performance Assessment (see [1])

The input response $u(t)$ of the real system Fig. 2.1 from the zero initial conditions to the unit step demand satisfies the bound

$$|u(t)- u^{(1)}(t)| \leq \varepsilon(t) \triangleq \frac{N_t(W_A)}{1 - N_t(W_A)} \max_{o\leq t'\leq t} |\xi(t')| \tag{2.17}$$

where

$$u^{(1)}(t) = u_A(t) + \xi(t) \quad t \geq o \tag{2.18}$$

$u_A(t)$ is the input response of the scheme (Fig. 2.2) to a step input demand and $\xi(t)$ is the response of $(1+ KFG_A)^{-1}KF$ to the input $W_A(t)$.

3. SMITH PREDICTOR SCHEME

Consider the single-input/single-output, linear plant expressed in the separable form GT, where the element $T = e^{-s\tau}$ represents an output delay and the element G represents strictly proper delay-free dynamics.

The destabilizing effect of the delay T can be offset with a considerable improvement in performance by the use of the Smith Predictor scheme illustrated in Fig. 3.1, (Marshall, 1979 [7], Owens and Raya, 1982 [8]) where K represents a delay free controller (for this report K is given by (1.5)), and G_A and $T_A = e^{-s\tau_A}$ represent models of G and T respectively. It is well-known that this scheme can be represented in the standard feedback form of Fig. 3.2 where the forward path controller

$$K^*(s) = \frac{K}{1 + KG_A - KG_AT_A} \tag{3.1}$$

and the transfer function is given by

$$\frac{KGT}{1 + KG_A + K(GT - G_AT_A)} \tag{3.2}$$

The mismatch term $GT - G_AT$ between the plant and model can be a serious source of stability and performance problems especially when GT is structurally and parametrically uncertain. When $G = G_A$ and $T = T_A$, the Smith control scheme (see Fig. 3.3) is equivalent to the approximate system of Fig. 2.2 except that the output is delayed.

3.1 Stability and Performance of Smith Predictor Scheme

The results of sections 2.3 and 2.4 are valid for the Smith control scheme with $G - G_A$ replaced by $GT - G_AT_A$, $F(s) \equiv 1$ and noting that

$$\frac{K^*}{1 + K^*G_AT_A} = \frac{K}{1 + KG_A} \tag{3.3}$$

Hence stability and performance degradation can be analysed for Smith control scheme in the presence of mismatch using approximation ideas introduced by Owens and Chotai [1].

4. CHOICE OF PARAMETERS IN SIMPLE MODELS

In this section we will discuss simple procedures for choosing the parameters in the specified simple approximate plant models given the step

response (Y(t)) of the real system to a unit step from zero initial conditions. The techniques involve only simple graphical operations on Y(t). They are no 'opimal' in any sense but later examples verify that even these rough and ready methods can lead to successful designs.

4.1 First-order Models

Consider the model given by

$$G_A(s) = \frac{A}{1 + Ts} \tag{4.1}$$

The parameter A will be chosen to match the steady-state value of the real plant response Y(t), that is

$$A = \lim_{s \to o} G(s) = \lim_{t \to \infty} Y(t) \tag{4.2}$$

and the time constant T will be roughly estimated as the time taken for Y(t) to reach 60% of its steady-state value.

$$Y(T) = 60\% \text{ of steady-state value} \tag{4.3}$$

If 'A' is chosen to satisfy (4.2), then

$$Y(T) = \frac{3}{5} \times A \tag{4.4}$$

4.2 First-order Models with Delay

Consider the model of the form

$$G_A(s) = \frac{A\, e^{-s\tau}}{1+T_1 s} \tag{4.5}$$

The parameter A will be chosen as in section 4.1. The time-delay τ will be chosen by graphical means e.g. by visual assessment of Y(t) or by rough and ready numerical procedures such as choosing τ to satisfy

$$Y(\tau) \simeq 10\% \text{ of steady-state value} \tag{4.6}$$

The time constant will then be taken as $T_1 = T - \tau$, where T will be found using (4.3).

4.3 Second-order Models

For under-damped systems, the second-order model of the form

$$G_A(s) = \frac{A\omega_n^2 e^{-s\tau}}{s^2 + 2\xi\omega_n s + \omega_n^2} \quad \tau \geq 0 \ , \ 0 < \xi < 1 \tag{4.7}$$

will be chosen. Here, we have

τ - Time delay

ξ - Damping ratio

ω_n - Natural frequency

A - Steady-state value

The parameters A and τ are chosen as in section 4.2. The damping ratio ξ is calculated from

$$\text{maximum \% overshoot of } Y(t) = 100\, e^{-\frac{\xi\pi}{(1-\xi^2)^{\frac{1}{2}}}} \quad 0 < \xi < 1 \tag{4.8}$$

(see Fig. 4.1)

The natural frequency ω_n is obtained either by matching the first peak of the step response or using settling band arguments. The peak overshoot for a unit step input Y(t) occurs when

$$t_p - \tau = \frac{\pi}{\omega_n\sqrt{1 - \xi^2}} \tag{4.9}$$

From (4.9)

$$\omega_n = \frac{\pi}{(t_p - \tau)(1-\xi^2)^{\frac{1}{2}}} \tag{4.10}$$

Alternatively, for ± 5% settling band, with a settling time, t_s, we could choose

$$\omega_n = \frac{3}{(t_s - \tau)\xi} \tag{4.11}$$

(Remark: The parameters ω_n and ξ can be obtained by other means but for the purpose of this report we will use (4.8) and (4.10) or (4.11). They have the advantage of simplicity yet still enable successful designs to be obtained).

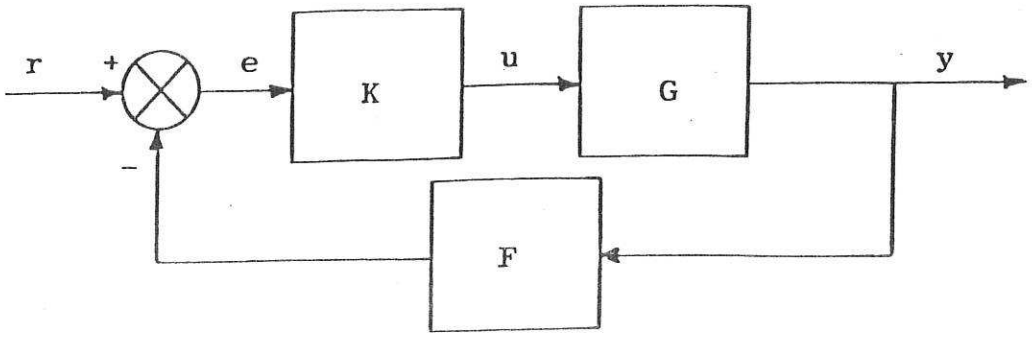

Fig. 2.1

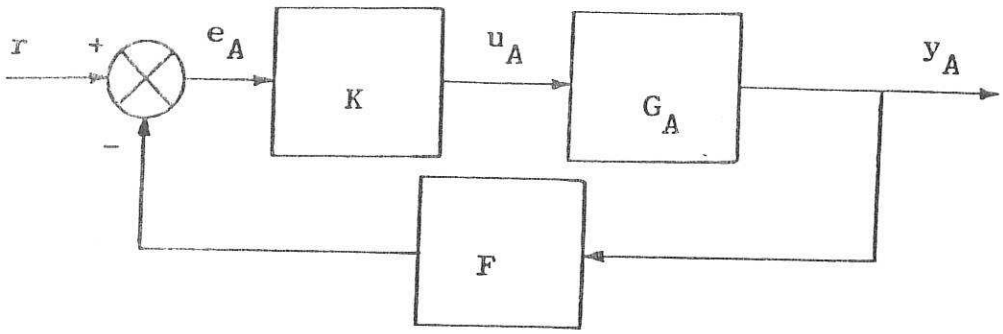

Fig. 2.2

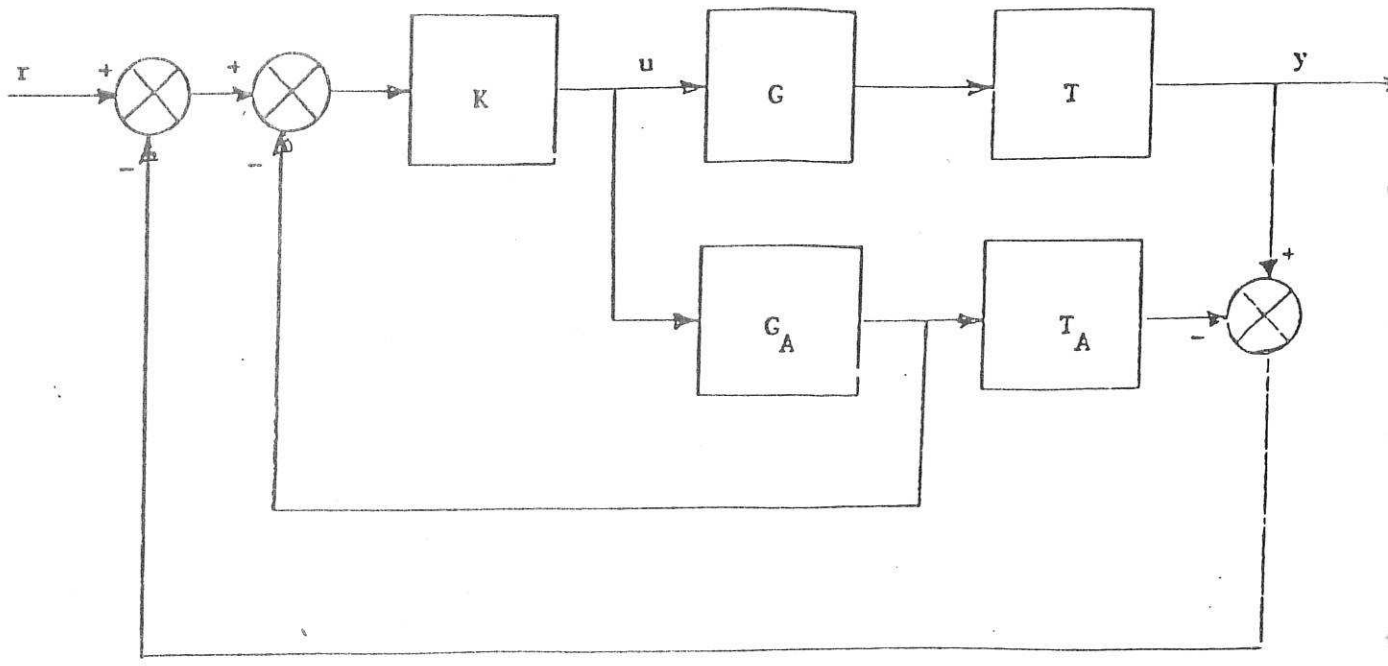

Fig. 3.1

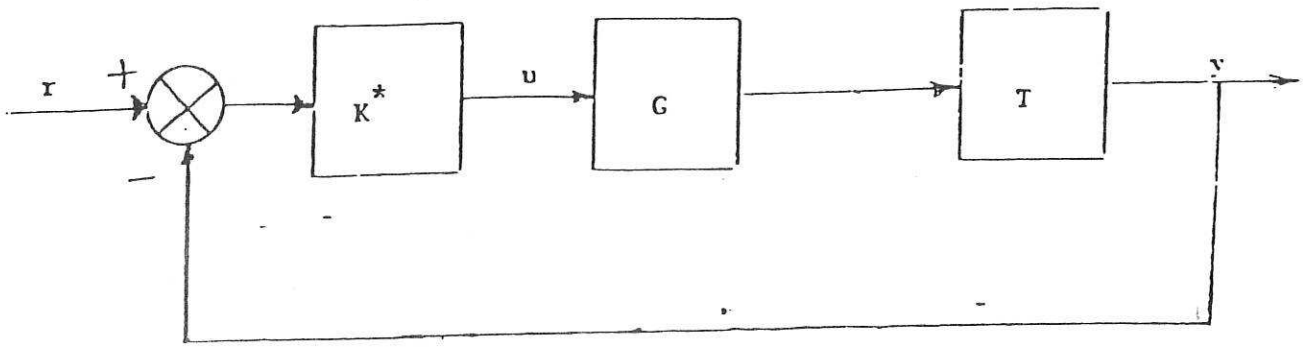

Fig. 3.2

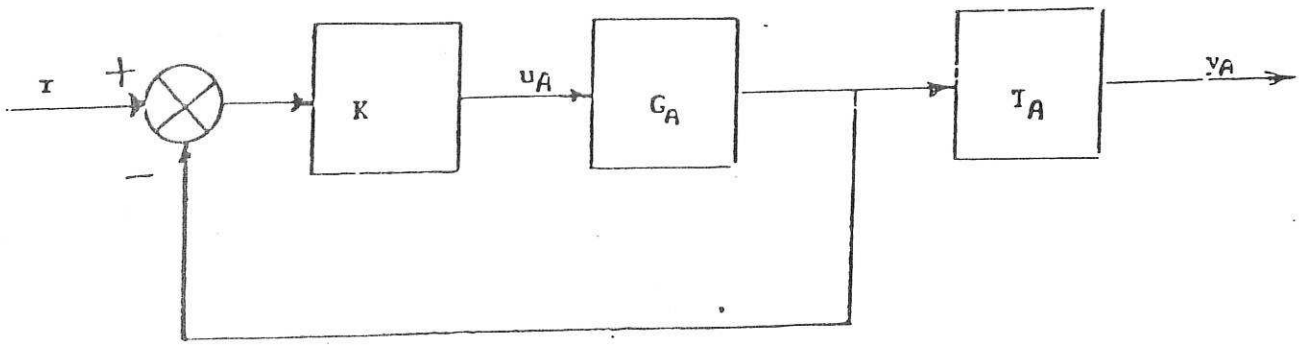

Fig. 3.3

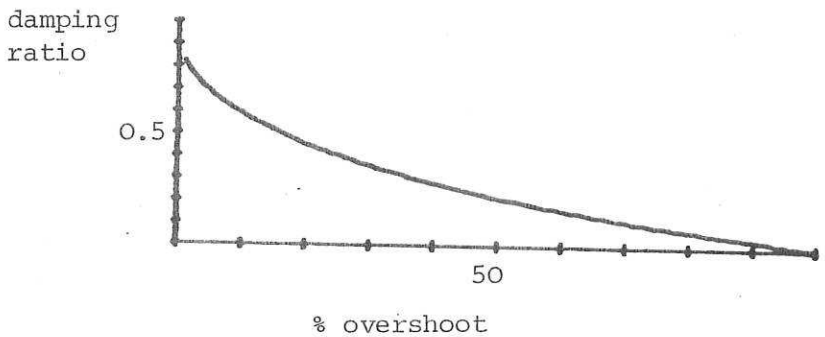

Fig. 4.1

5. EXAMPLE 1

Suppose that a single-input/single-output plant has an (unknown) transfer function

$$G(s) = \frac{1}{(s+1)^3} \tag{5.1}$$

and that plant step tests yield the step response Y(t) illustrated in Fig. 5.1. Four different models of the form

$$\text{(a)} \quad G_A^a(s) = \frac{1}{1+3.1s} \tag{5.2}$$

$$\text{(b)} \quad G_A^b(s) = \frac{e^{-0.7s}}{1+2.4s} \tag{5.3}$$

$$\text{(c)} \quad G_A^c(s) = \frac{1}{2s^2+3s+1} \tag{5.4}$$

$$\text{(d)} \quad G_A^d(s) = \frac{e^{-0.5s}}{2s^2+3s+1} \tag{5.5}$$

were fitted with step responses denoted by $Y_A^a(t)$, $Y_A^b(t)$, $Y_A^c(t)$ and $Y_A^d(t)$ respectively. (see Figs: 5.2, 5.3, 5.4 and 5.5).

(Remark: The models (a) and (b) were obtained by using the methods of sections 4.1 and 4.2 and models (c) and (d) were obtained by trial and error visual curve fitting).

The modelling error functions $E^a(t)$, $E^b(t)$, $E^c(t)$ and $E^d(t)$ are shown in Fig. 5.6 and using (2.8) it was found that

$$N_\infty(E^a) = 0.57, \qquad N_\infty(E^b) = 0.36$$

$$N_\infty(E^c) = 0.25 \qquad N_\infty(E^d) = 0.16$$

showing that the modelling error (represented by the total variation) reduces with complexity of the models.

A proportional-plus-integral controller of the form $K(s) = k_1 + s^{-1}k_2$ was used with $F(s) = 1$. The stability region deduced from the frequency domain technique is shown in Fig. 5.7 for all four models together with

the stability regions of the actual plant. It is evident from Fig. 5.7 that conservatism decreases as model complexity increases, also that all models are good for predicting gains k_1 and k_2 for standard closed-loop damping ($\xi = \frac{1}{\sqrt{2}}$) conditions (see Appendix A), but none of the models can predict the Ziegler-Nichols tuning points. (see appendix B).

Since the radii of the confidence circles are 'proportional' to the total variation of the modelling error, they decrease in width as the complexity of the model is increased and this is shown in Fig. 5.8 for $k_1 = 1$ and $k_2 = 0.5$.

So far we have only used information about the total variation of the modelling error to bound $|G(s) - G_A(s)|$. Using information about integrated modelling error and derivative of modelling error (i.e. using (2.12),

$$\Delta(s) = \min (N_\infty(E), E(\infty) + |s| N_\infty(Z), |s|^{-1} N_\infty(\dot{E}))$$

a better bound can be obtained and this is illustrated in Figs. 5.9 and 5.10 for models (a) and (c). It is clear from Fig. 5.11 that by using (2.12) for $\Delta(s)$, the frequency-domain method permits slightly higher gains.

The stability regions deduced from the time-domain technique are illustrated in Fig. 5.12 for all four models together with the actual stability region of the real plant. From Fig. 5.12 we observe that all models are good for predicting gains k_1 and k_2 for standard damping of the system, that model (d) can also predict both P and P + I, Ziegler-Nichols tuning points and that model (c) can describe the P Ziegler-Nichols tuning point. From Fig. 5.13 and comparing Figs. 5.7 and 5.12, it is clear that the time-domain method is less conservative than the frequency-domain technique. Other examples will strengthen this observation.

Taking $k_1 = 1.0$ and $k_2 = 0.5$ as before, it was found that

$$N_\infty(W_A^a) = 0.68 \quad , \quad N_\infty(W_A^b) = 0.50$$

$$N_\infty(W_A^c) = 0.36 \quad , \quad N_\infty(W_A^d) = 0.26$$

The correction term $\eta(t)$ and the error bound $\varepsilon(t)$ depend on the choice of approximate model $G_A(s)$, the better the model, the smaller the value of $\eta(t)$ and $\varepsilon(t)$. These facts are illustrated in Fig. 5.14 and Fig. 5.15.

For all four models, bounds $y^{(1)} \pm \varepsilon$ together with y and y_A are illustrated in Figs. 5.16, 5.17, 5.18 and 5.19.

Using model (d) and setting controller $K(s)$ to the P+I Ziegler-Nichols tuning point (i.e. $k_1 = 3.6$ and $k_2 = 1.2$), it was found that $N(W_A^d) = 0.54$. The closed-loop responses y and y_A are shown in Fig. 5.20 indicating that controller gains are probably too high, since the responses are very oscillatory.

Finally consider the above example in a Smith Predictor context when we use a delay-lag model of the form (b). More precisely,

$$G(s) = \frac{1}{(s+1)^3} \quad , \quad T(s) = 1$$

and

$$G_A(s) = \frac{1}{1+2.4s} \quad , \quad T_A(s) = e^{-0.7s}$$

The stability regions deduced from the time-domain technique using the Smith predictor scheme and standard feedback scheme are shown in Fig. 5.21, indicating that the Smith scheme permits higher gains and mismatch can have benefits in stabilizability. Using the Smith Predictor scheme with controller $K(s) = 1.0 + s^{-1}0.5$, the response $W_A(t)$ was computed to be as in Fig. 5.22 and graphical analysis of this response leads to the conclusion that $N_\infty(W_A) = 0.39 < 1$, hence verifying the stability predictions. The correction term $\eta(t)$ is shown in Fig. 5.23 and bounds $y^{(1)} \pm \varepsilon$ together with y and y_A, are illustrated in Fig. 5.24, where y is the output response of the mismatched Smith control scheme of Fig. 3.1 and y_A is the output response of the ideal Smith scheme of Fig. 3.3.

5.1 Summary and Discussion

The above example has demonstrated the following results on control system design using approach developed by the authors [1].

(1) By using very simple models ((a) -(d)), a highly satisfactory design can be achieved. In fact all four models can predict standard damping design conditions.

(2) The predicted stability regions increase as the complexity of the model increases.

(3) Conservatism and the total variation $N_\infty(E)$ decrease as the complexity of the model increases.

(4) Although the model (a) verifies the stability prediction for the controller $K(s) = 1.0 + s^{-1}0.5$, it gives large error bounds (maximum of 40% error) which are not regarded as acceptable in this report. For the purpose of this report error bound $\leq$ 25% are regarded as ideal. The model (b) gives a maximum error bound of 15% < 25%, hence yielding a satisfactory design.

(5) The time-domain method is better than the frequency-domain method in the sense that it permits higher gains to be used for a given model.

(6) For the delay-lag model, the Smith predictor scheme gives much better performance than a standard feedback scheme and increases the stability margin in the sense that it permits higher control gain to be used.

(7) Although only model (d) can predict the P + I Ziegler-Nichols tuning point, the maximum % overshoot obtained by this setting is 72% (which is unacceptable as, for this report, the maximum % overshoot permitted is (arbitrarily) set at 10%) which is greater than 10% and hence design is unsatisfactory and the controller gains are too high.

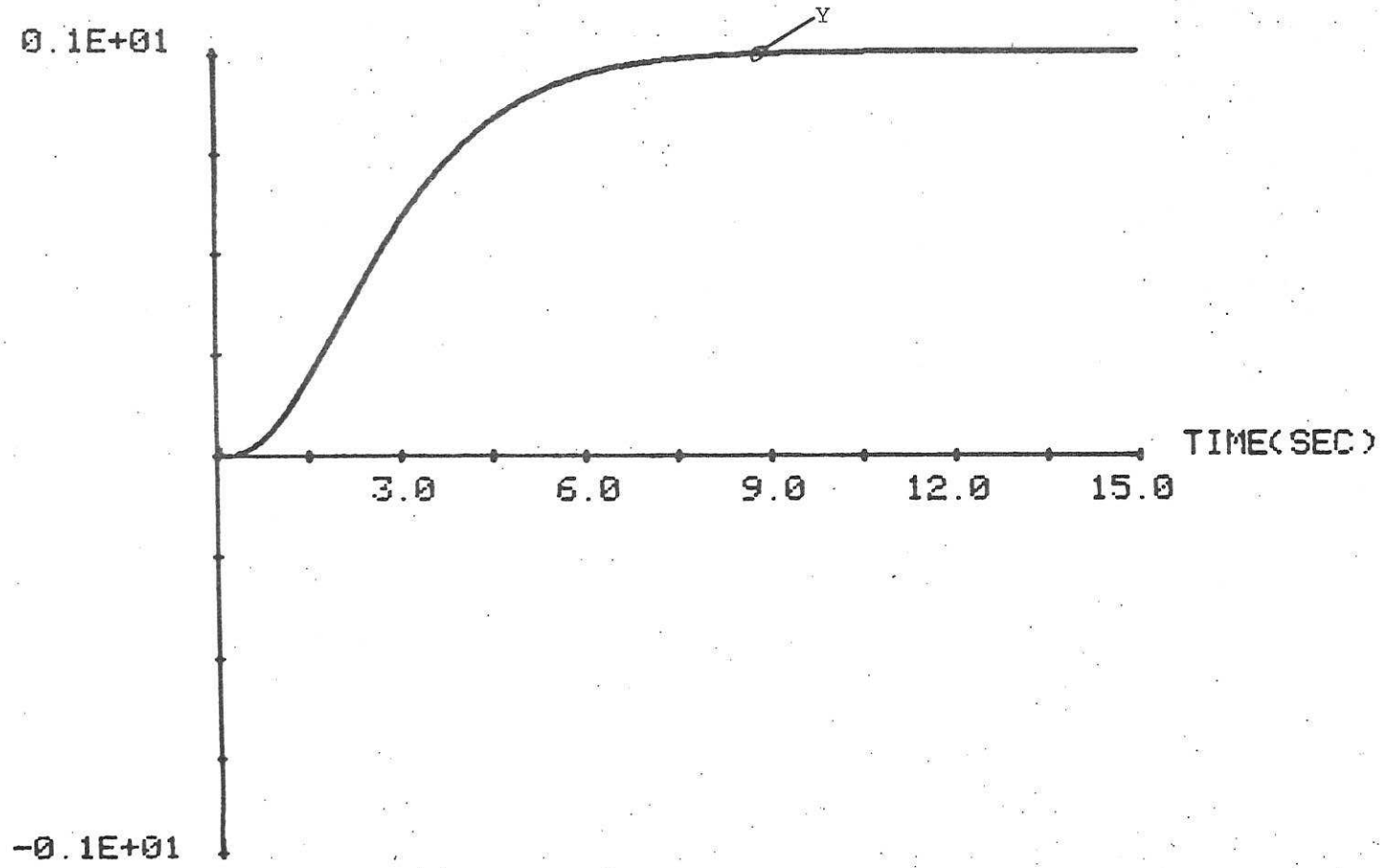

Fig. 5.1

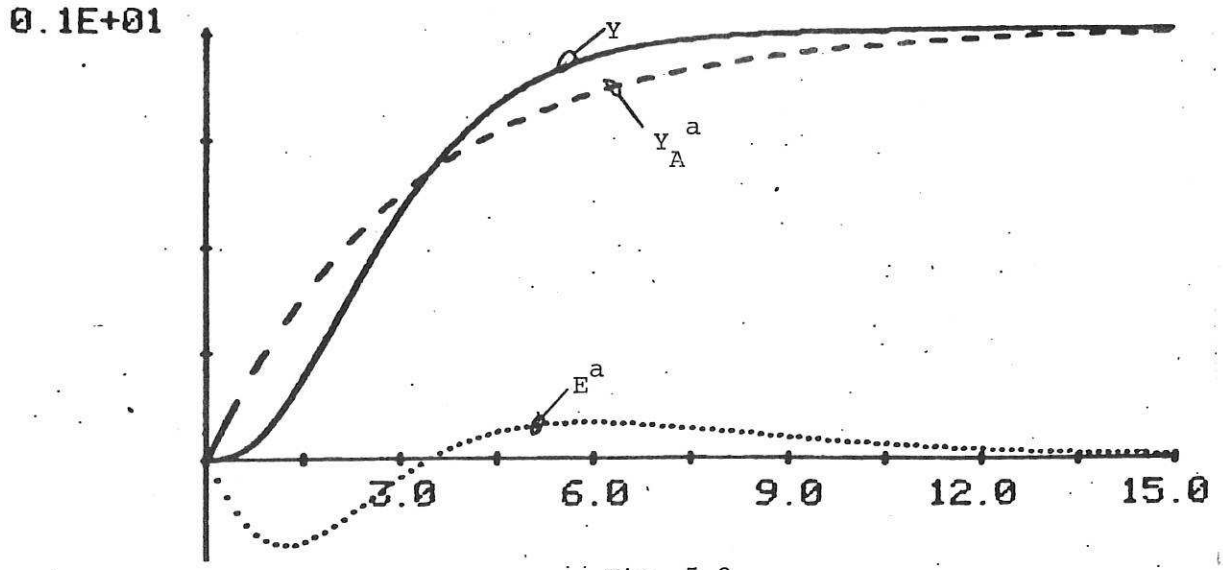

Fig. 5.2

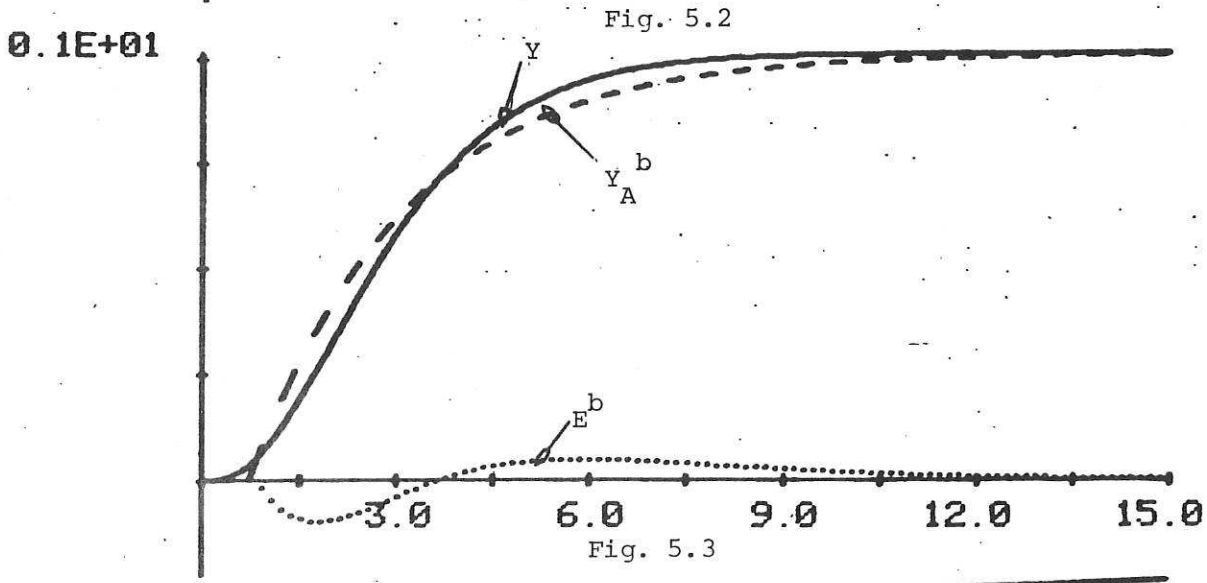

Fig. 5.3

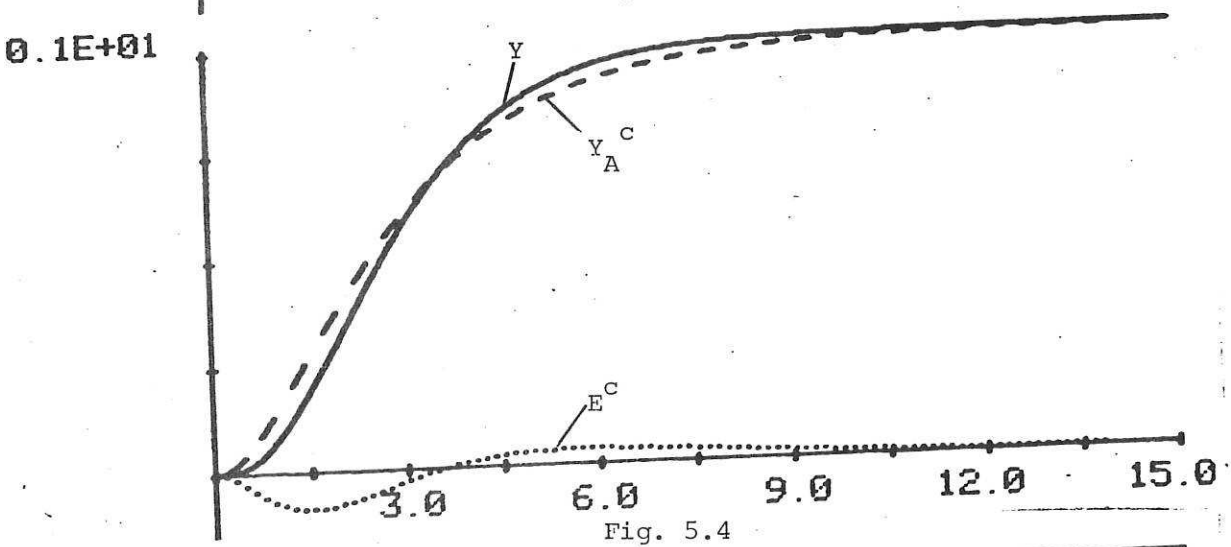

Fig. 5.4

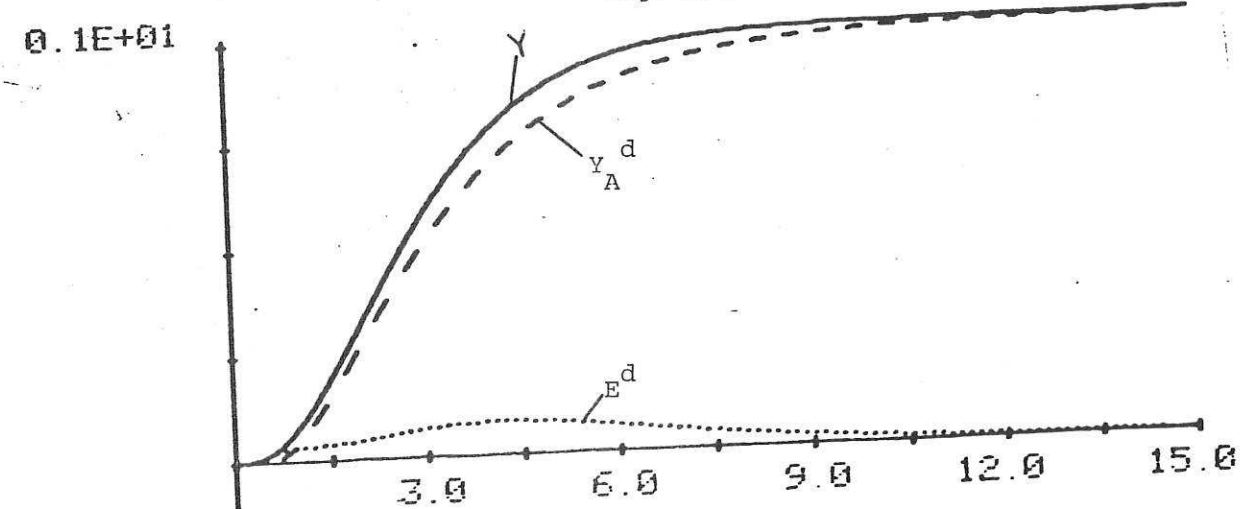

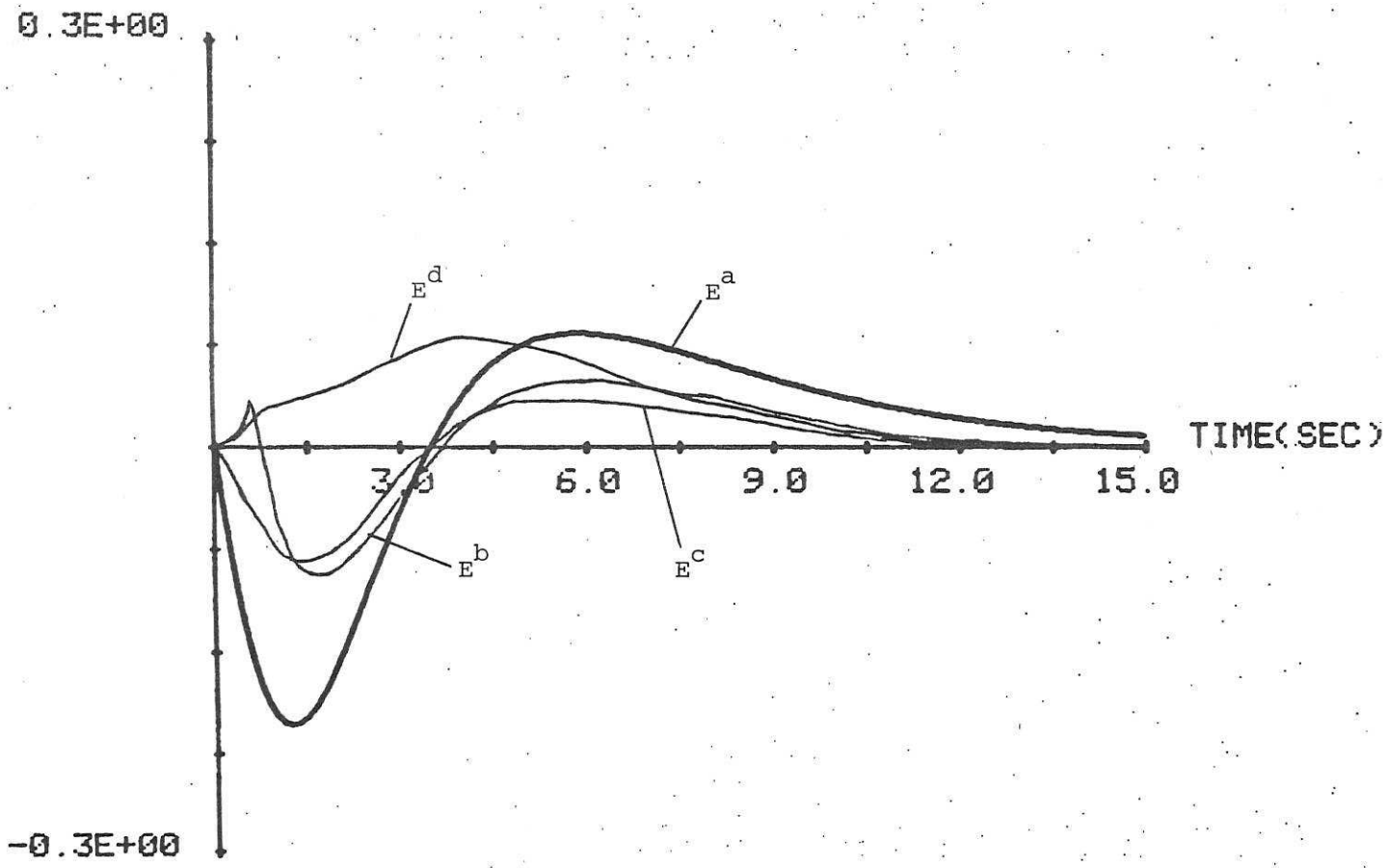

Fig. 5.6

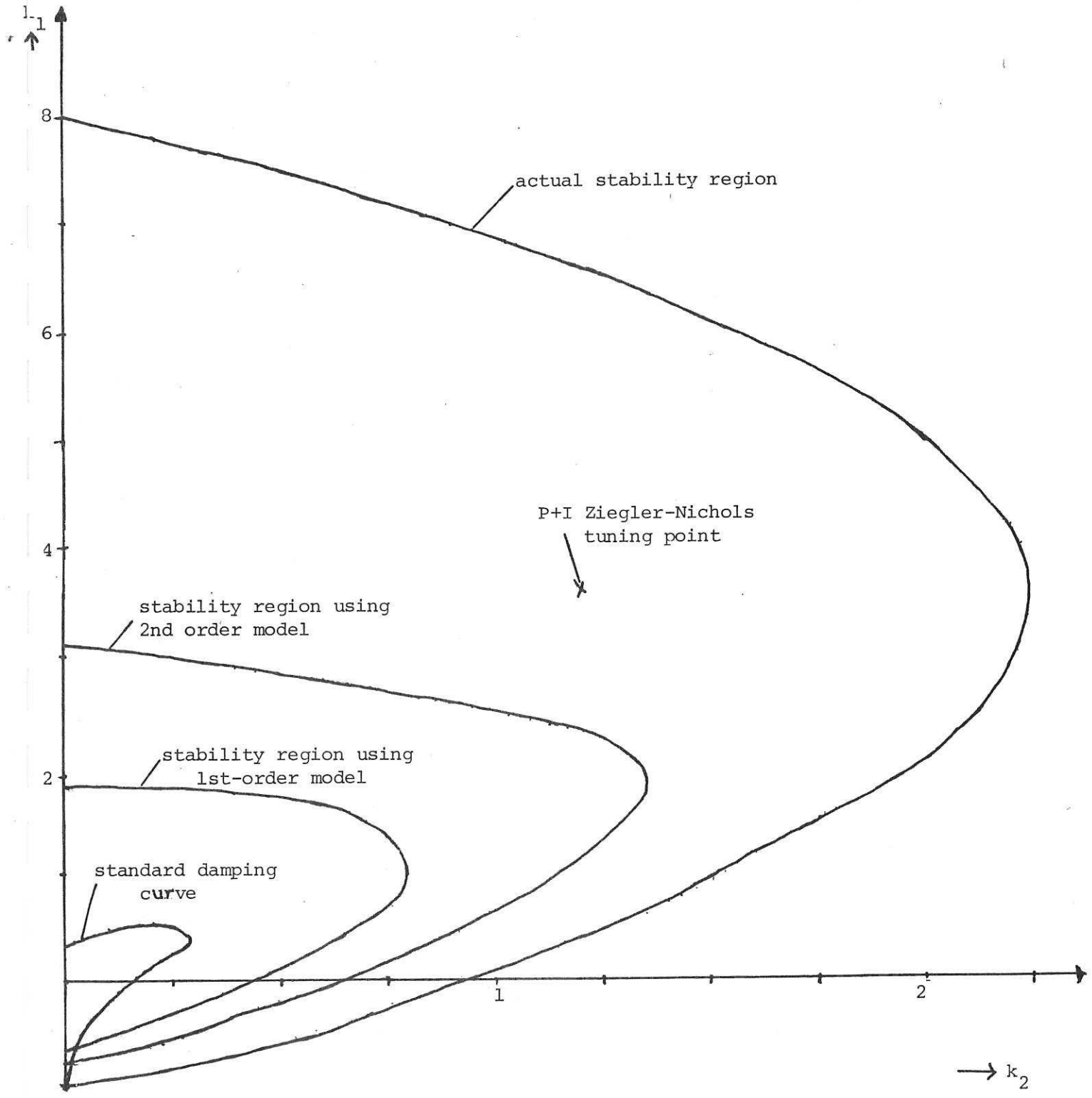
k_1
8
6
4
2
actual stability region
P+I Ziegler-Nichols
tuning point
stability region using
2nd order model
stability region using
1st-order model
standard damping
curve
1
2
k_2

Fig. 5.7

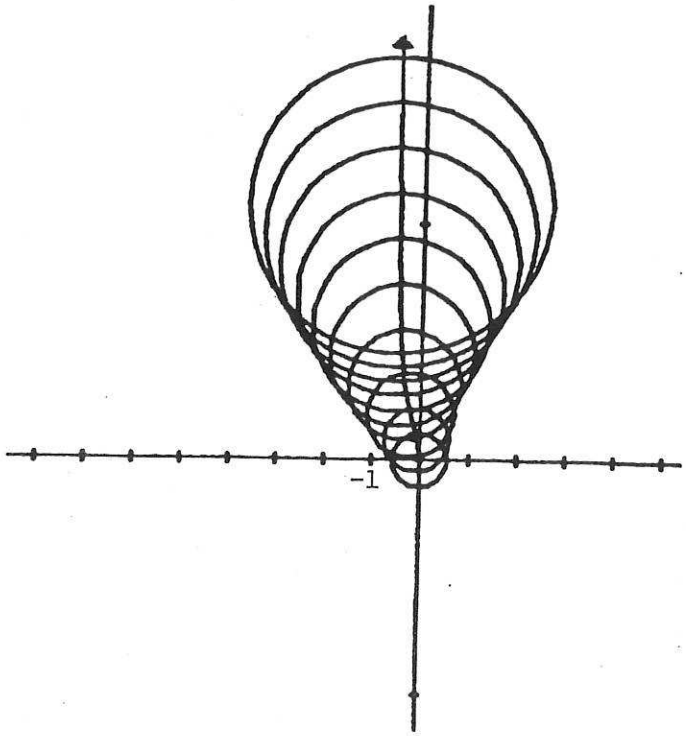

Fig. 5.8(a)

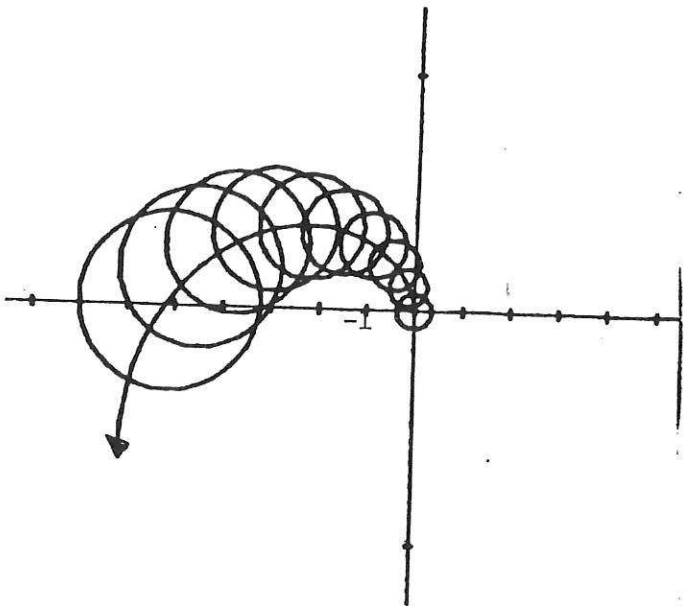

Fig. 5.8(b)

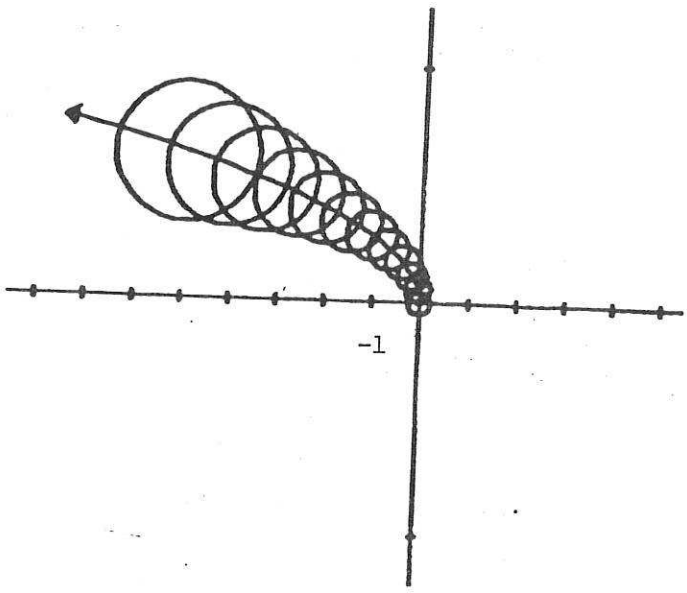

Fig. 5.8(c)

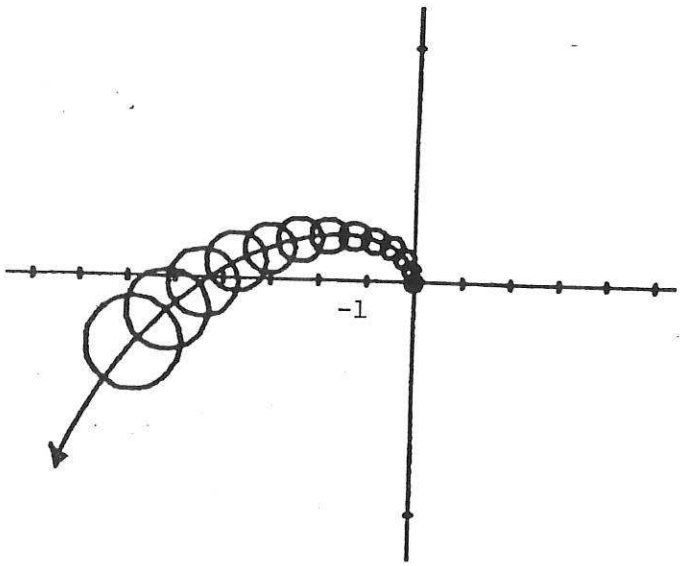

Fig. 5.8(d)

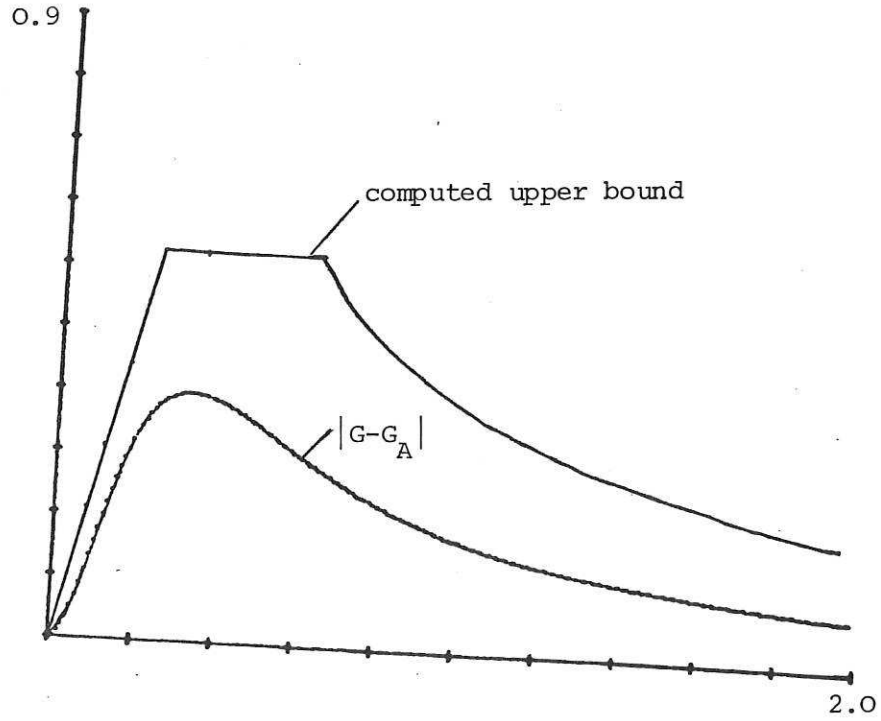

Fig. 5.9

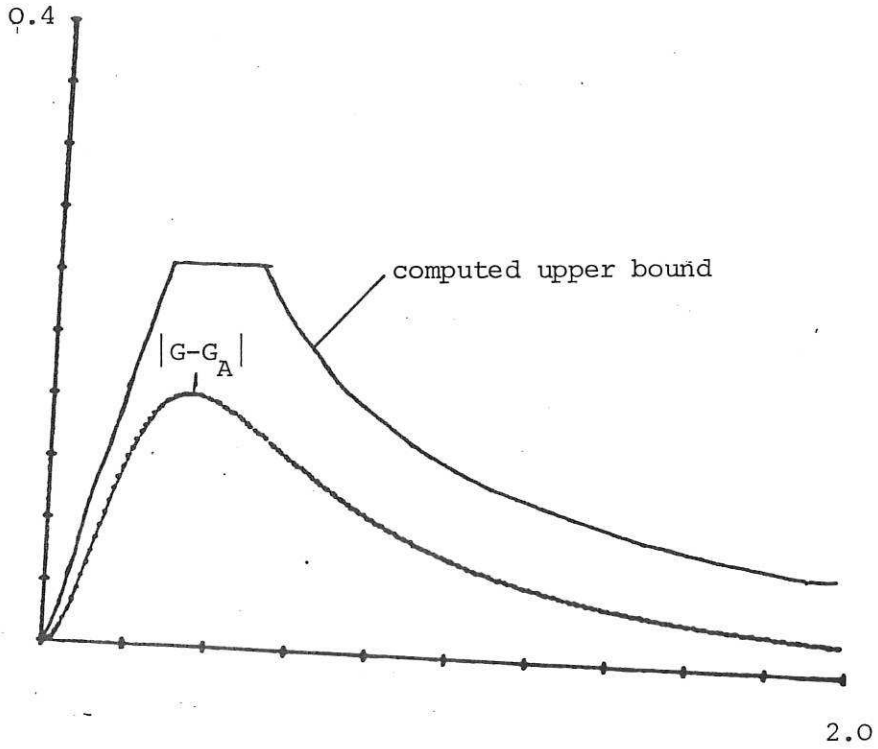

Fig. 5.10

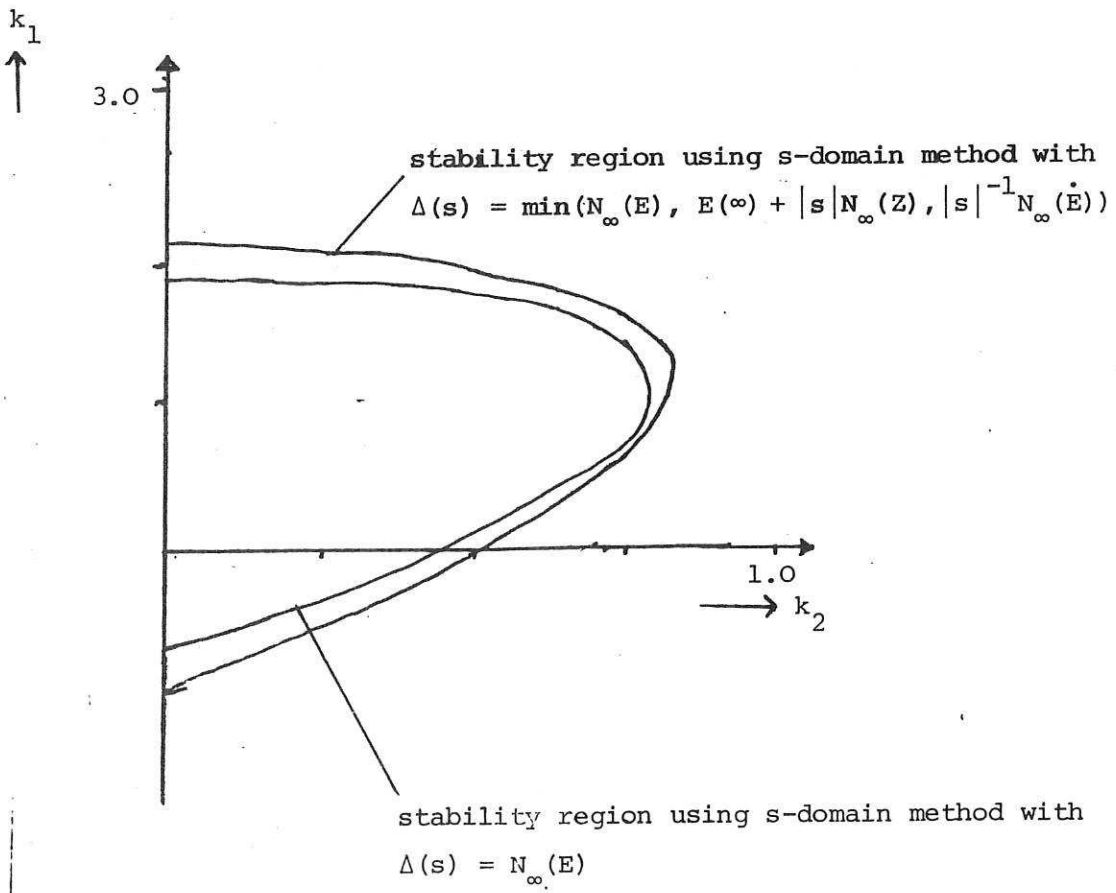
k_1
3.0
stability region using s-domain method with
$\Delta(s) = \min(N_\infty(E),\ E(\infty) + |s|N_\infty(Z), |s|^{-1}N_\infty(\dot{E}))$
1.0
k_2
stability region using s-domain method with
$\Delta(s) = N_\infty(E)$

Fig. 5.11

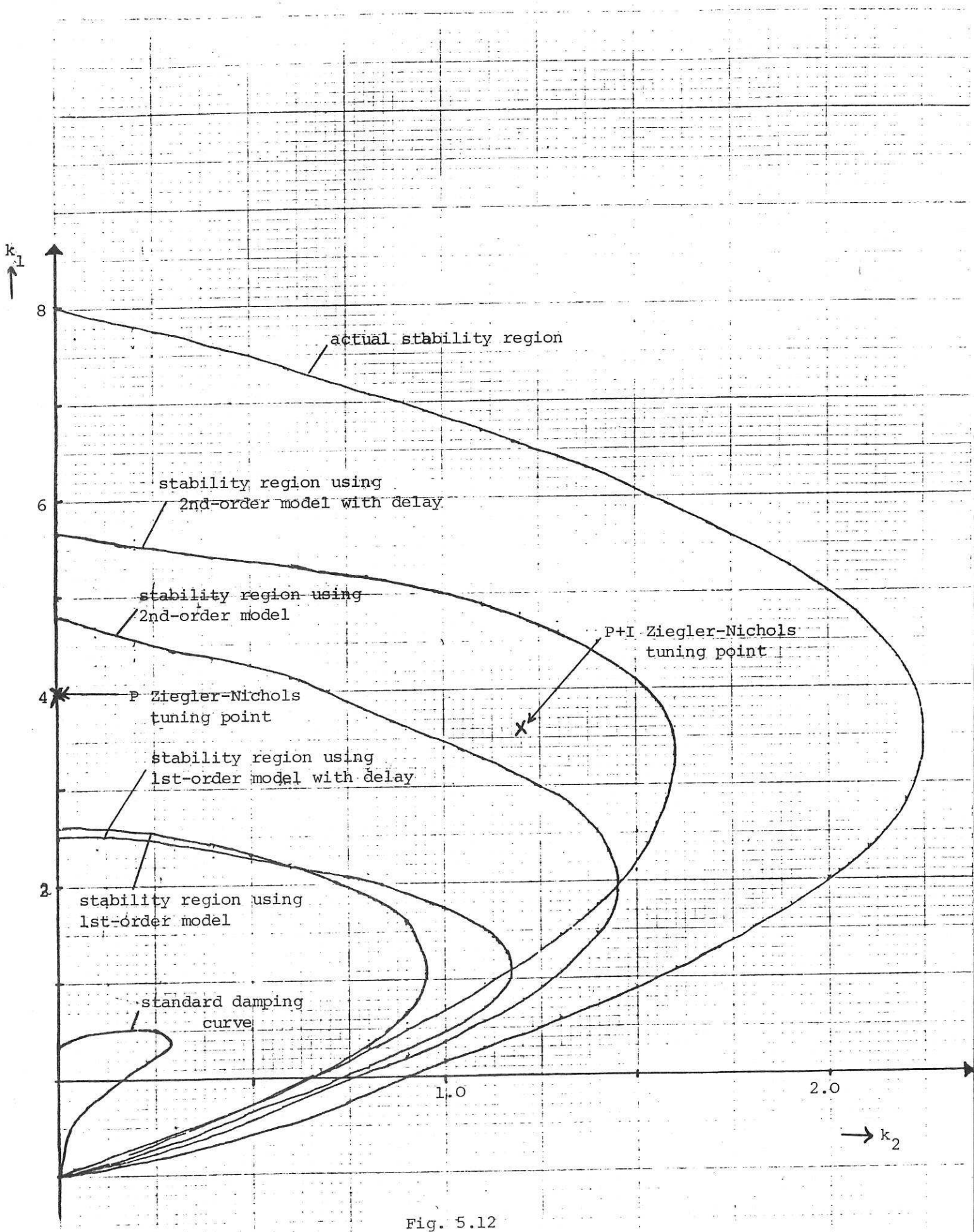
k1
8
6
4
2
actual stability region
stability region using
2nd-order model with delay
stability region using
2nd-order model
P+I Ziegler-Nichols
tuning point
P Ziegler-Nichols
tuning point
stability region using
1st-order model with delay
stability region using
1st-order model
standard damping
curve
1.0
2.0
k2

Fig. 5.12

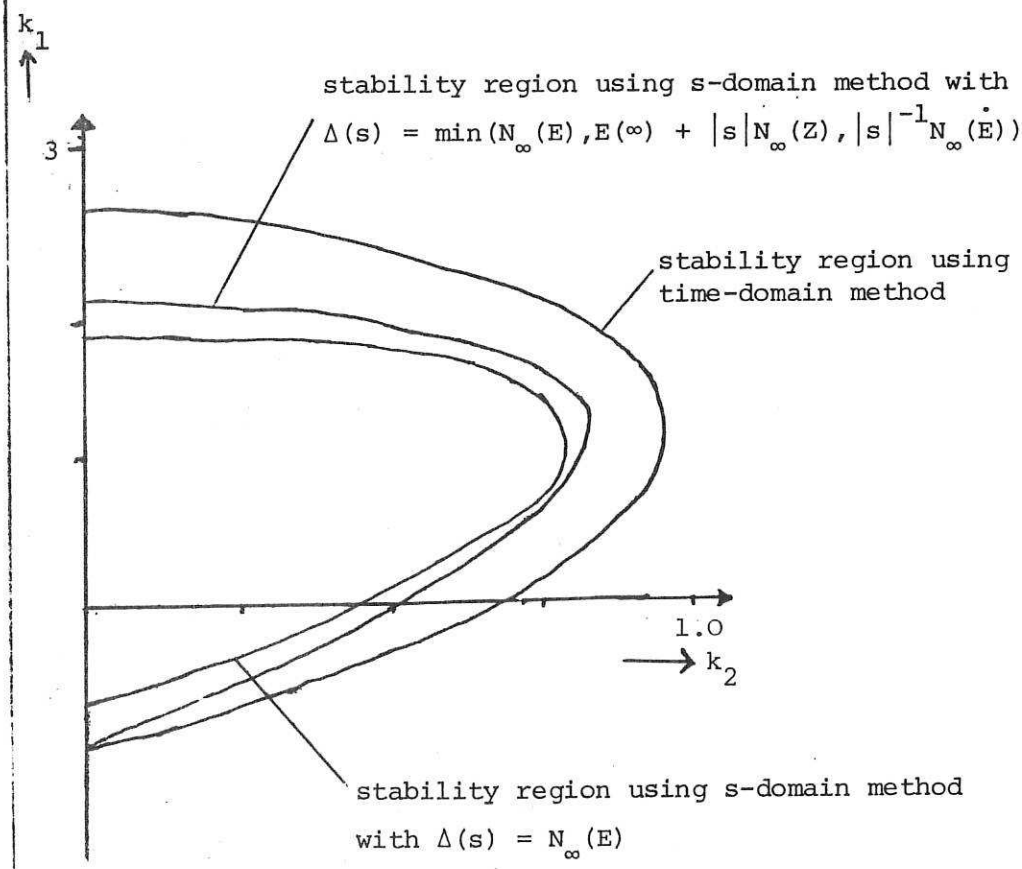
k_1
3
stability region using s-domain method with
$\Delta(s) = \min(N_\infty(E), E(\infty) + |s|N_\infty(Z), |s|^{-1}\dot{N}_\infty(E))$
stability region using
time-domain method
1.0
k_2
stability region using s-domain method
with $\Delta(s) = N_\infty(E)$

Fig. 5.13

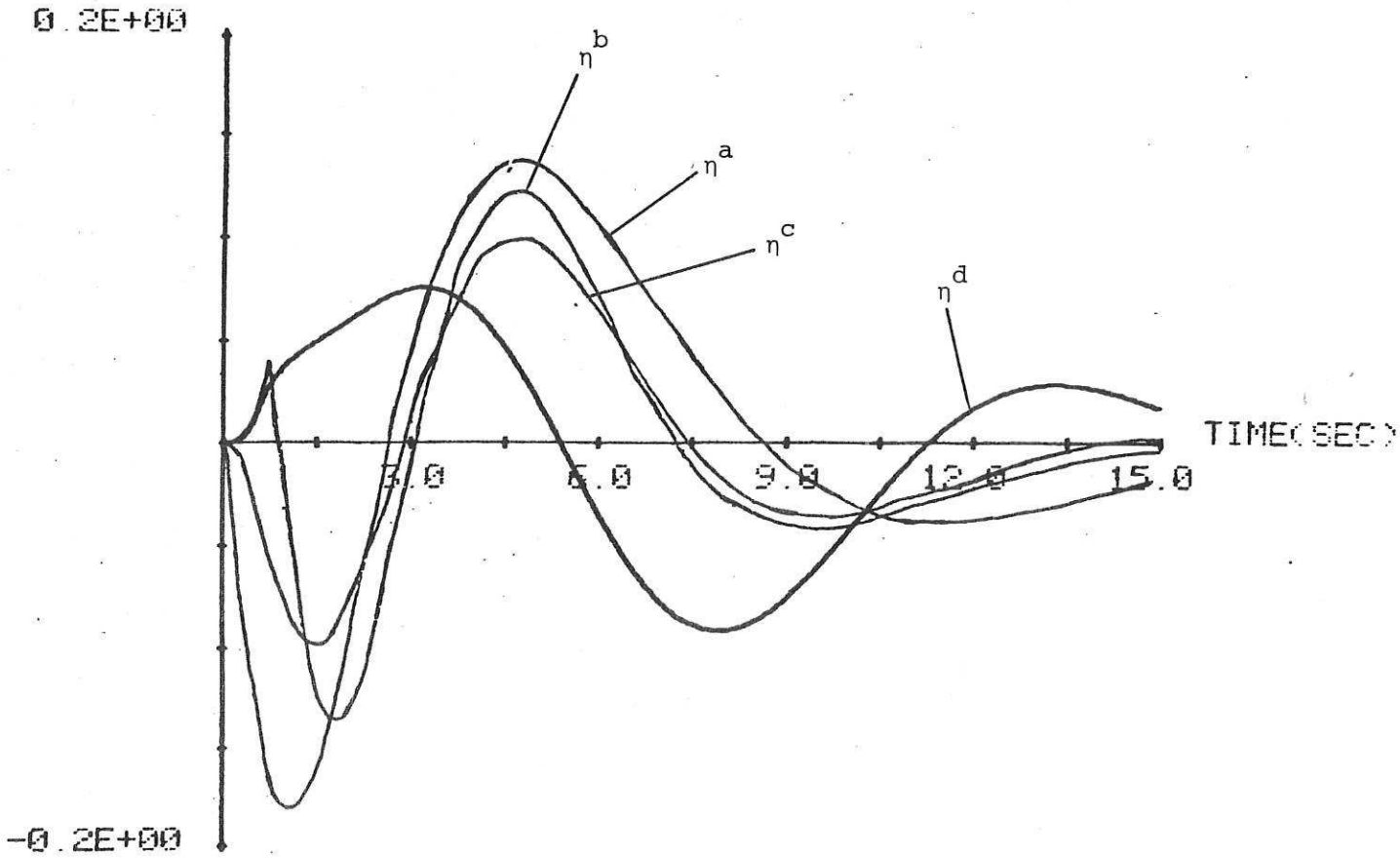

Fig. 5.14

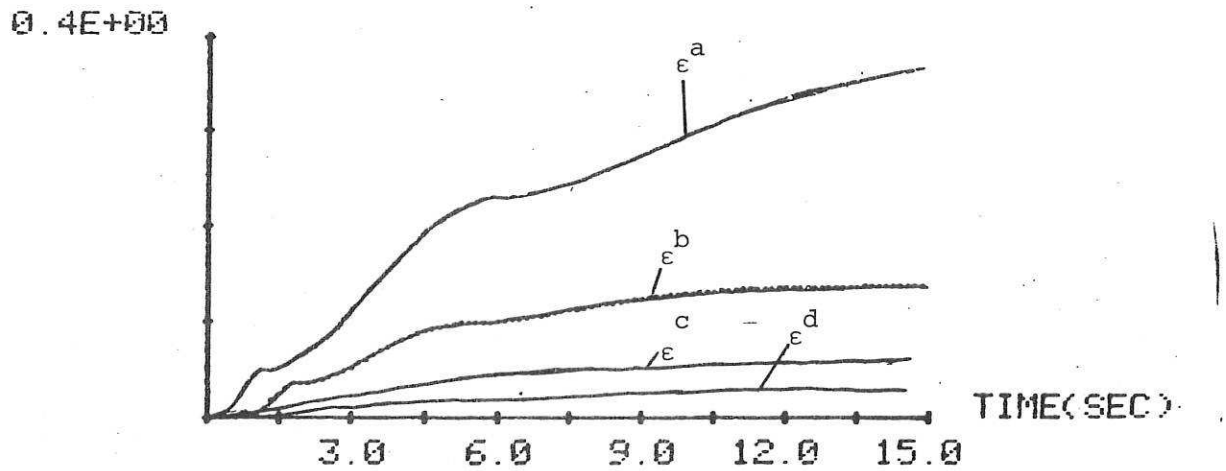

Fig. 5.15

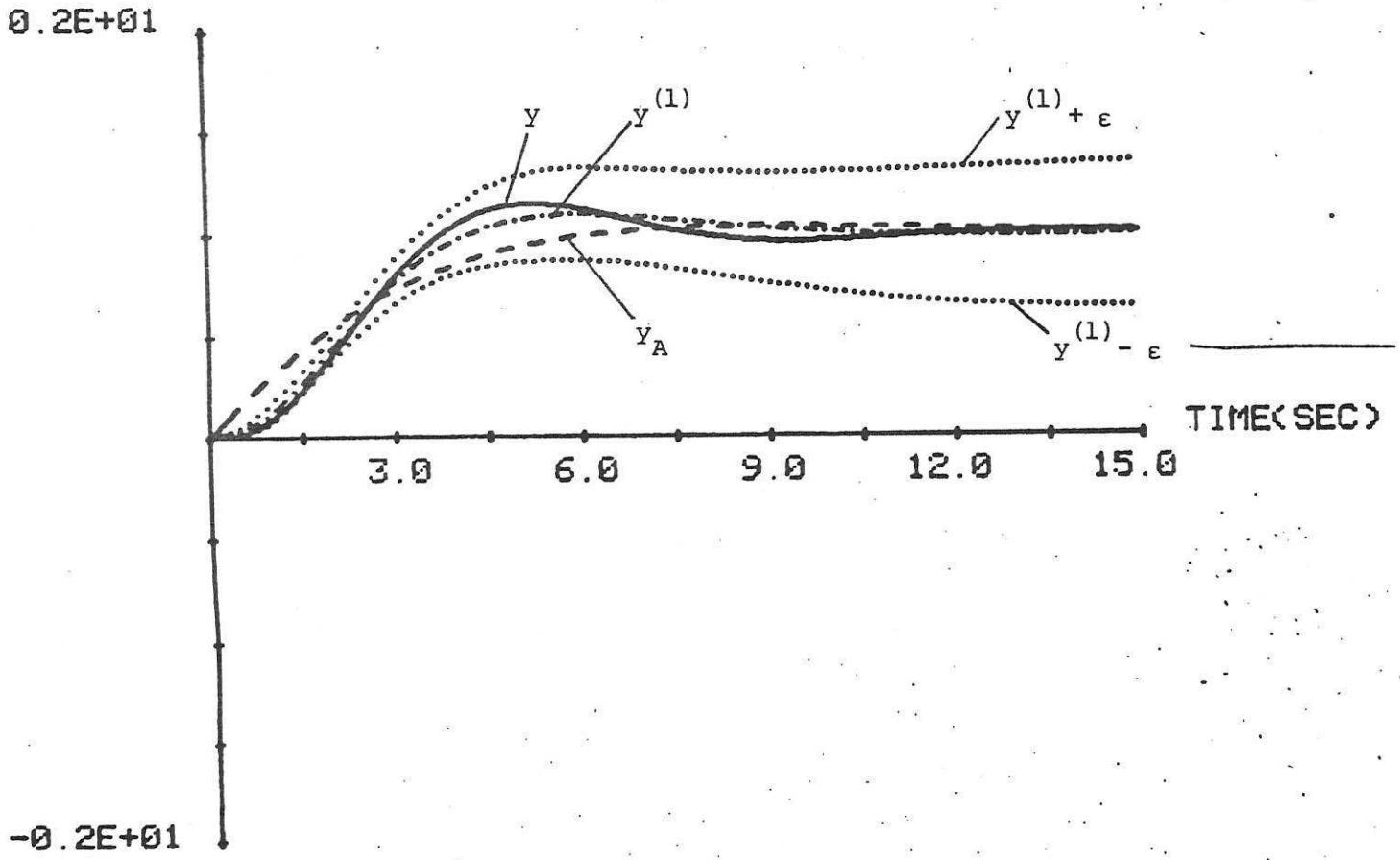
0.2E+01
y
$y^{(1)}$
$y^{(1)} + \varepsilon$
y_A
$y^{(1)} - \varepsilon$
TIME(SEC)
3.0
6.0
9.0
12.0
15.0
-0.2E+01

Fig. 5.16

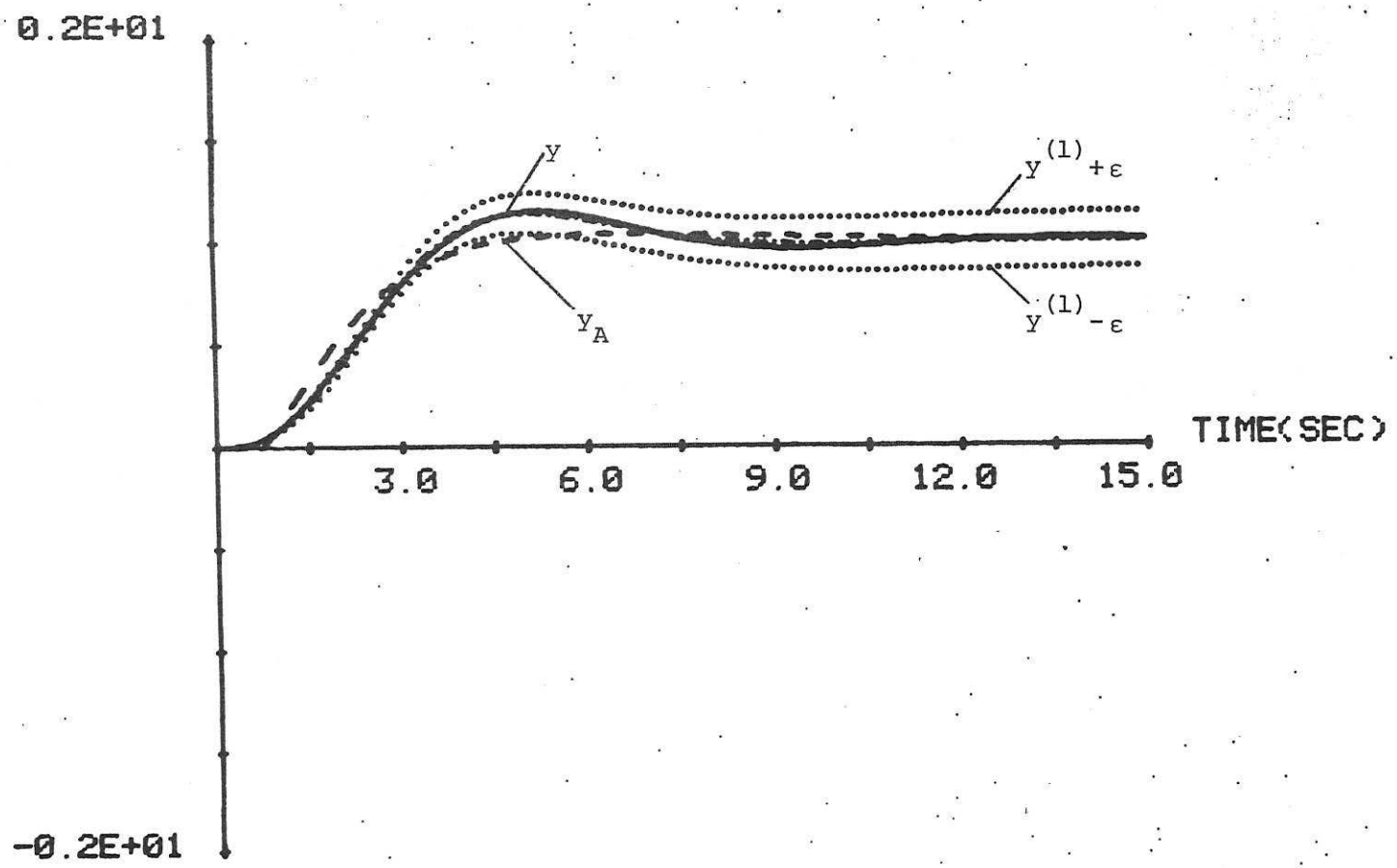
0.2E+01
-0.2E+01
y
$y^{(1)}_{+\varepsilon}$
y_A
$y^{(1)}_{-\varepsilon}$
TIME(SEC)
3.0
6.0
9.0
12.0
15.0

Fig. 5.17

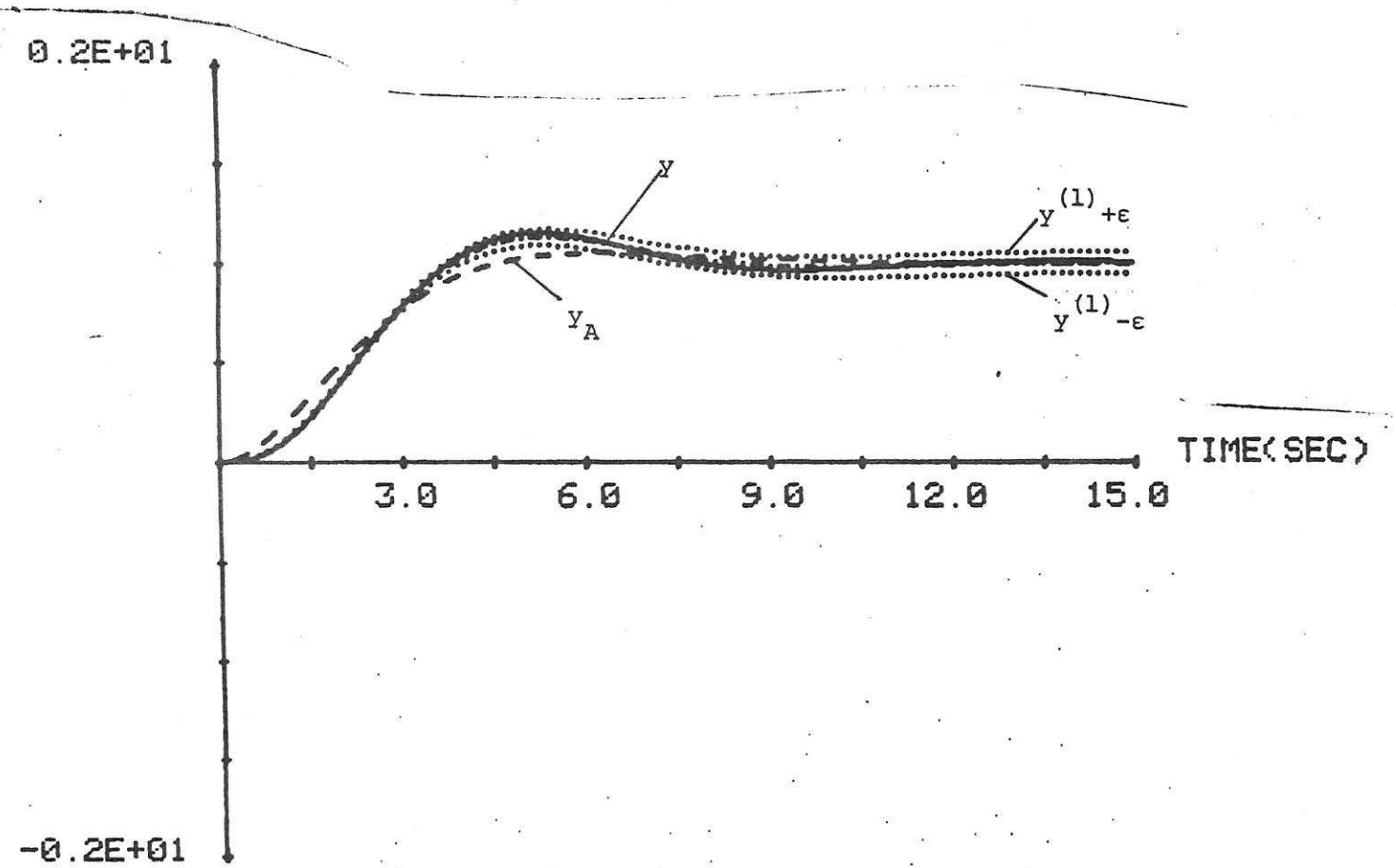
0.2E+01
-0.2E+01
y
$y^{(1)}_{+\varepsilon}$
$y^{(1)}_{-\varepsilon}$
y_A
TIME(SEC)
3.0
6.0
9.0
12.0
15.0

Fig. 5.18

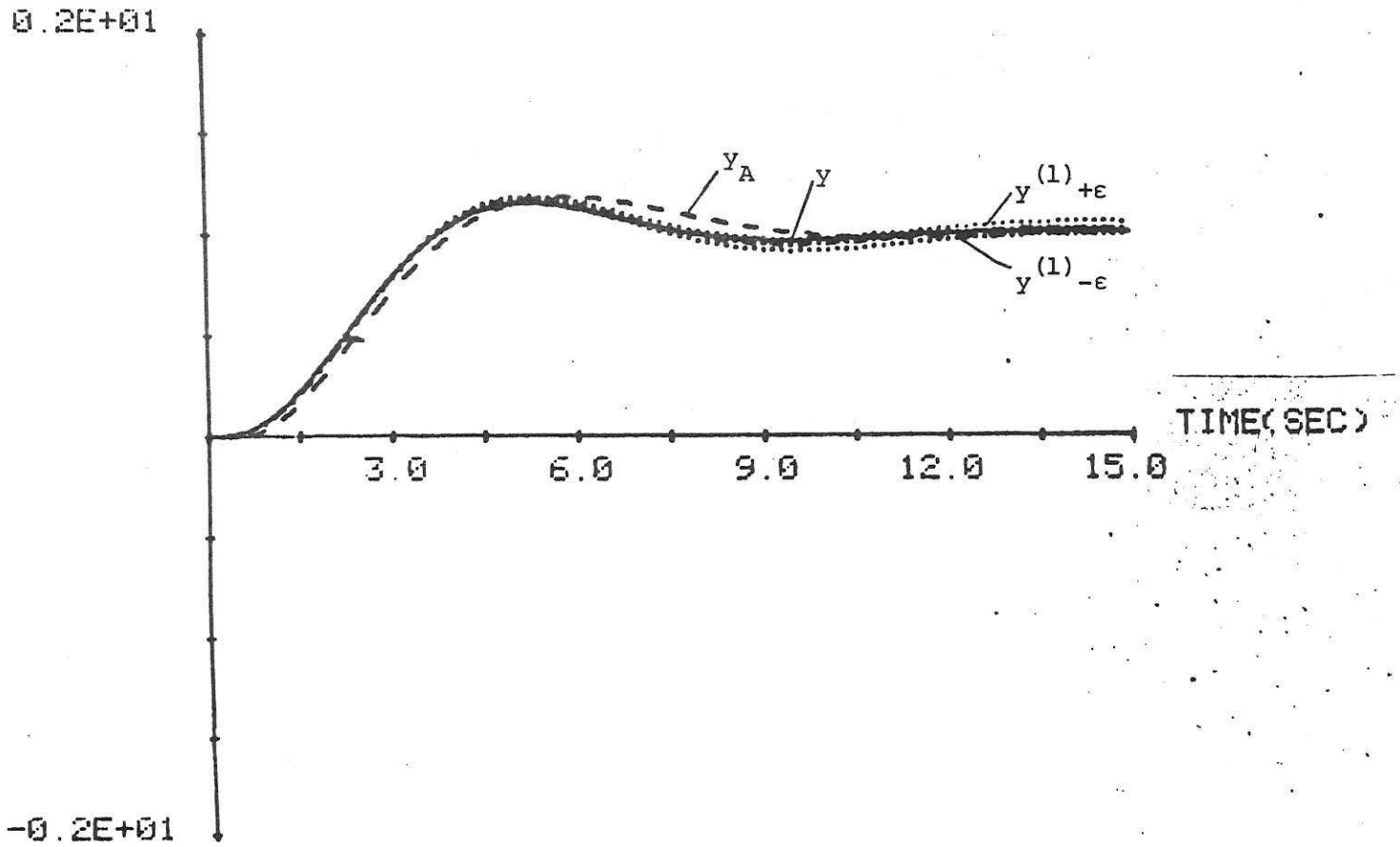
0.2E+01
-0.2E+01
y_A
y
$y^{(1)}_{+\varepsilon}$
$y^{(1)}_{-\varepsilon}$
TIME(SEC)
3.0
6.0
9.0
12.0
15.0

Fig. 5.19

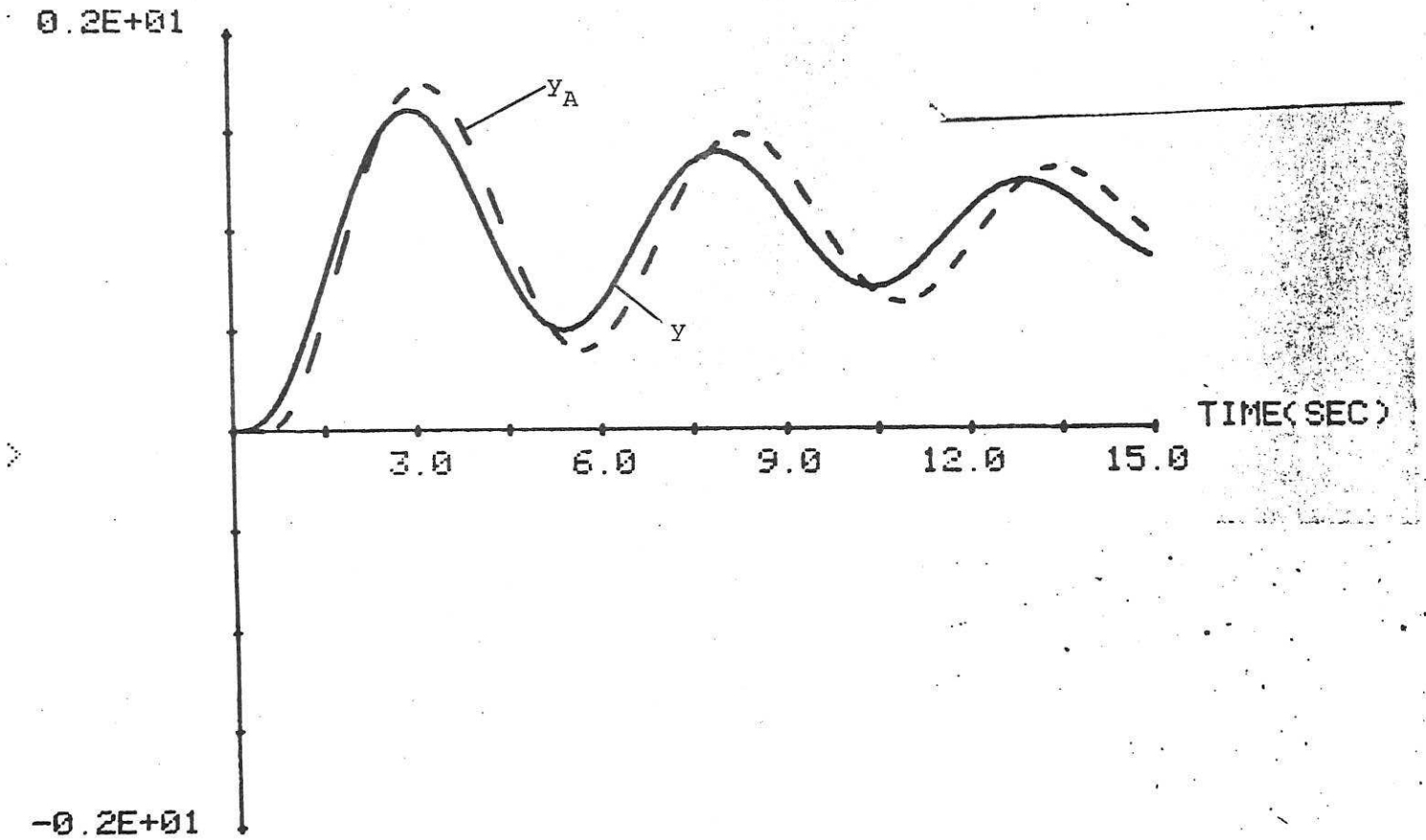

Fig. 5.20

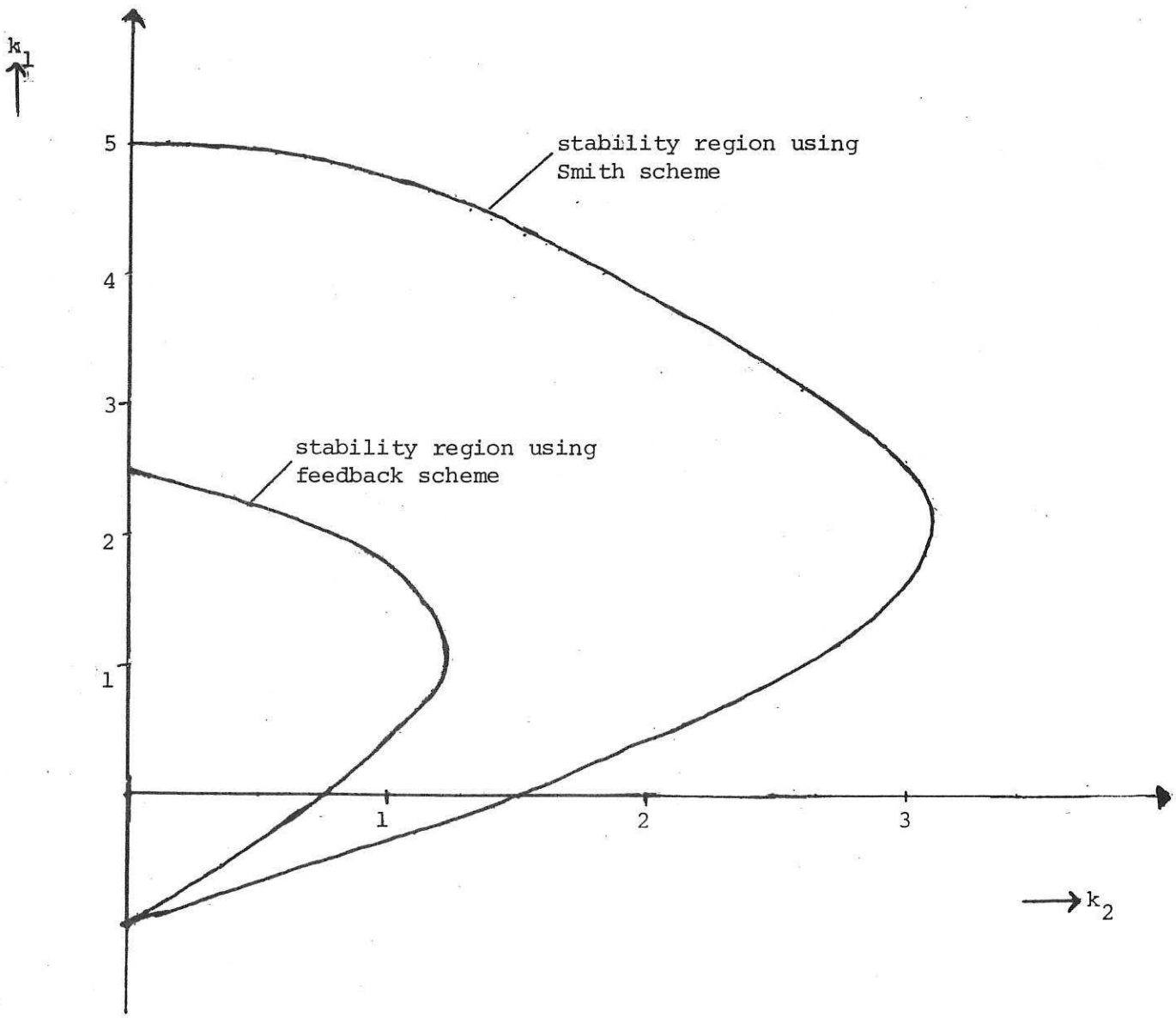
k_1
5
4
3
2
1
stability region using
Smith scheme
stability region using
feedback scheme
1
2
3
k_2

Fig. 5.21

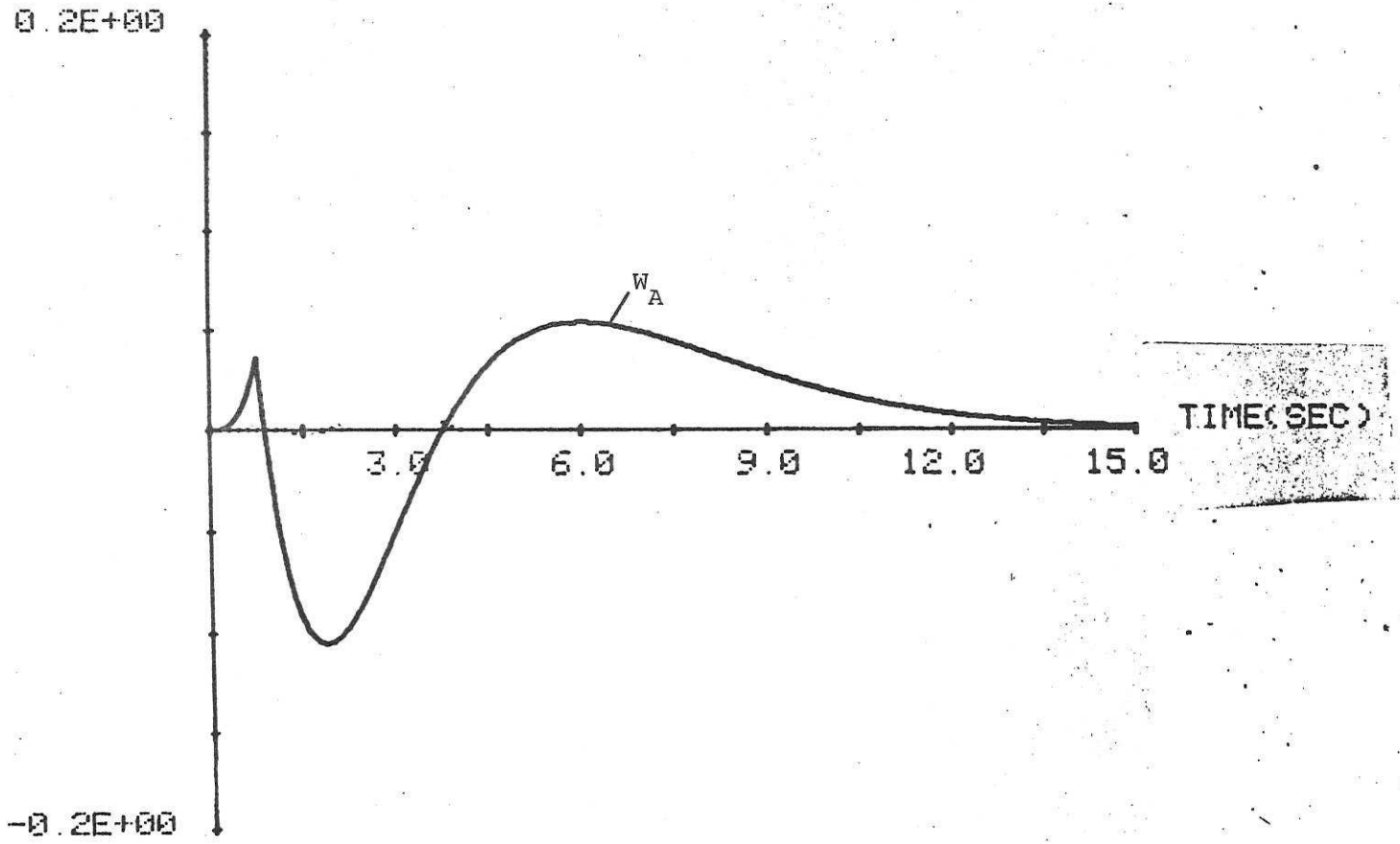

Fig. 5.22

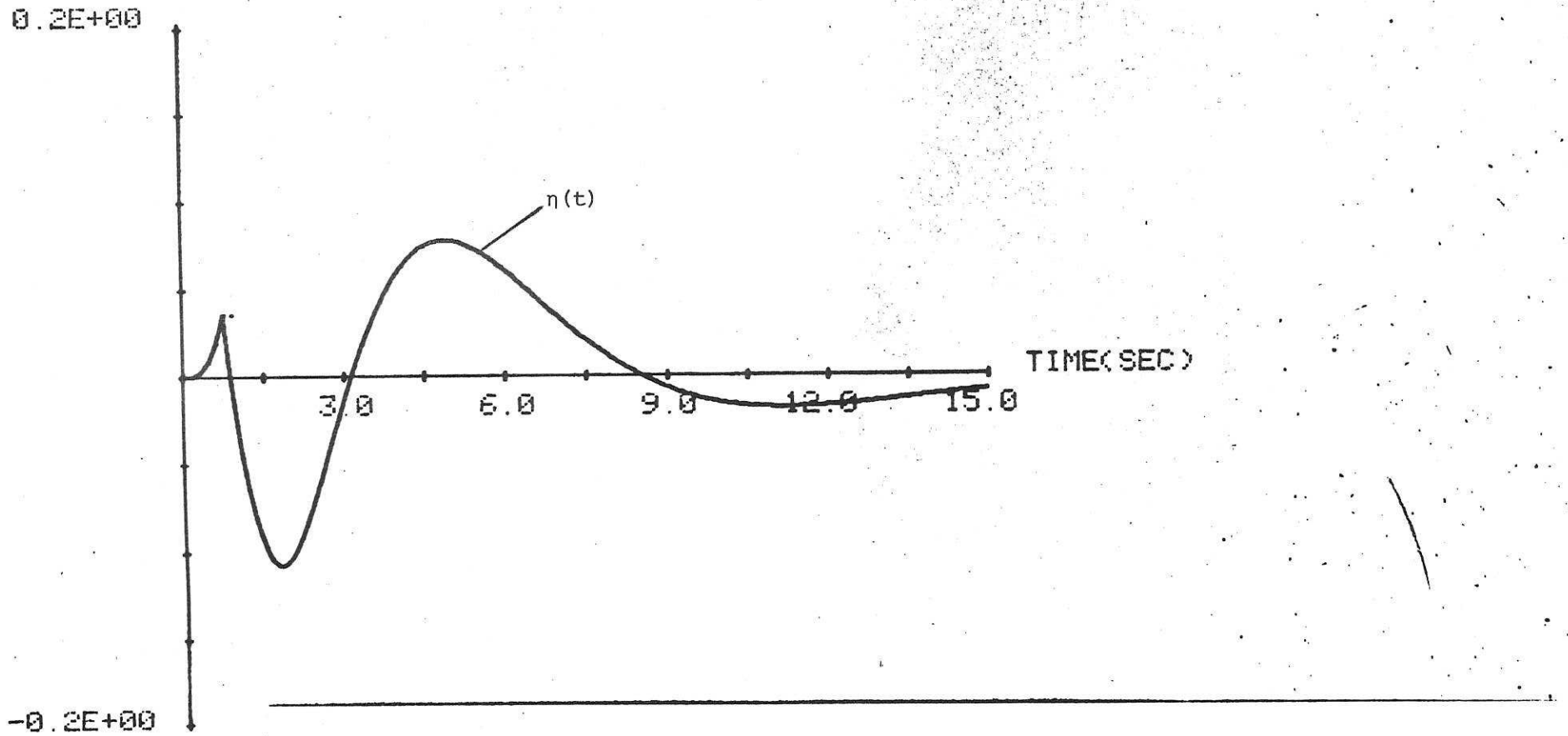

Fig. 5.23

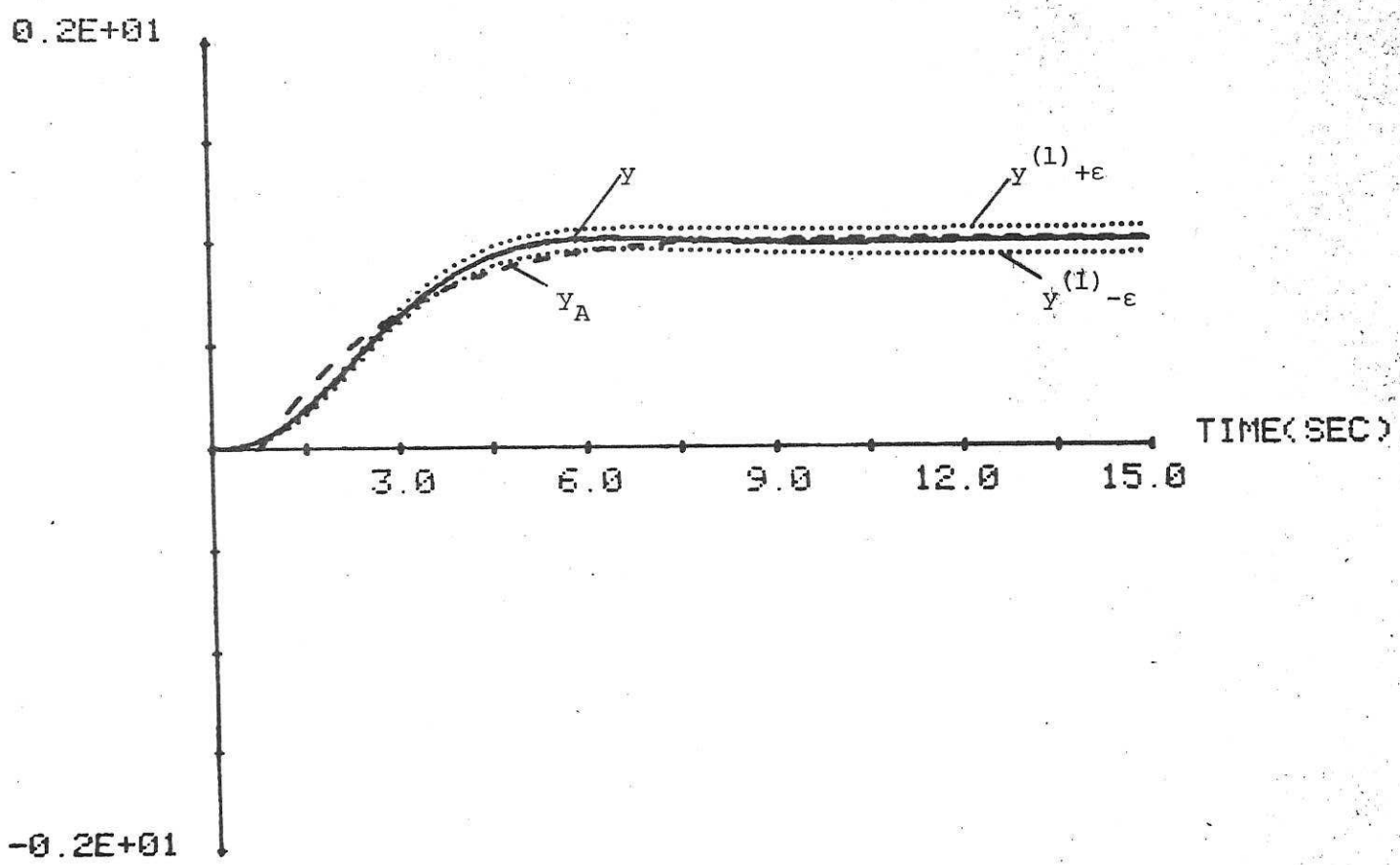
0.2E+01
-0.2E+01
y
$y^{(1)}_{+\varepsilon}$
y_A
$y^{(1)}_{-\varepsilon}$
TIME(SEC)
3.0
6.0
9.0
12.0
15.0

Fig. 5.24

6. EXAMPLE 2

Consider a process with transfer function

$$G(s) = \frac{1}{(s+1)^6} \tag{6.1}$$

with step response Y shown in Fig. 6.1 (a). Using the technique of Section 4.1 the first-order model of the form

$$G_A(s) = \frac{1}{1+5.9s} \tag{6.2}$$

was fitted, with step response Y_A again illustrated in Fig. 6.1 (a) and the error $E = Y - Y_A$ shown in Fig. 6.1(b). The total variation, $N_\infty(E)$ was found to be 0.87. Consideration of G_A suggests the P+I controller

$$K(s) = 0.6 + s^{-1}0.15 \tag{6.3}$$

to stabilise G_A and produce the acceptable closed-loop characteristic indicated in Fig. 6.3. This choice clearly satisfies equation (2.5) and the inverse Nyquist plot of $G_AKF = G_AK$ with superimposed confidence circles shown in Fig. 6.2 indicates that the (-1,0) point does not lie in or on the confidence band. Stability of real plant is hence guaranteed provided that the controllability and observability condition is satisfied and this is so for the above plant.

Finally, for comparative purposes, the closed-loop response of the real feedback scheme is also shown in Fig. 6.3.

Using the time-domain method for the above example, the response $W_A(t)$ was computed to be as in Fig. 6.4 and graphical analysis of this response leads to the conclusion that $N_\infty(W_A) = 0.64 < 1$, hence verifying the stability predictions for the real plant. The correction term $\eta(t)$ is shown in Fig. 6.5 and the error bound $\varepsilon(t)$ is shown in Fig. 6.6. The bounds $y^{(1)} \pm \varepsilon(t)$, together with y and y_A, are illustrated in Fig. 6.7. Although the first-order model of the form (6.2) verifies the stability prediction for the P+I controller of the form (6.3), it clearly gives large error bounds (with a maximum of 38% error) and to reduce these we

must choose a better model (say) of the delay-lag system

$$G_A(s) = \frac{e^{-2.5s}}{1+3.4s} \qquad (6.4)$$

The open-loop step responses Y and Y_A are shown in Fig. 6.8 and modelling error E(t) is illustrate in Fig. 6.9. Using the same controller as before (equantion (6.3)), the response $W_A(t)$ is shown in Fig. 6.10 and graphical analysis of this response leads to the conclusion that $N_\infty(W_A) = 0.4$. The correction term $\eta(t)$ is shown in Fig. 6.11 and the improved bound $\varepsilon(t)$ is shwon in Fig. 6.12 indicating that the maximum error is 8%. (compared with 38%). The bounds $y^{(1)} \pm \varepsilon$, together with y and y_A are illustrated in Fig. 6.13. The stability regions deduced from the time-domain technique are illustrated in Fig. 6.14 for both models together with the actual stability region of the real plant. From Fig. 6.14 it is clear that for stability purposes, both the models are good for predicting Ziegler-Nichols tuning points.

Using the Smith Predictor scheme for the delay-lag model of the form of (6.4), with the same controller gains as before, it was also found that $N_\infty(W_A) = 0.3$ and the bound $\varepsilon(t)$ is shown in Fig. 6.15. The responses y, y_A and $y^{(1)} \pm \varepsilon$ are illustrated in Fig. 6.16 for the Smith control scheme and the maximum error was found be 4% only.

6.1 Summary and Discussion:

We make the following observations from the above example.

(1) Again we notice that, by using highly simplified process models, a successful design can be achieved.

(2) For stability purposes, both models (first-order and first-order model with delay) can predict the standard P and P+I Ziegler-Nichols tuning points. Also note that both models predict the substantial part of the actual stability region.

(3) The first-order model verifies the stability prediction for the controller $K(s) = 0.6 + \frac{0.15}{s}$ but gives large performance error bounds which are not regarded as acceptable. The error bounds are reduced by using a better model (i.e. a first-order model with delay).

(4) For the delay-lag model, the Smith Predictor scheme gives much better performance predictions than a standard feedback scheme in the sense that it reduces the maximum error bound from 8% to 4%.

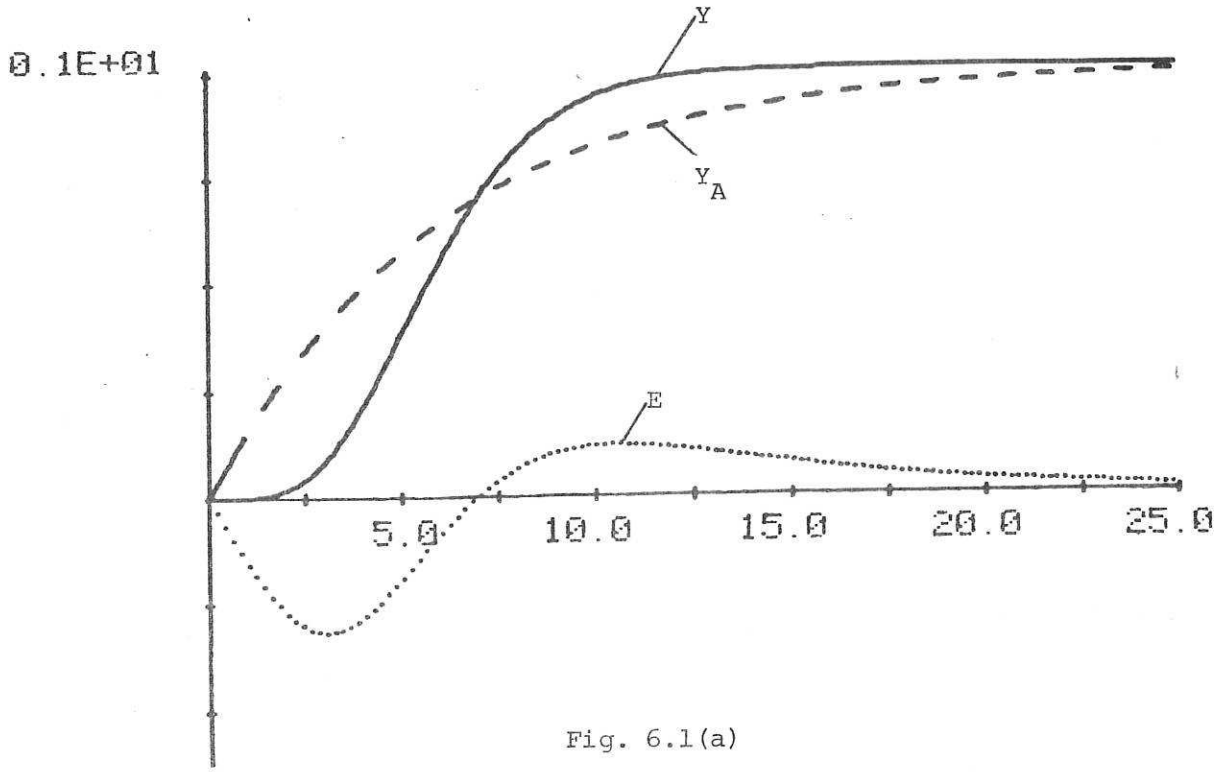

Fig. 6.1(a)

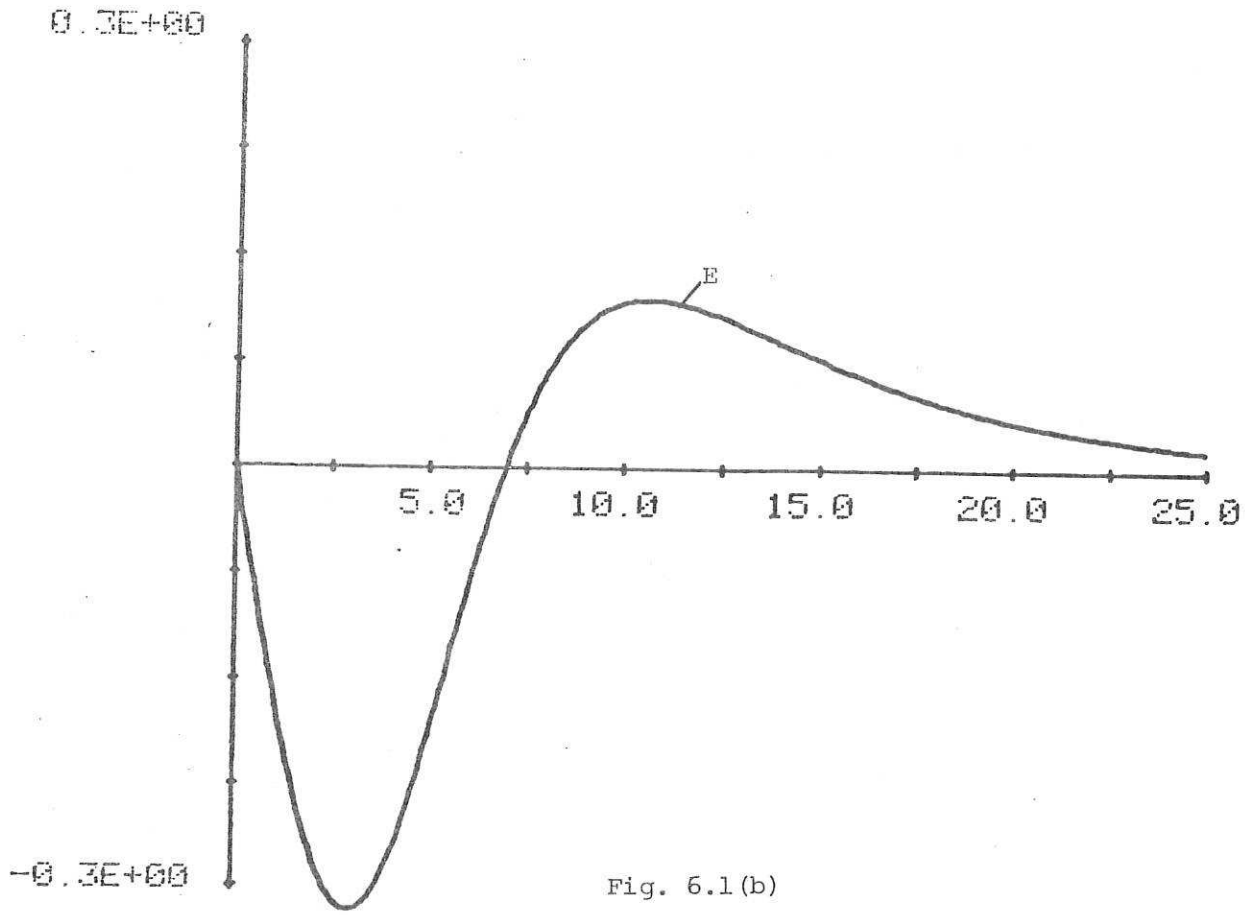

Fig. 6.1(b)

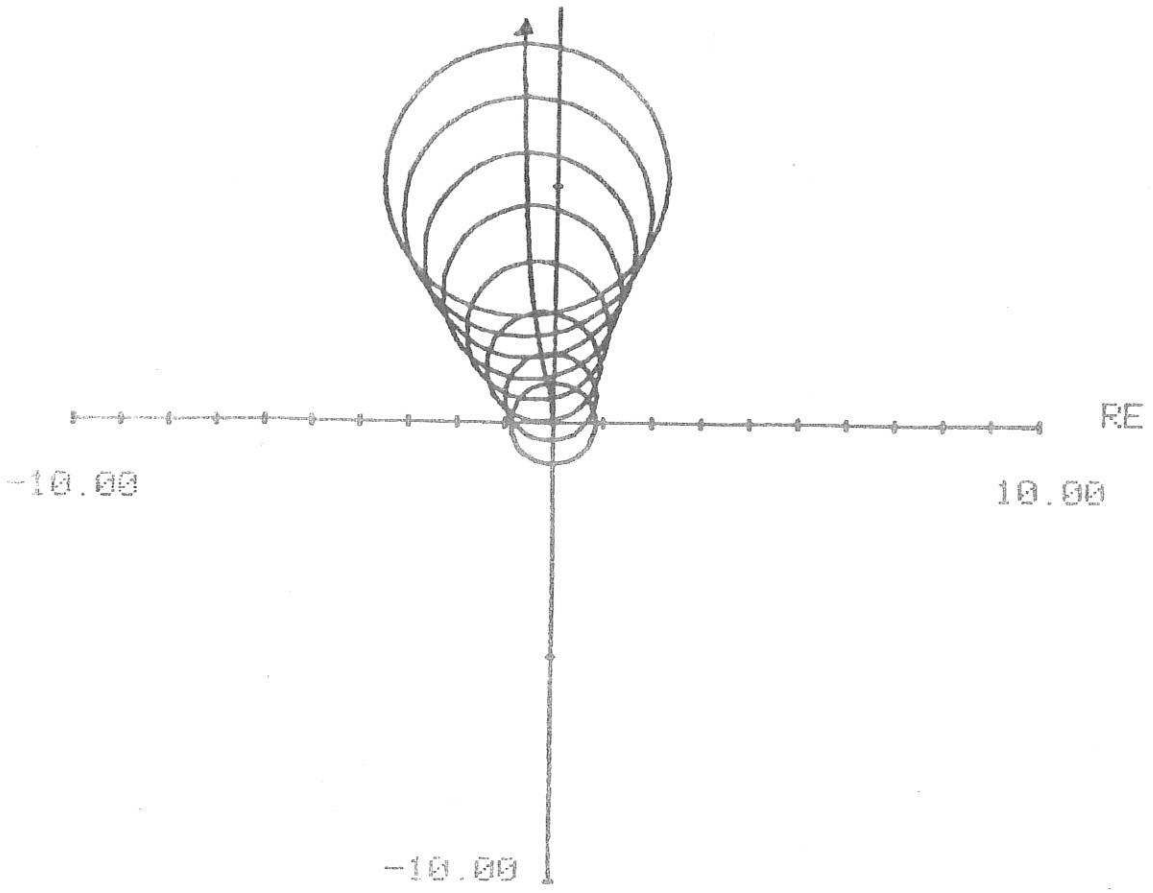

Fig. 6.2

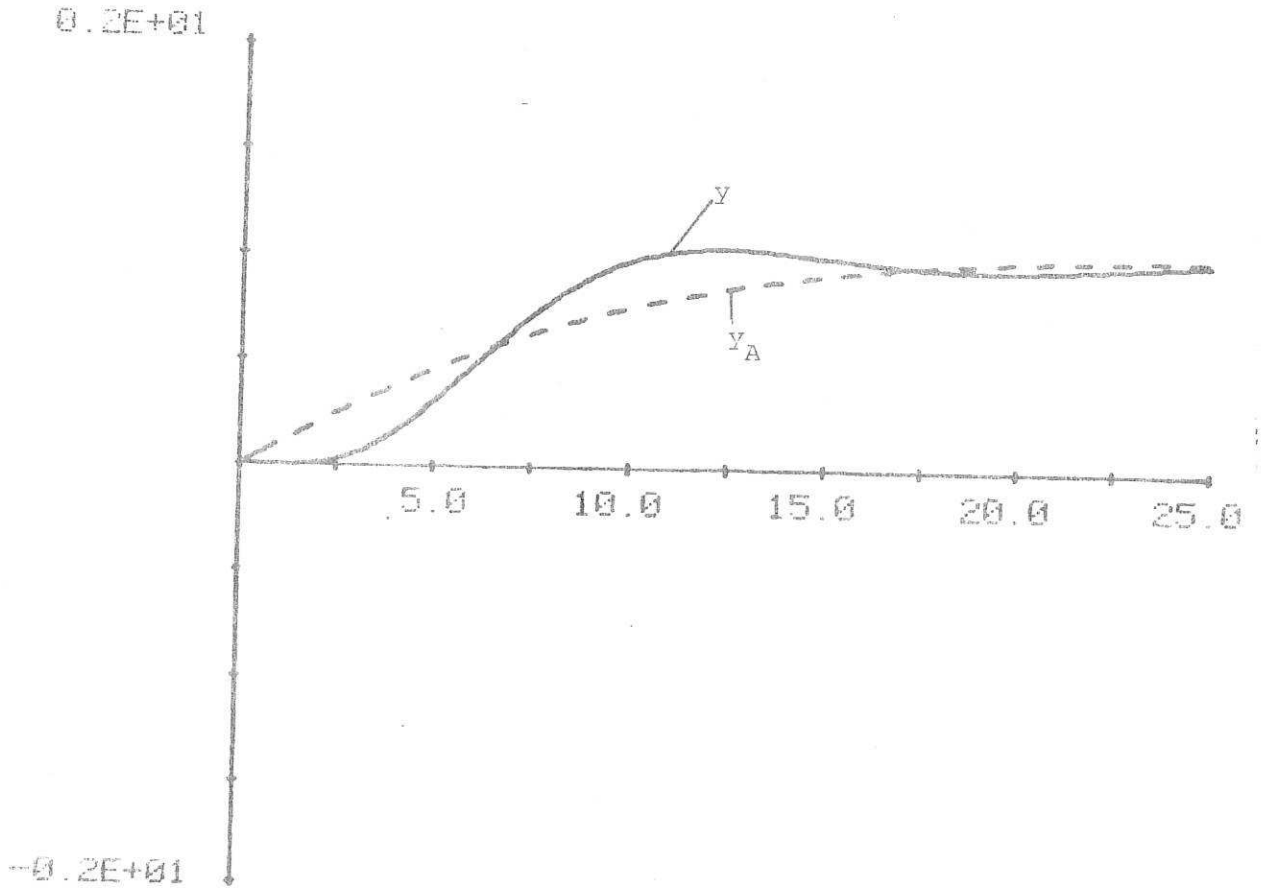

Fig. 6.3

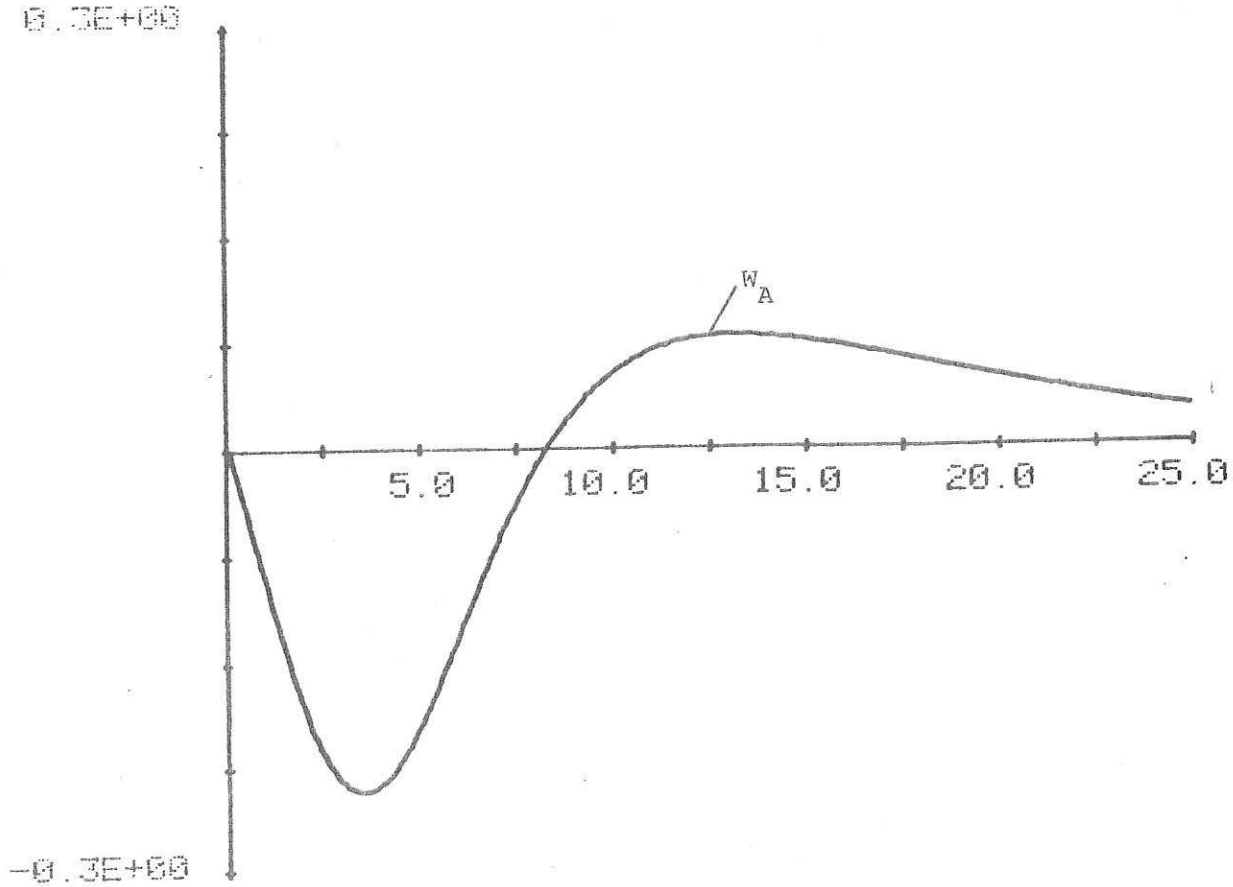
0.3E+00
W_A
5.0
10.0
15.0
20.0
25.0
-0.3E+00

Fig. 6.4

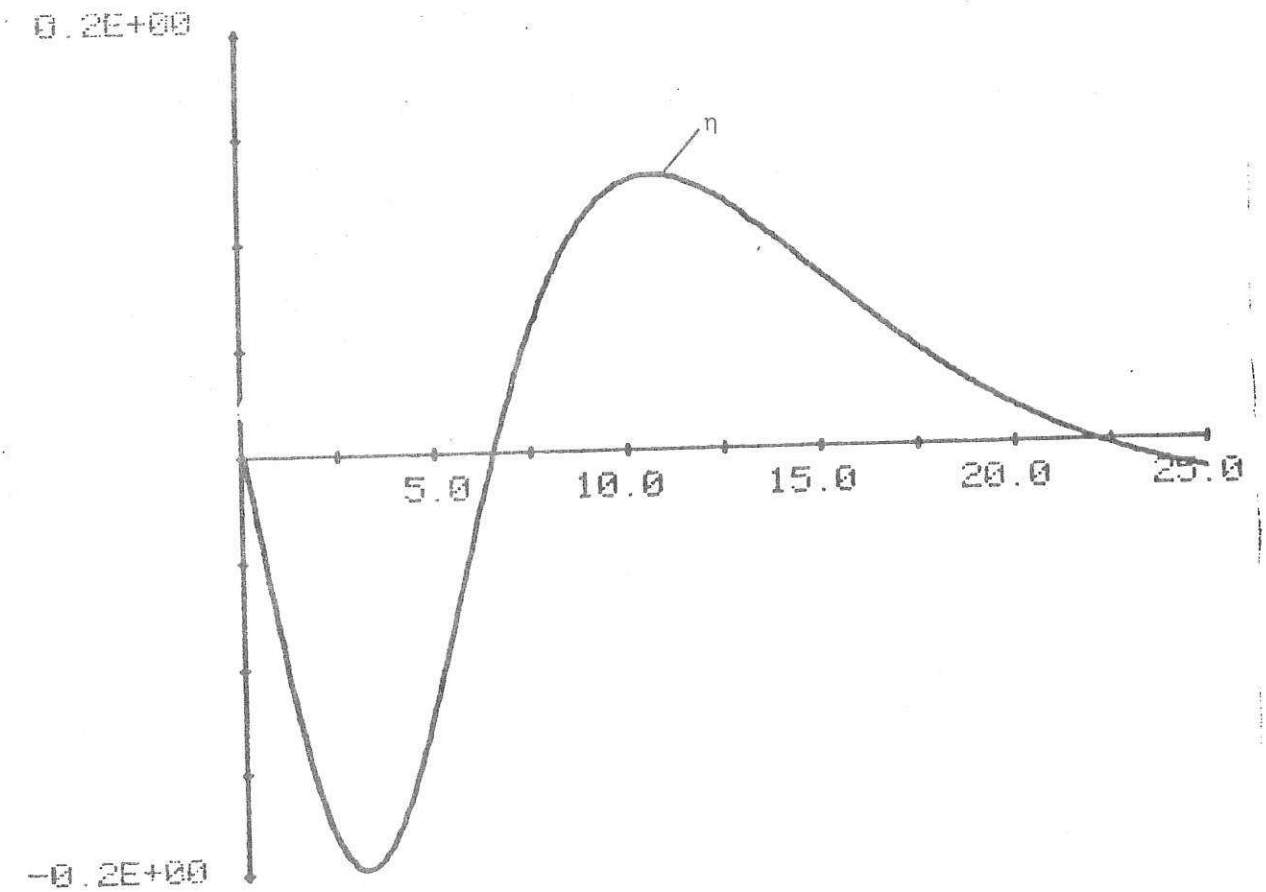
0.2E+00
η
5.0
10.0
15.0
20.0
25.0
-0.2E+00

Fig. 6.5

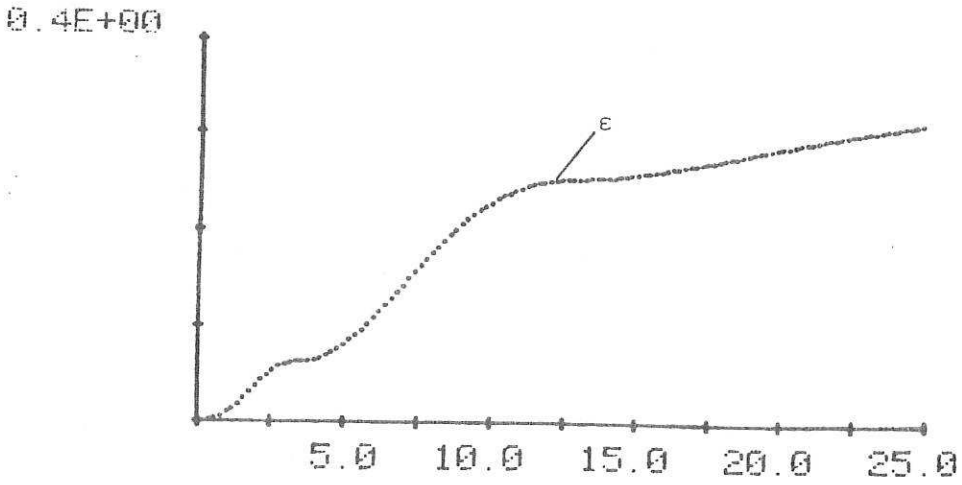
0.4E+00
ε
5.0
10.0
15.0
20.0
25.0

Fig. 6.6

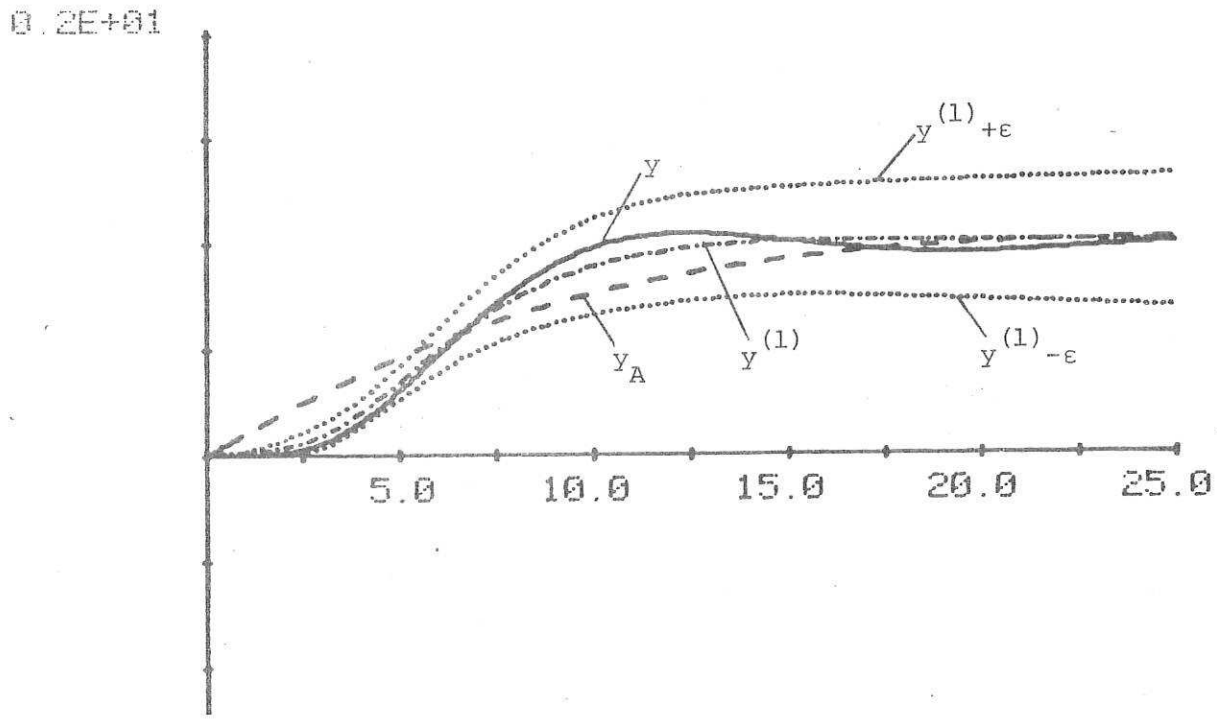
0.2E+01
y
$y^{(1)}_{+\varepsilon}$
y_A
$y^{(1)}$
$y^{(1)}_{-\varepsilon}$
5.0
10.0
15.0
20.0
25.0

Fig. 6.7

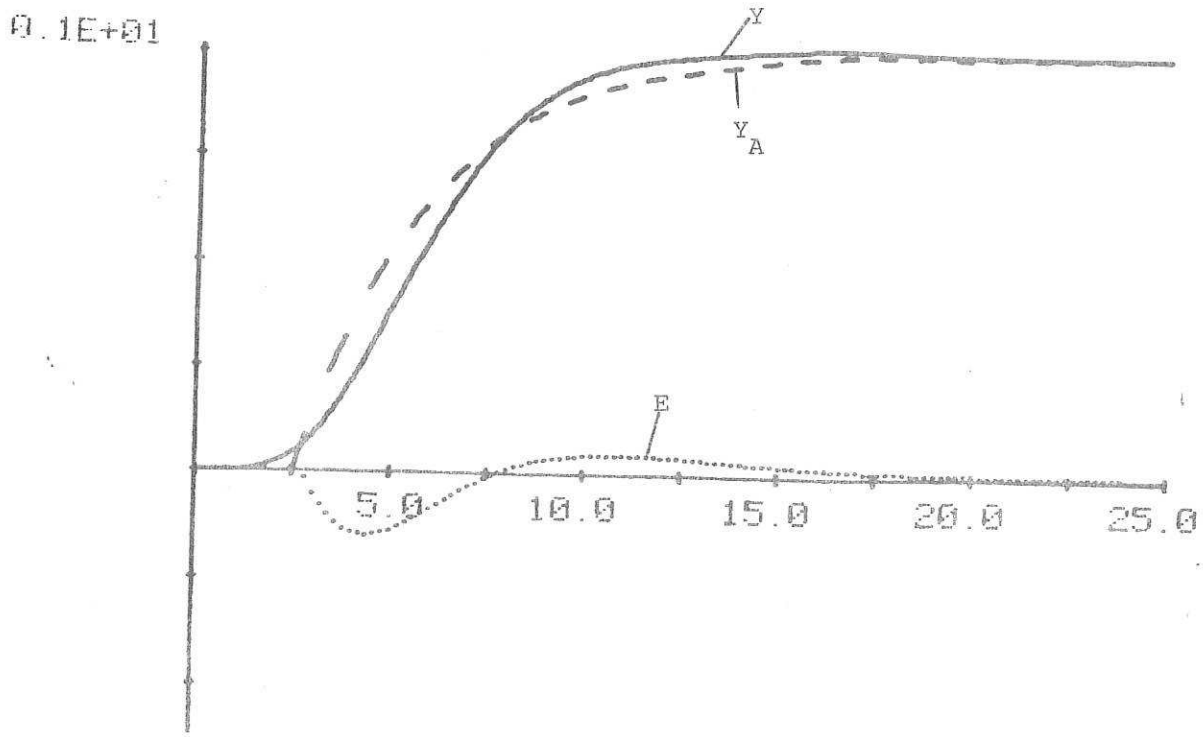

Fig. 6.8

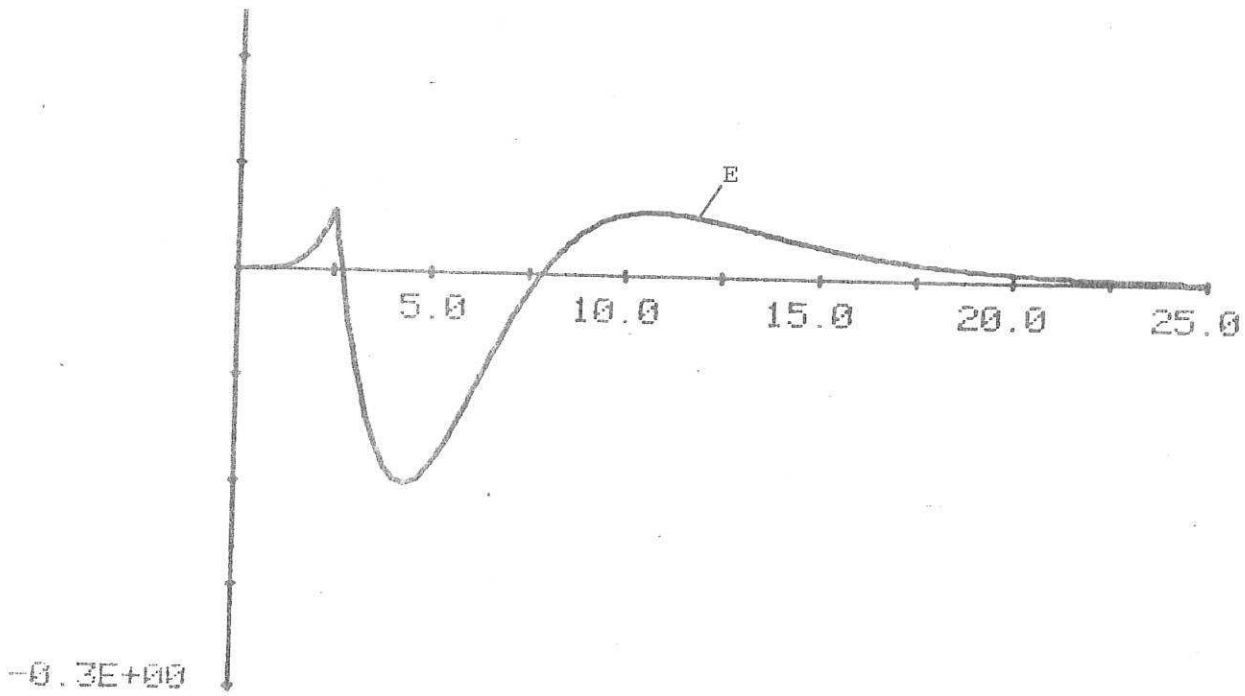

Fig. 6.9

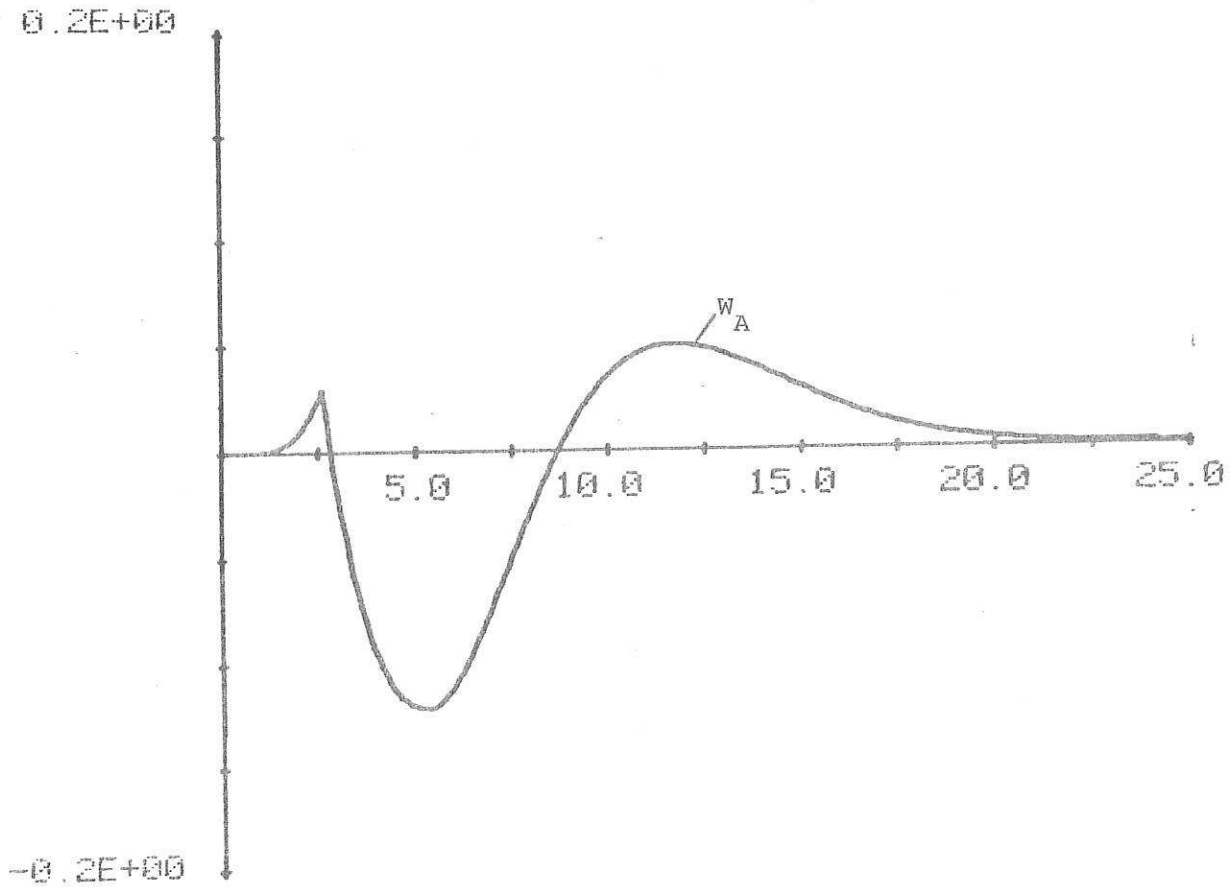

Fig. 6.10

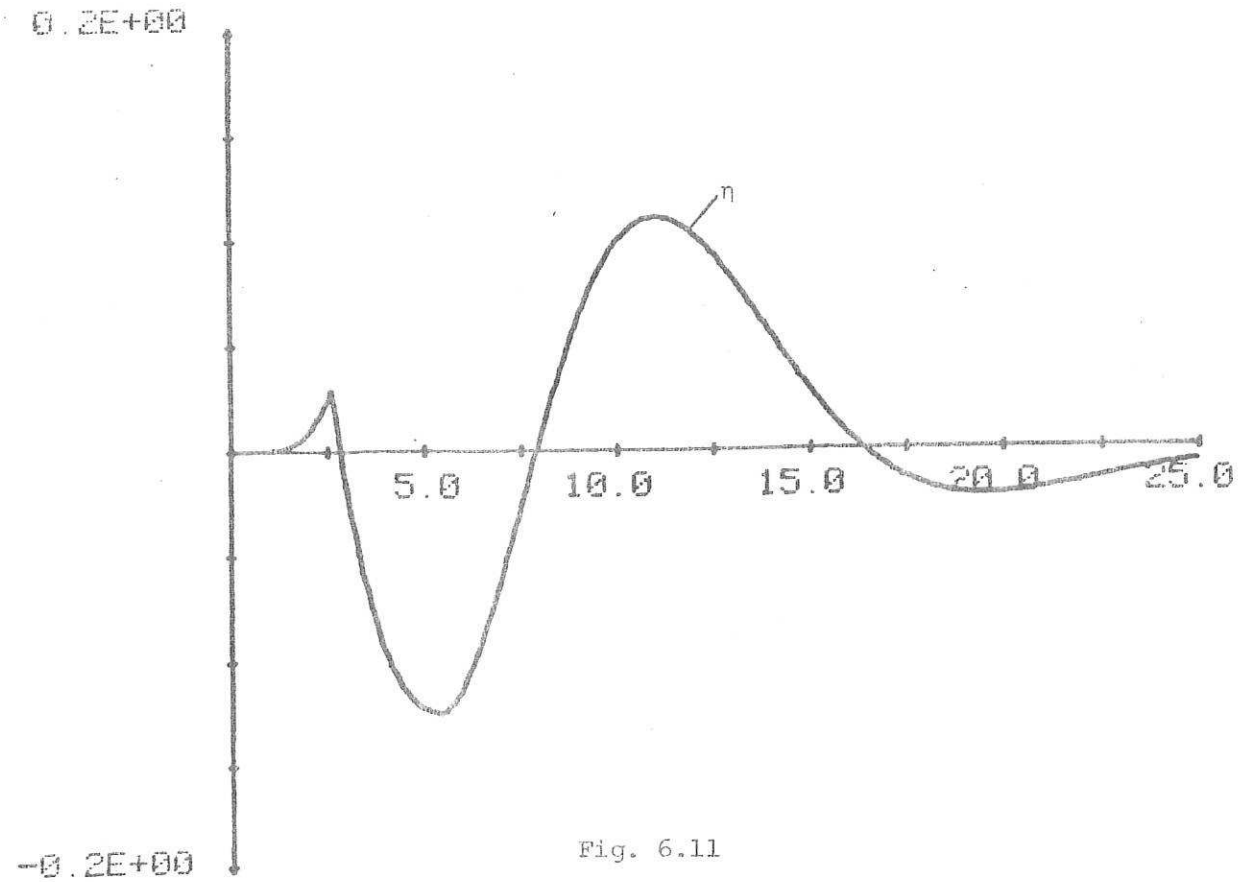

Fig. 6.11

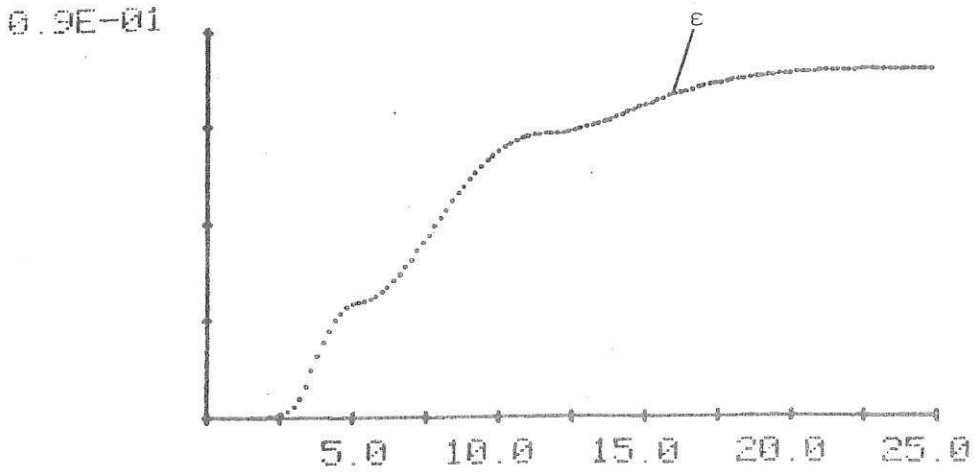

Fig. 6.12

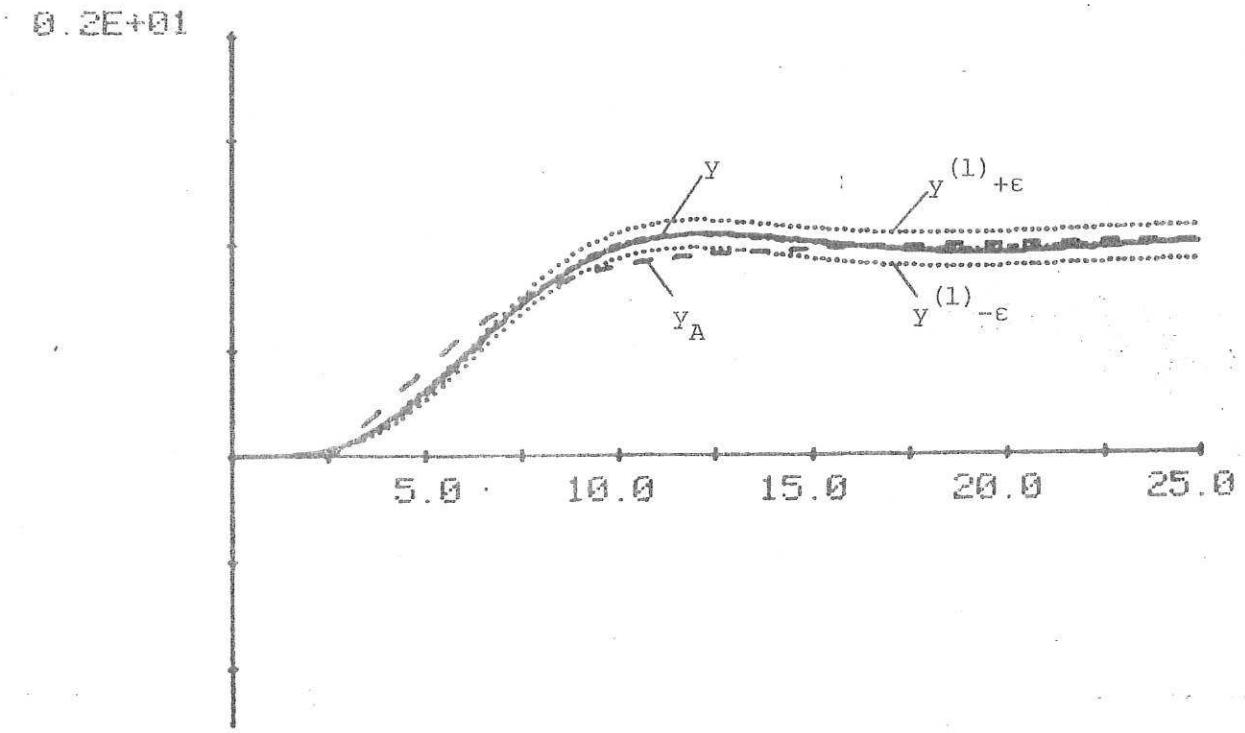

Fig. 6.13

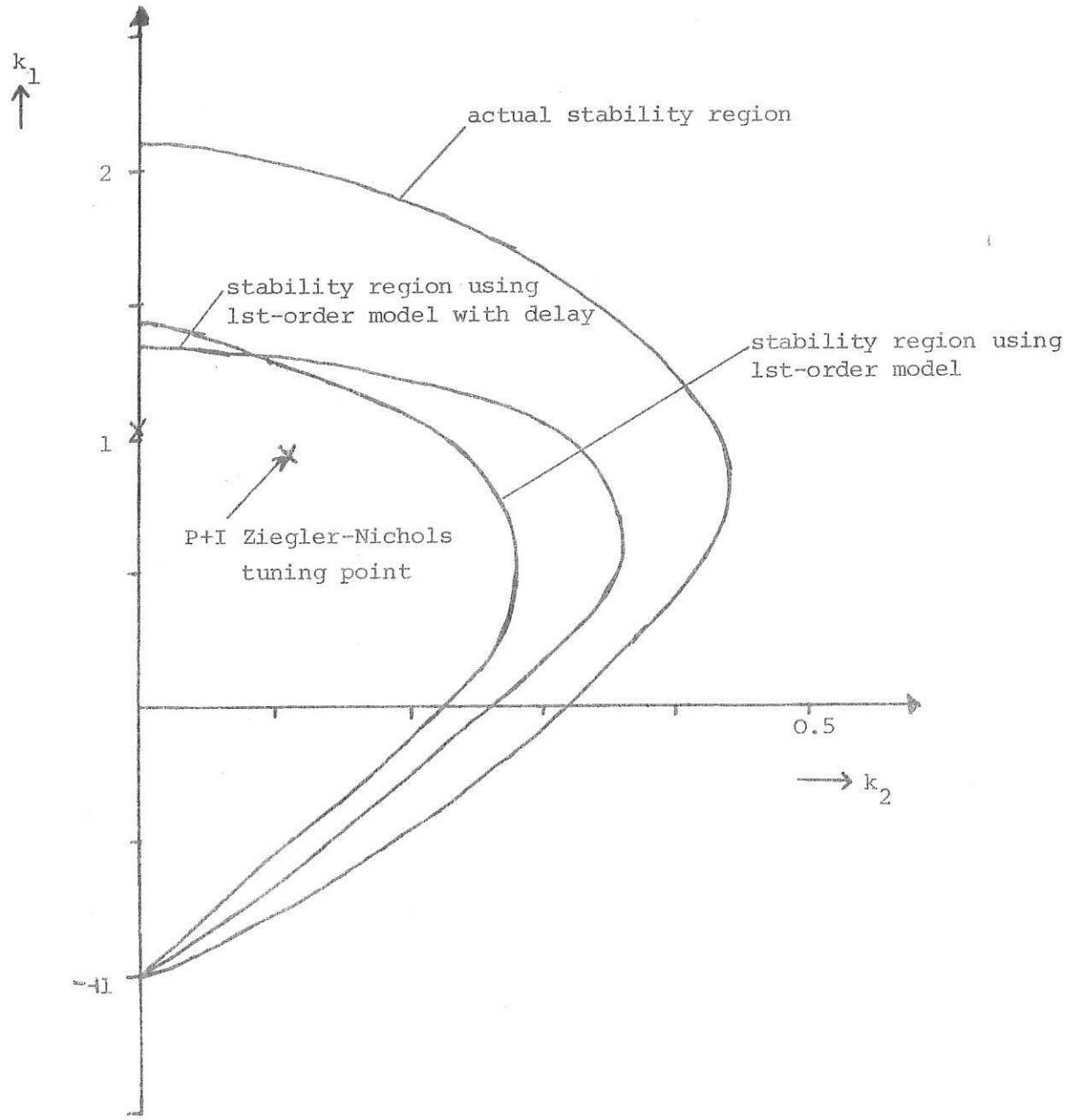
k_1
actual stability region
2
stability region using
1st-order model with delay
stability region using
1st-order model
1
P+I Ziegler-Nichols
tuning point
0.5
k_2
-1

Fig. 6.14

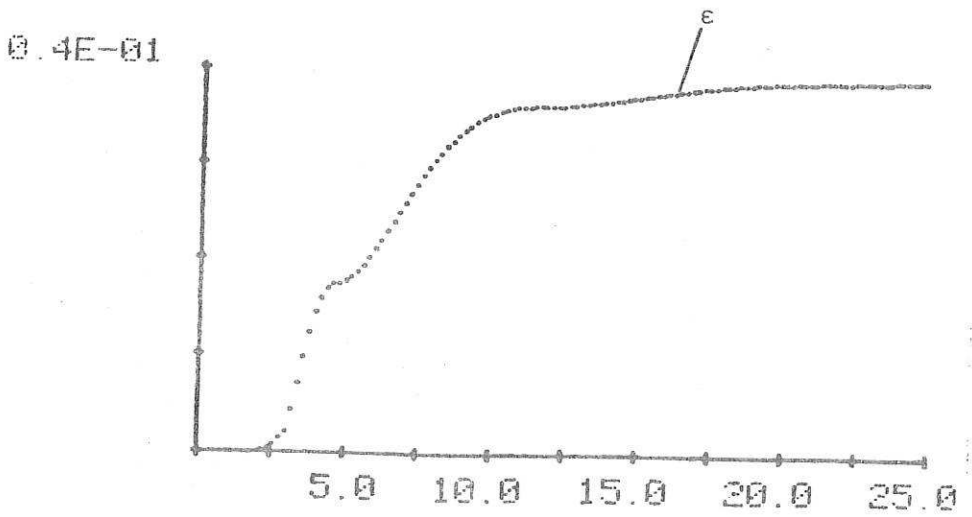

Fig. 6.15

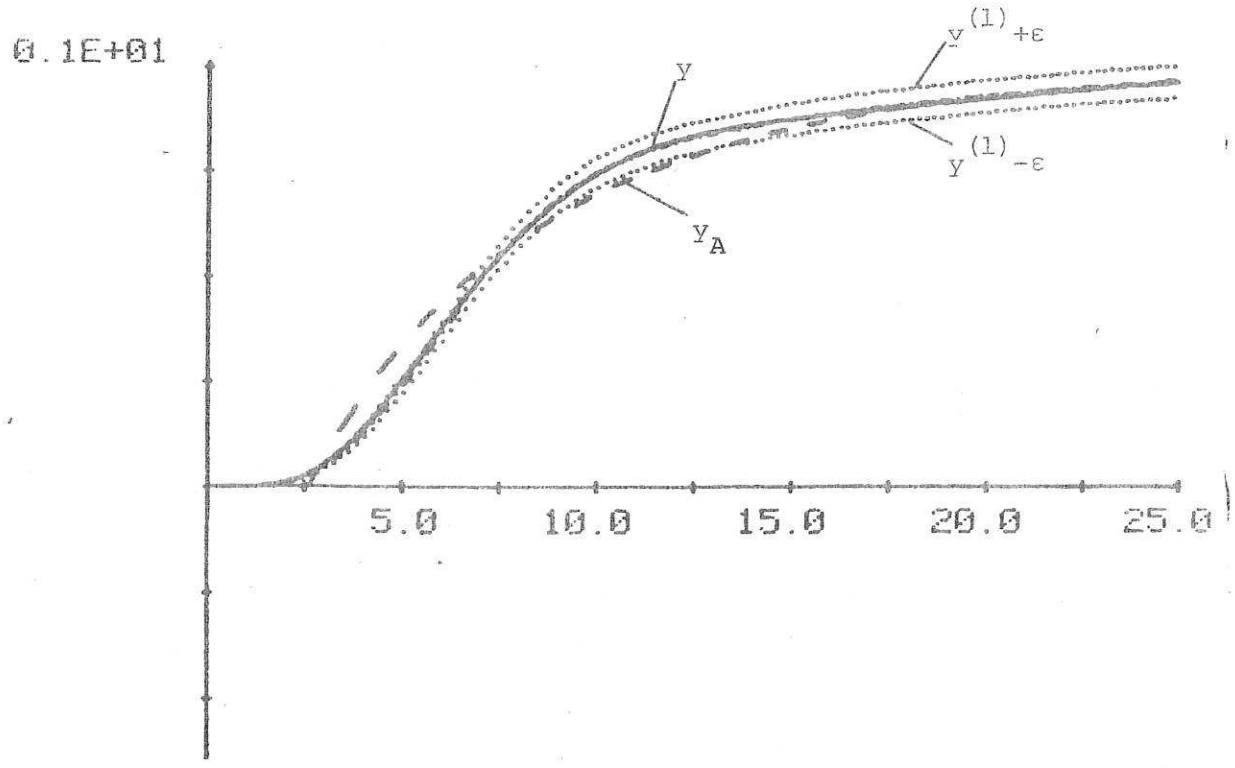

Fig. 6.16

7. EXAMPLE 3

Suppose that a single-input/single-output system has an (unknown) transfer function

$$G(s) = \frac{4}{(s^2+2s+4)(s+1)} \tag{7.1}$$

Two simple models of the form

$$\text{(a)} \quad G_A^a(s) = \frac{1}{1+1.6s} \tag{7.2}$$

and

$$\text{(b)} \quad G_A^b(s) = \frac{e^{-0.6s}}{1+s} \tag{7.3}$$

were fitted with step responses denoted by $Y_A^a(t)$ and Y_A^b respectively. (see Figs. 7.1 and 7.2). The modelling error functions $E^a(t)$ and $E^b(t)$ are shown in Fig. 7.3 and it was found that

$$N_\infty(E^a) = 0.72$$
$$N_\infty(E^b) = 0.45 \tag{7.4}$$

The stability regions deduced from the time-domain technique are illustrated in Fig. 7.4 for both models together with the stability region of the real systems, for the P+I controller of (1.5) with $F(s) = 1$. From Fig. 7.4 it is clear that both models predict the substantial part of the actual stability region.

Taking $k_1 = 1$ and $k_2 = 0.5$ in (1.5), i.e.

$$K(s) = 1.0 + \frac{0.5}{s} \tag{7.5}$$

The responses $W_A^a(t)$ and $W_A^b(t)$ are shown in Fig. 7.5 and it was noticed that

$$N_\infty(W_A^a) = 0.72$$
and $$N_\infty(W_A^b) = 0.62 \tag{7.6}$$

For both models, the performance bounds $y^{(1)} \pm \varepsilon$ together with the responses y and y_A are illustrated in Figs. 7.6 and 7.7. The maximum error bound using model (a) is 46% and for model (b) is 22%. It is important to note

that the error bounds can be reduced by decreasing gains or by using a better mode, but for this report error bounds up to 25% are acceptable, hence the model (b) yields a satisfactory design.

7.1 Design Based on Smith Predictor Scheme

Consider the above example in a Smith Predictor context. More precisely consider the scalar system with transfer function

$$T(s)G(s) = \frac{4\, e^{-s\tau}}{(s^2+2s+4)(s+1)} \quad , \quad \tau \geq 0 \tag{7.7}$$

and a simple model (Owens and Chotai, 1984, [9]) having the delay-lag structure

$$T_A(s)G_A(s) = \frac{e^{-s\tau_A}}{1+s} \quad , \tau_A = \tau + 0.6 \tag{7.8}$$

where we identify $T_A(s)$ with $e^{-s\tau_A}$. The use of the approximate model (7.8) to represent the plant (7.7) in unity feedback control has been discussed in detail in the case of $\tau = o$ by Owens and Chotai (1983) and in Section 7. We concentrate here on the general case of $\tau \geq o$ and the use of the Smith control scheme to demonstrate that the permissible errors in the Predictor scheme can be larger than the errors allowed under normal feedback conditions and to indicate the improvements in input/output performance.

The total variations of E, $N_\infty(E) = 0.45$ independent of the value of $\tau \geq o$. Considering initially the case of proportional control $K(s) = k_1$ and using the frequency-domain method it can be verified that

$$k_1 < \frac{1}{0.45} = 2.22 \tag{7.9}$$

independent of the value of $\tau \geq o$. This should be compared with the lower maximum gains of $k_1 < 1.32$ allowed (Owens and Chotai, 1984) in the standard feedback configuration in the case of $\tau = o$ and $k_1 < 0.78$ when $\tau = 3$.

Turning our attention now to the case of proportional plus integral control $K(s) = k_1 + s^{-1}k_2$.

Choosing $k_1 = 1.5$ to obtain closed-loop fine-constants of 0.4 from the approximating predictor of Fig. 3.3 and $k_2 = 1.0$ to obtain reset times of the order of 1.0, the corresponding inverse Nyquist plot is given in Fig. 7.8 and indicates stability as the (-1,0) point does not lie in or on the confidence band. This prediction is verified by the closed-loop unit step responses given in Fig. 7.9 for the cases of $\tau = o$ and $\tau = 3$.

It is known (Marshall and Salehi, 1982 [10]) that mismatch of the plant delay can benefit performance of Smith schemes. The above example also indicates that overestimation of the plant delay can have benefits in stabiiizability. To demonstrate this, let τ and τ_A now vary independently and let $\delta\tau = \tau_A - \tau$. The plots of $N_\infty(E)$ against τ_A are given in Fig. 7.10 for the cases of $\tau = o$ and $\tau = 3$ and indicates that the stability predictions are least conservative by the choice of $\delta\tau = \delta\tau^* = 0.7$ as $N_\infty(E)$ is minimized for this choice of $\delta\tau$. (overestimation of the delay improves stability characteristics independent of the length of the plant delay).

Using the time-domain technique with controller $K(s) = 1.5 + s^{-1}1.0$, the response $W_A(t)$ was computed to be as in Fig. 7.11 in the case $\tau = o$ and hence $N_\infty(W_A) = 0.595 < 1$. Note that $N_\infty(W_A)$ is independent of τ as increasing τ simply delays E and hence W_A and has no effect on the total variation. This verifies the stability predictions of Fig. 3.1 and also indicates that the time-domain approach is less conservative than the frequency domain approach and that the Smith scheme permits higher gains than the standard feedback scheme. These observations can be substantiated in a quantitative way by considering the case of proportional control $K(s) = k_1$ and plotting the contraction constants for the feedback control and Smith scheme as a function of k_1 as illustrated in Fig. 7.12. The feedback scheme permits a maximum gain of $k_1^* = 1.55$ in the case of $\tau = o$ and $k_1^* = 1.02$ when $\tau = 3$ whilst the Smith scheme permits

a maximum gain of $k_1^* = 3.35$ independent of the value of $\tau \geq o$. Choosing the P+I controller with $k_1 = 1.5$ and $k_2 = 1.0$, the deterioration in input characteristics predicted by $u_A(t)$ are obtained by evaluation of $\xi(t)$, shown in Fig. 7.13 for $\tau = o$. (The $\xi(t)$ for $\tau = 3$ is obtained as a delayed version). The error bounds on the input are represented graphically in Figs. 7.14 and 7.15 the cases of $\tau = o$ and $\tau = 3$ respectively.

The deterioration in output characteristics predicted by $y_A(t)$ are obtained by evaluation of $\eta(t)$, given in Fig. 7.16 for the cases of $\tau = o$ and $\tau = 3$. The error bounds $y^{(1)} \pm \varepsilon$, together with y and y_A are illustrated in Fig. 7.17 for the cases of $\tau = o$, and $\tau = 3$. Note that the performance predicted by the ideal Smith scheme was a reasonable indicator of the performance to be expected of the implemented scheme.

7.2 Summary and Discussion:

The above example has demonstrated the following results.

(1) We note that both models (first-order and first-order model with delay) predict the substantial part of the actual stability region. For the purpose of this report, the model (b) achieves a successful design with a maximum error bound of 22% for the controller $K(s) = 1.0 + s^{-1}0.5$.

(2) The example has again demonstrated that the time-domain approach is better than the frequency-domain in the sense that it permits higher gains to be used for a given model.

(3) For the plant (7.7) with model (7.8), the Smith Predictor scheme gives much better performance than the standard feedback scheme and also increases the stability margin in the sense that it permits higher control gains to be used. Also note that stability region is independent of the value of delays $\tau \geq o$ for the Smith control scheme but for normal feedback the stability region decrease as the value of τ increases.

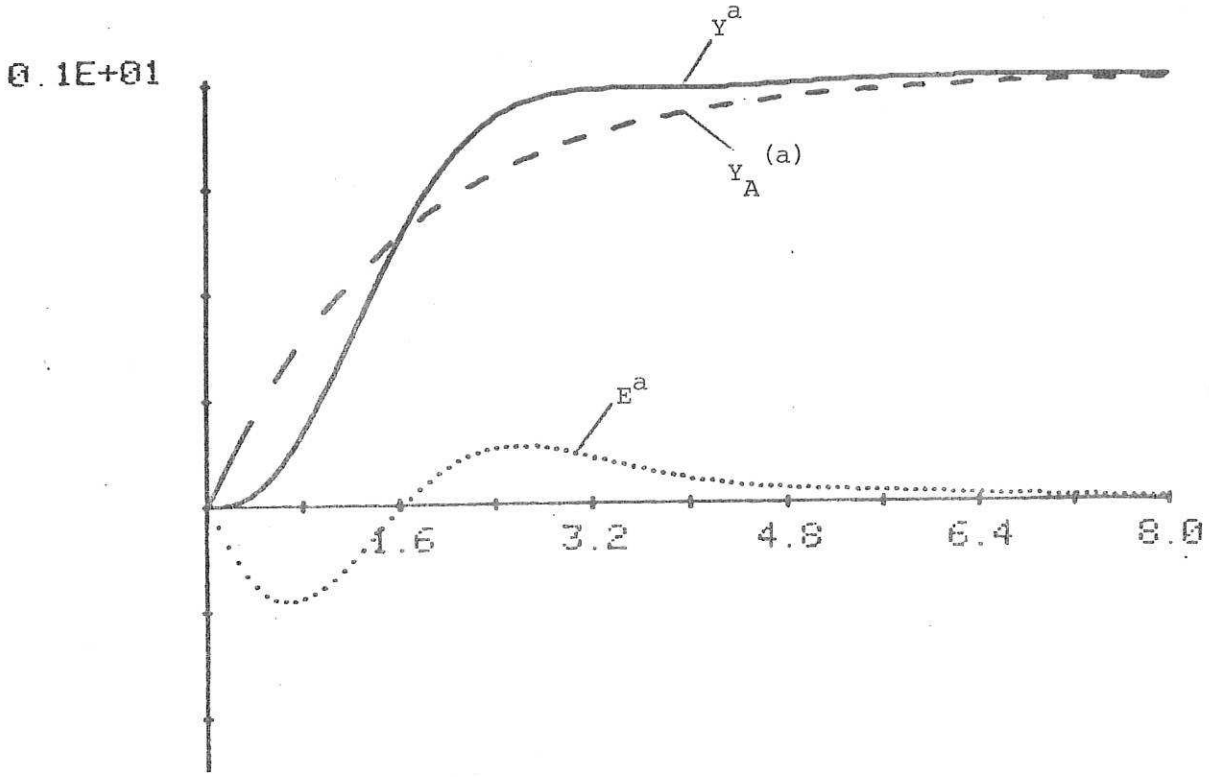

Fig. 7.1

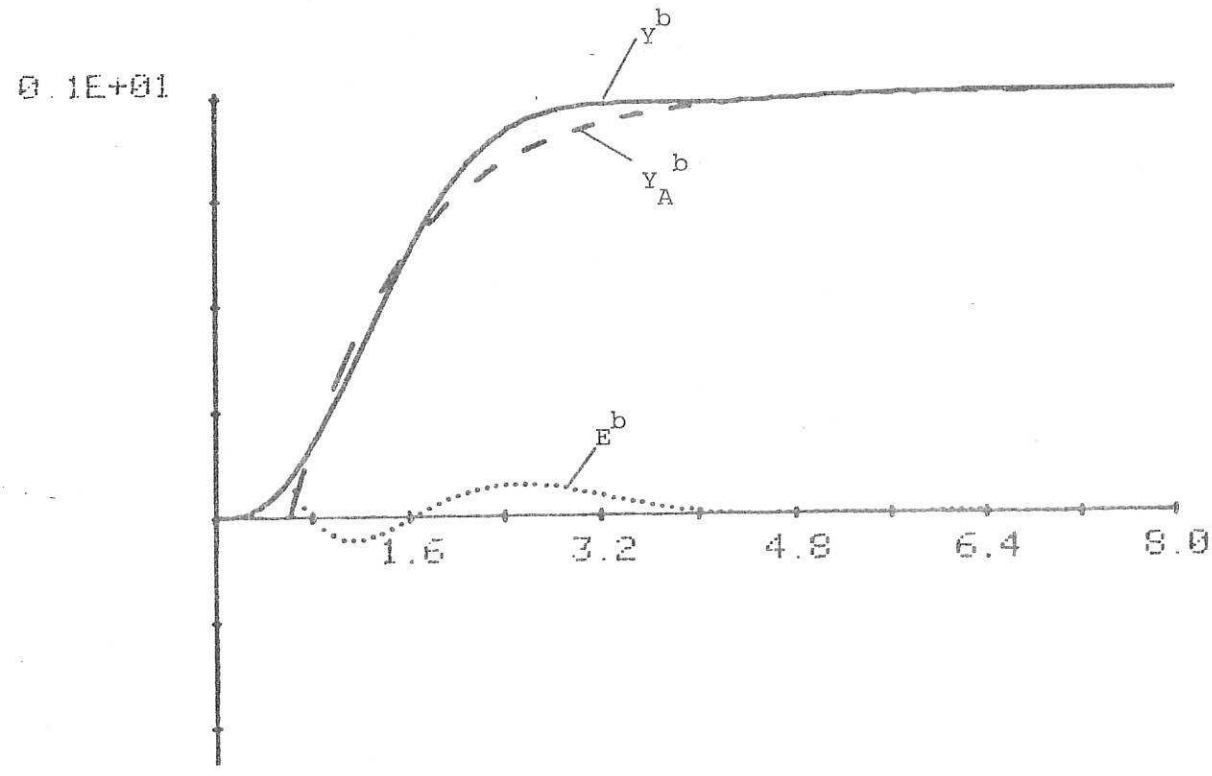

Fig. 7.2

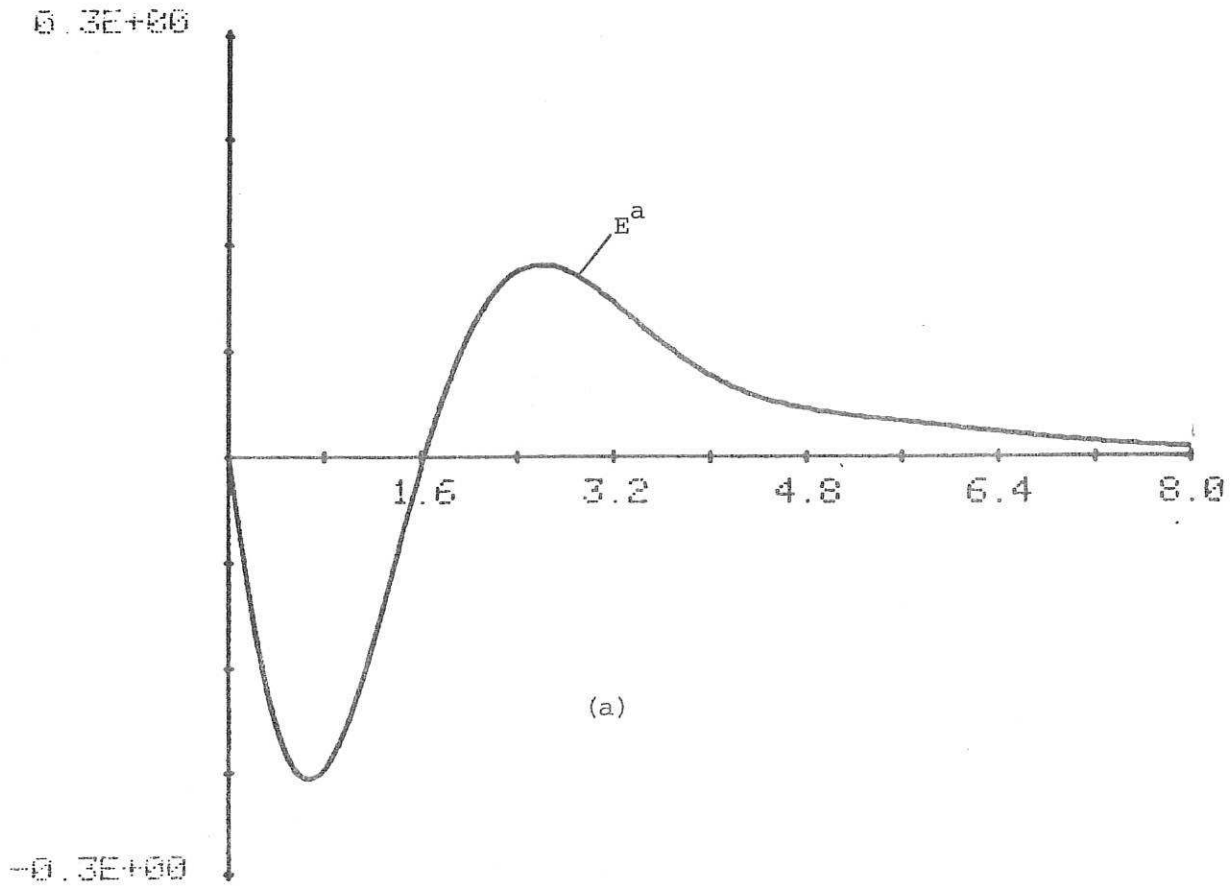

(a)

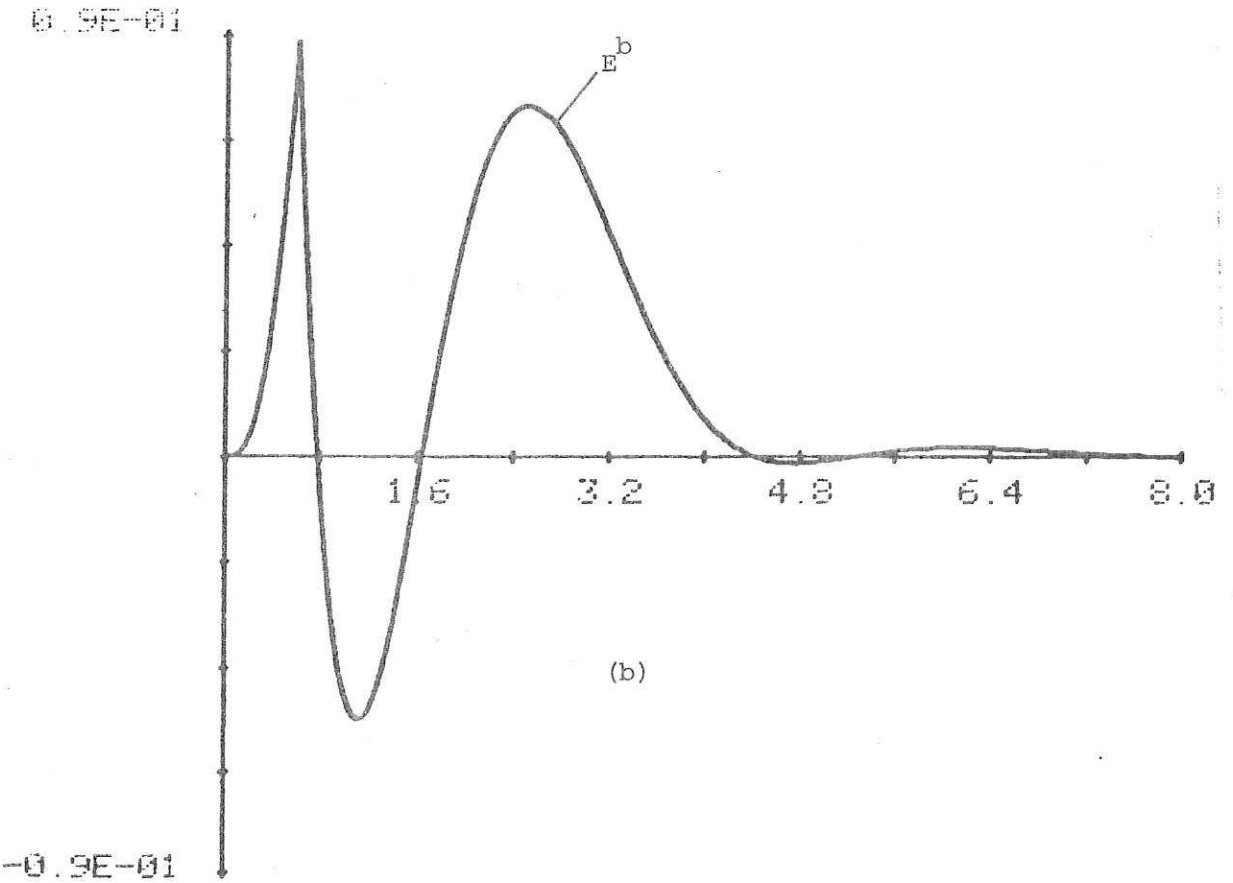

(b)

Fig. 7.3

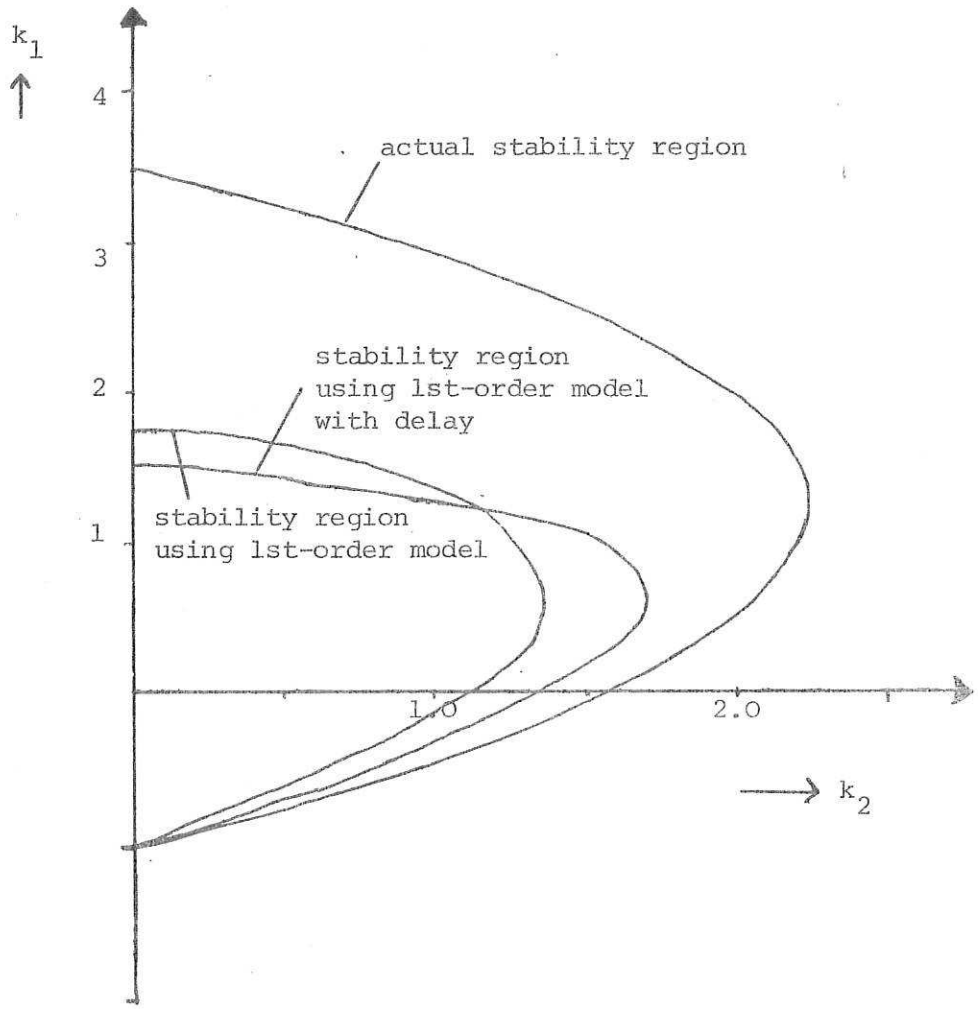
k_1
4
3
2
1
actual stability region
stability region
using lst-order model
with delay
stability region
using lst-order model
1.0
2.0
k_2

Fig. 7.4

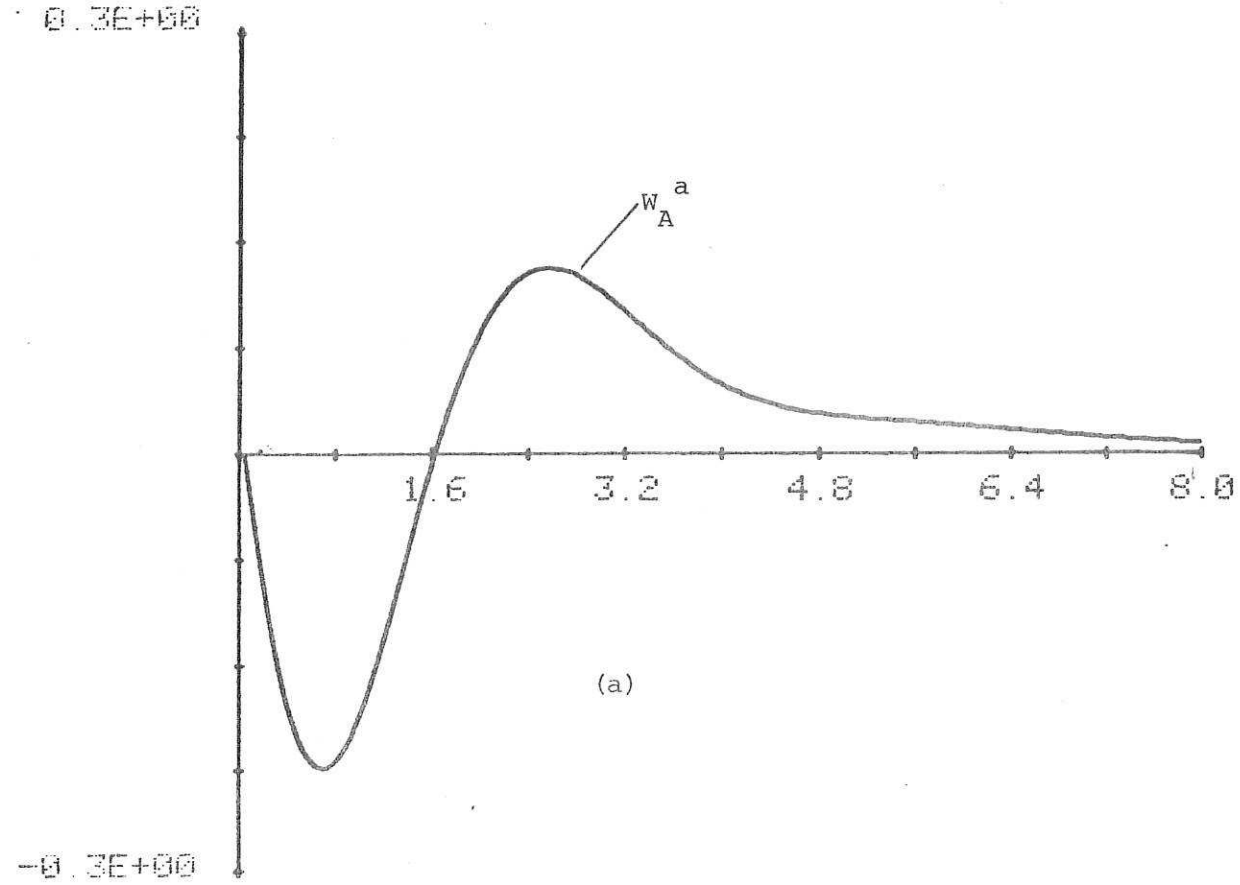

(a)

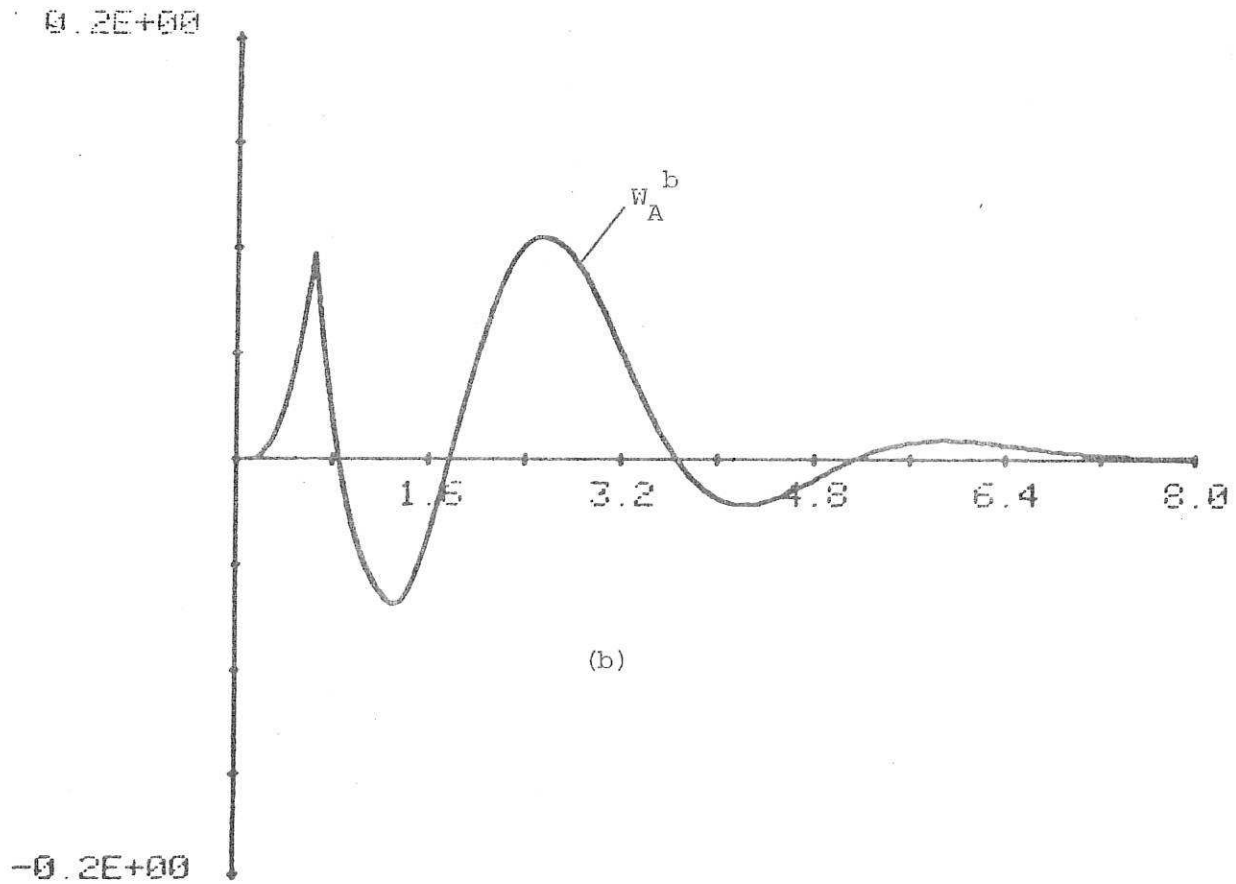

(b)

Fig. 7.5

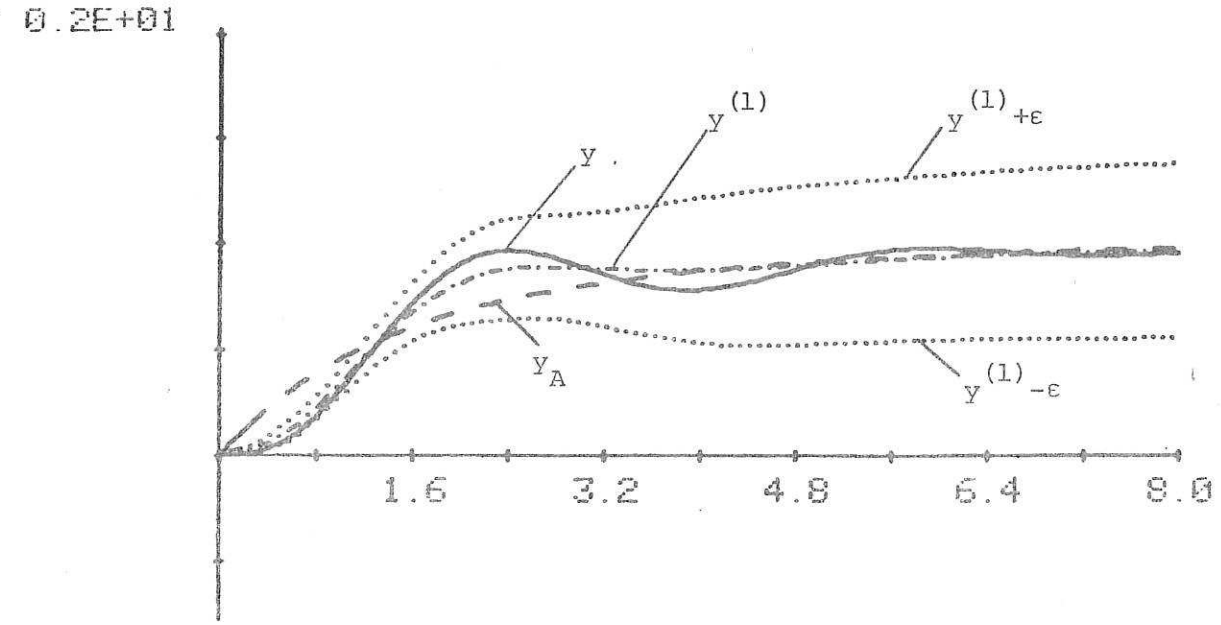
0.2E+01
y
y(1)
y(1)+ε
yA
y(1)-ε
1.6
3.2
4.8
6.4
8.0

Fig. 7.6

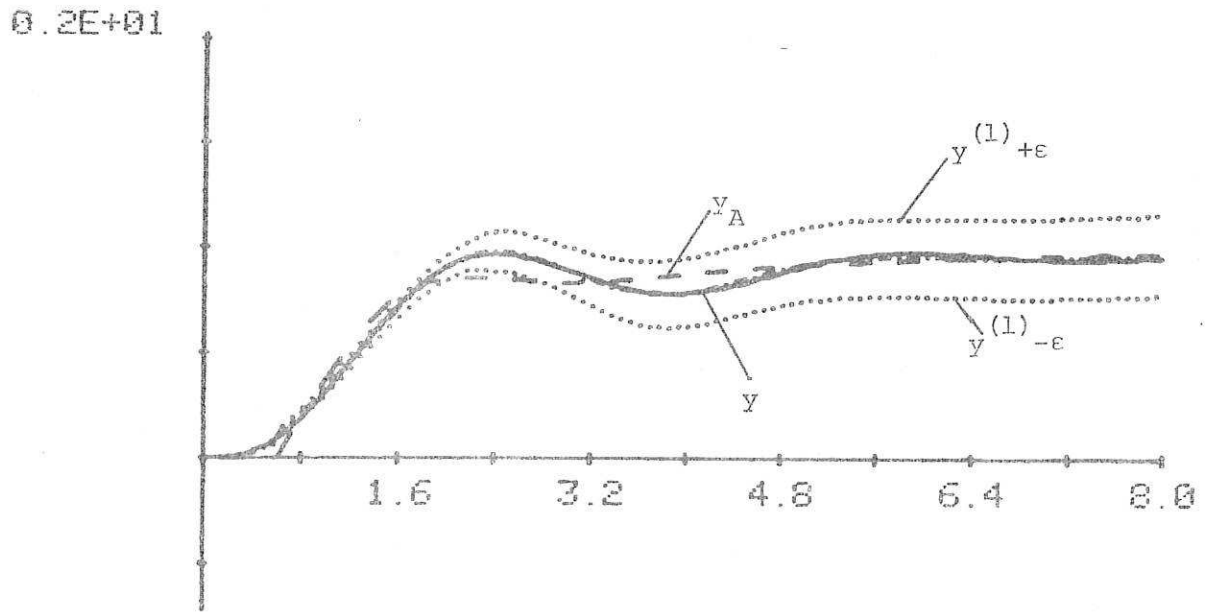
0.2E+01
y(1)+ε
yA
y(1)-ε
y
1.6
3.2
4.8
6.4
8.0

Fig. 7.7

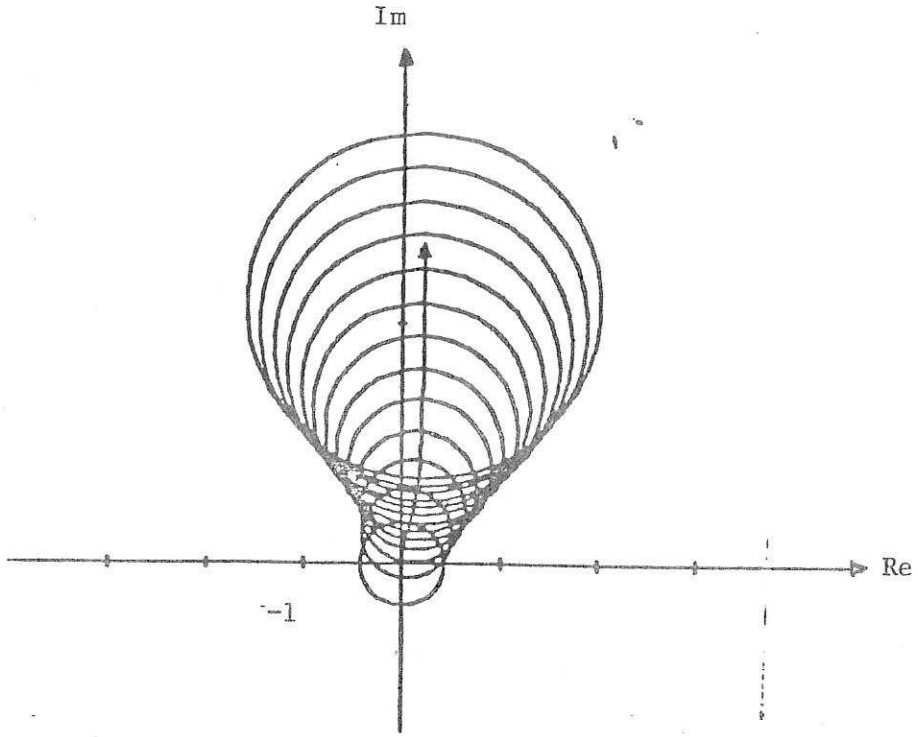

Fig. 7.8

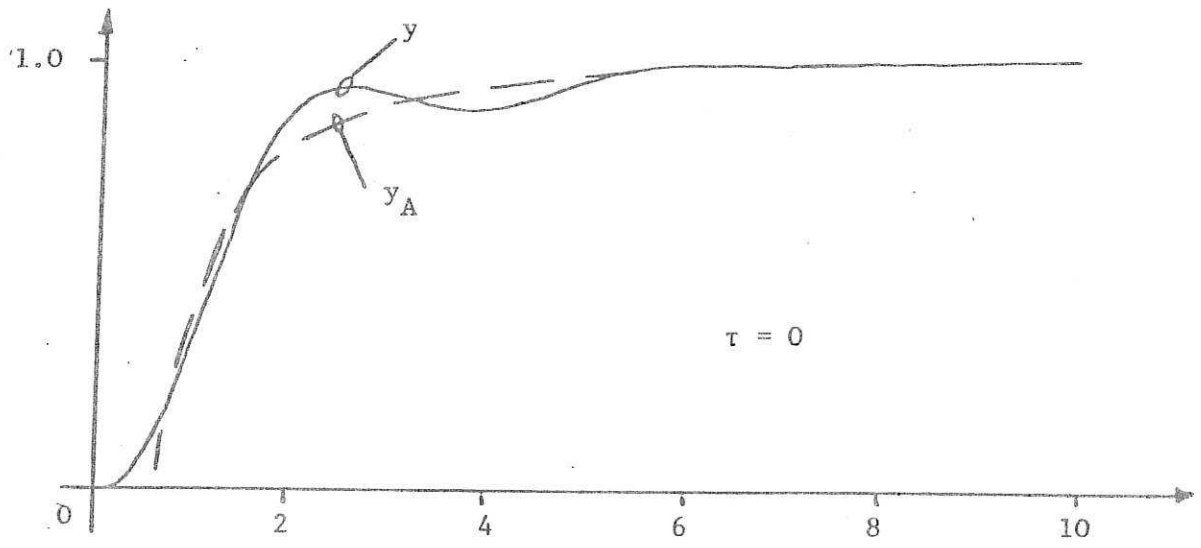

Fig. 7.9 (a)

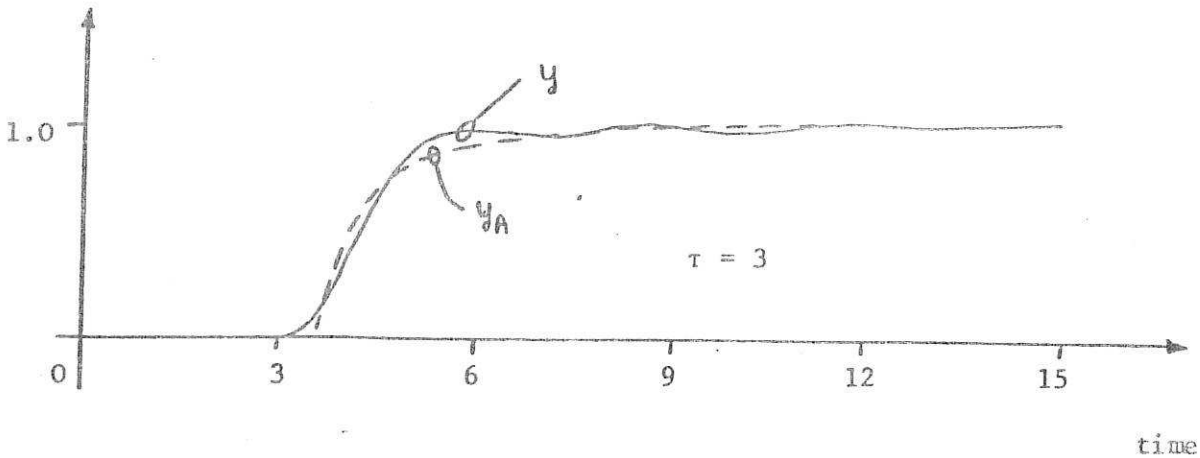

Fig. 7.9 (b)

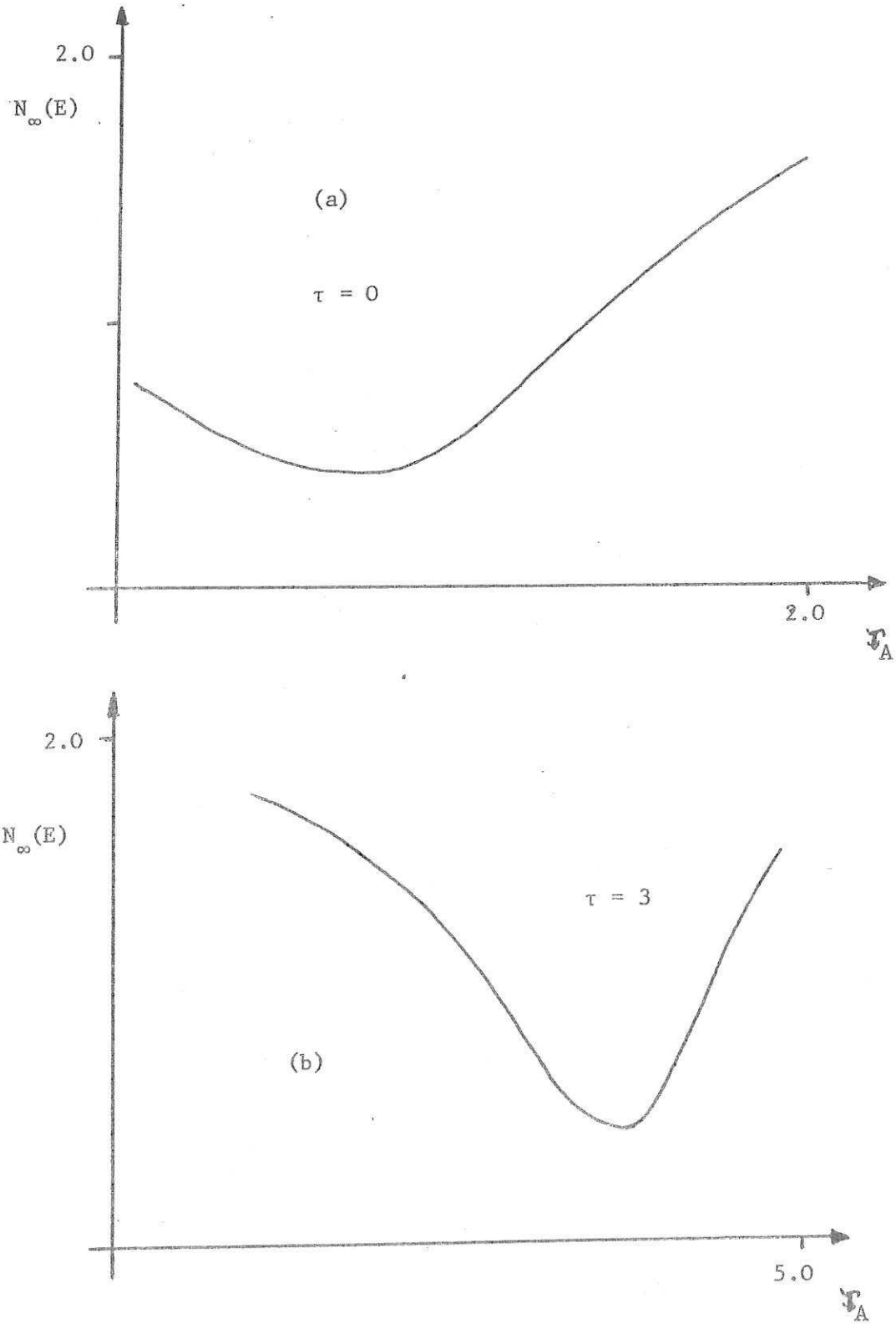
2.0
$N_\infty(E)$
(a)
$\tau = 0$
2.0
$\mathcal{E}_A$
2.0
$N_\infty(E)$
$\tau = 3$
(b)
5.0
$\mathcal{E}_A$

Fig. 7.10

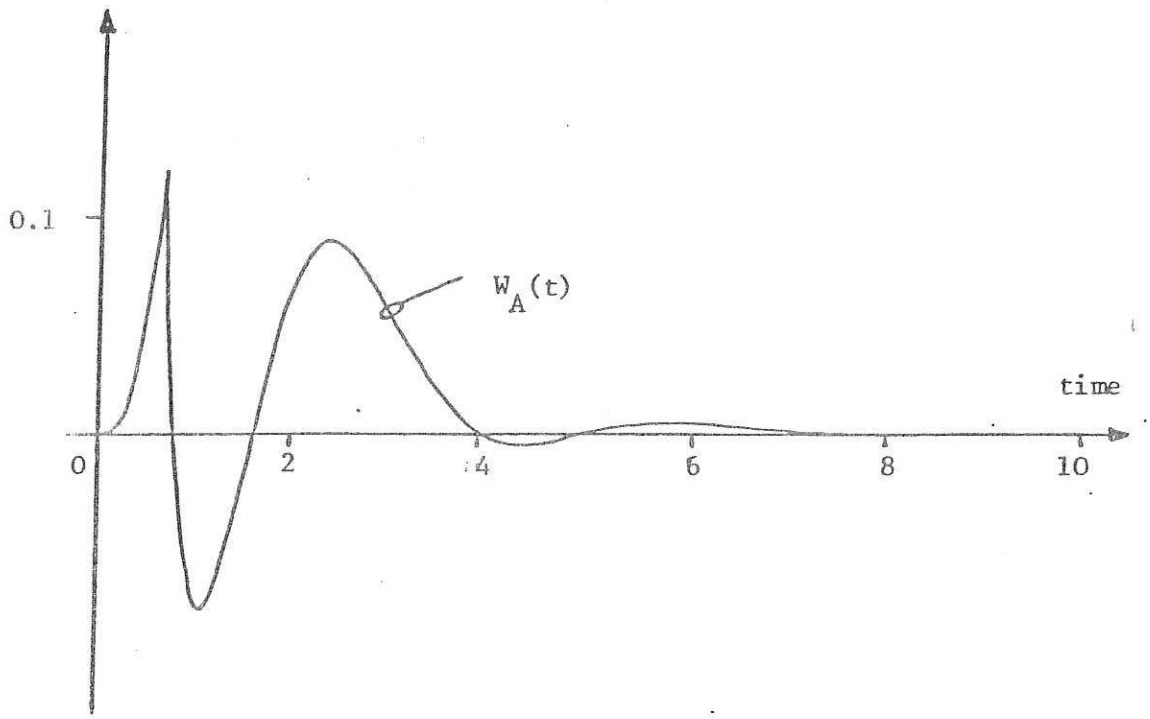

Fig. 7.11

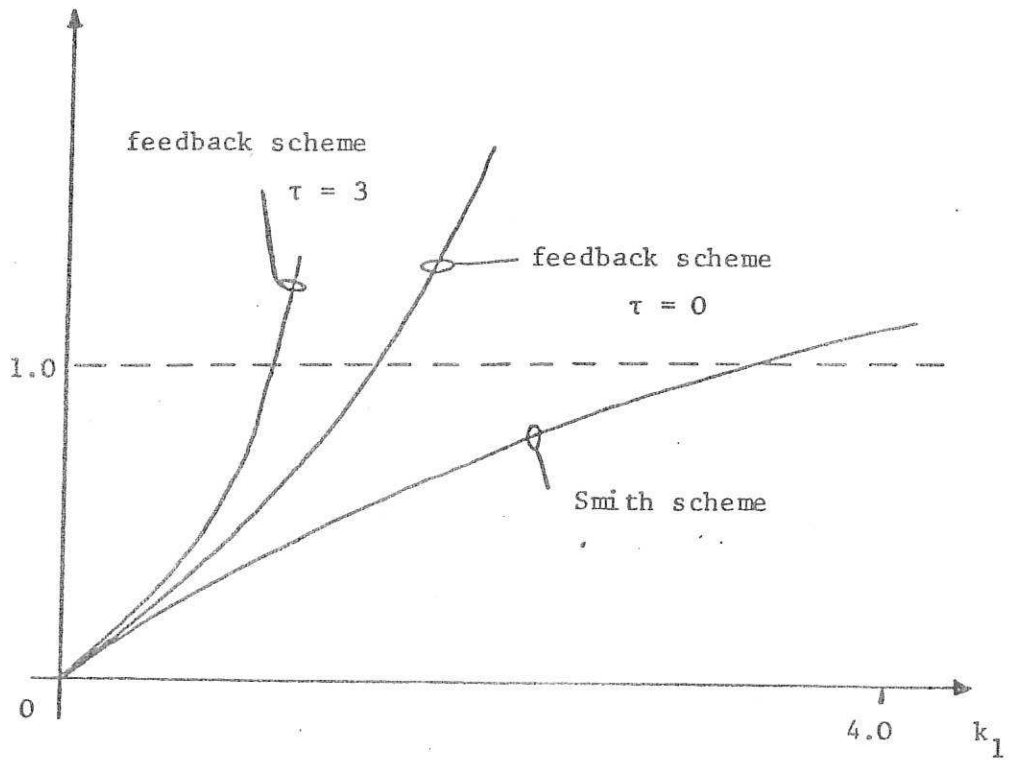

Fig. 7.12

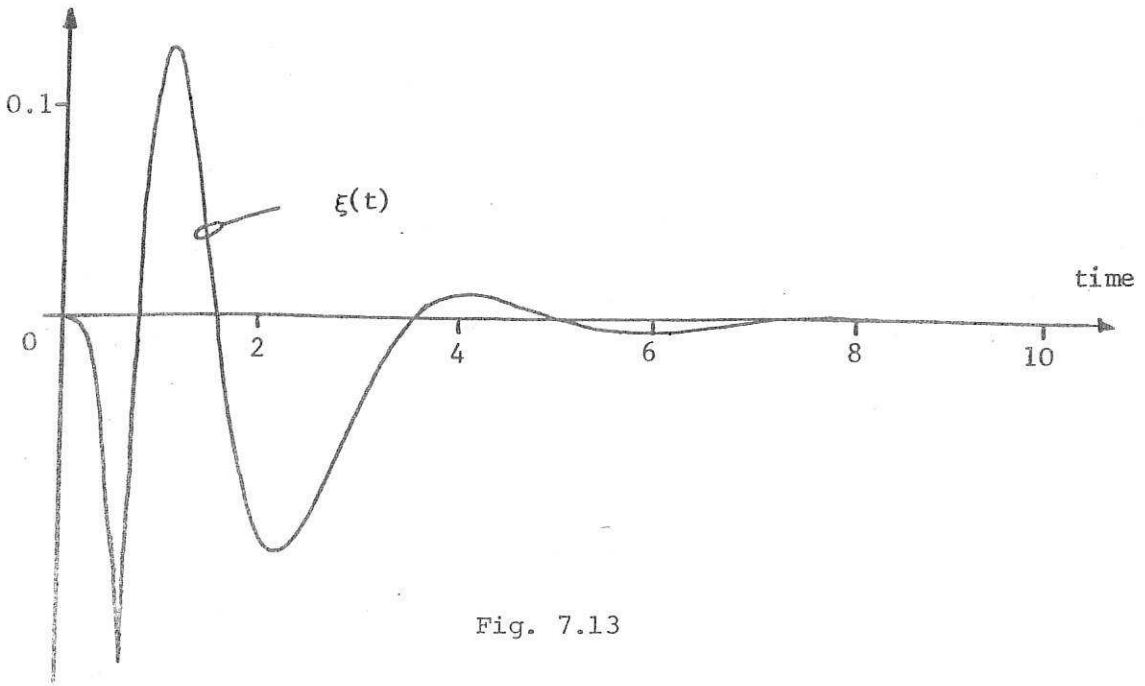

Fig. 7.13

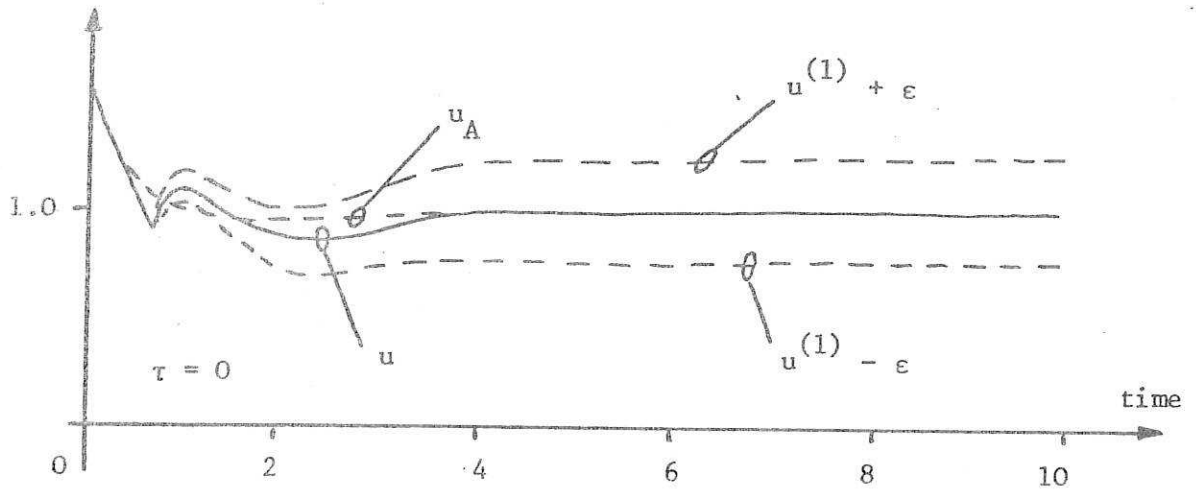

Fig. 7.14

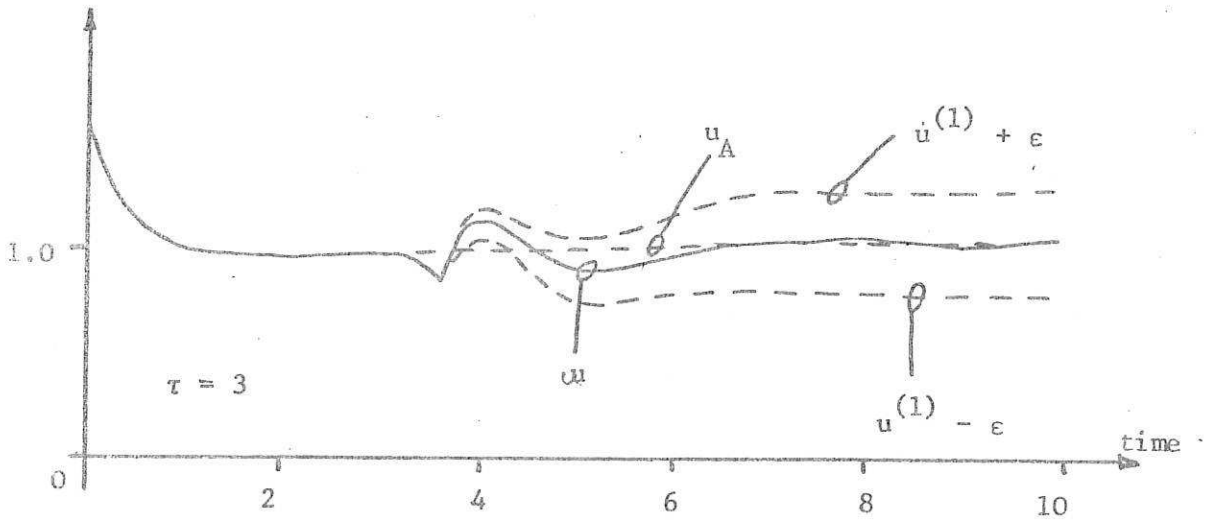

Fig. 7.15

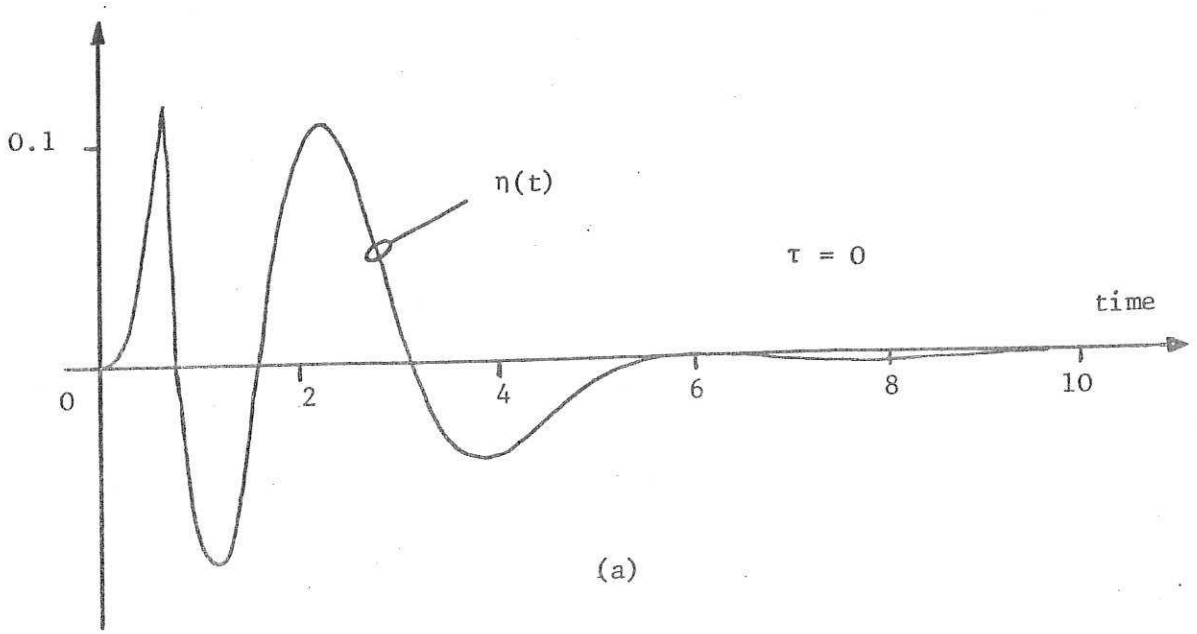

(a)

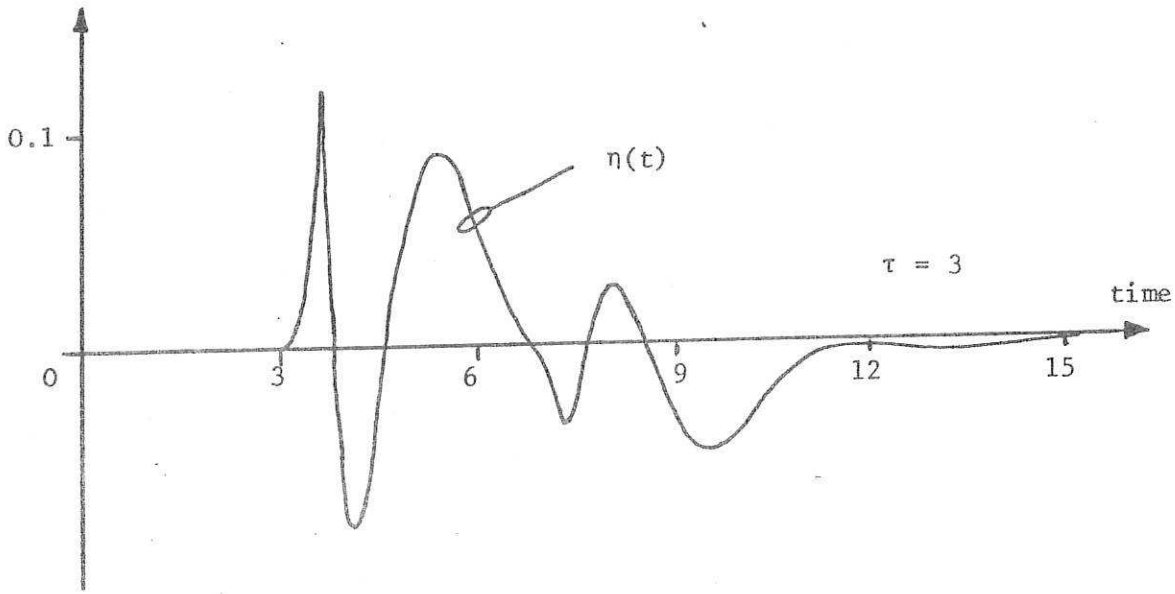

(b)

Fig. 7.16

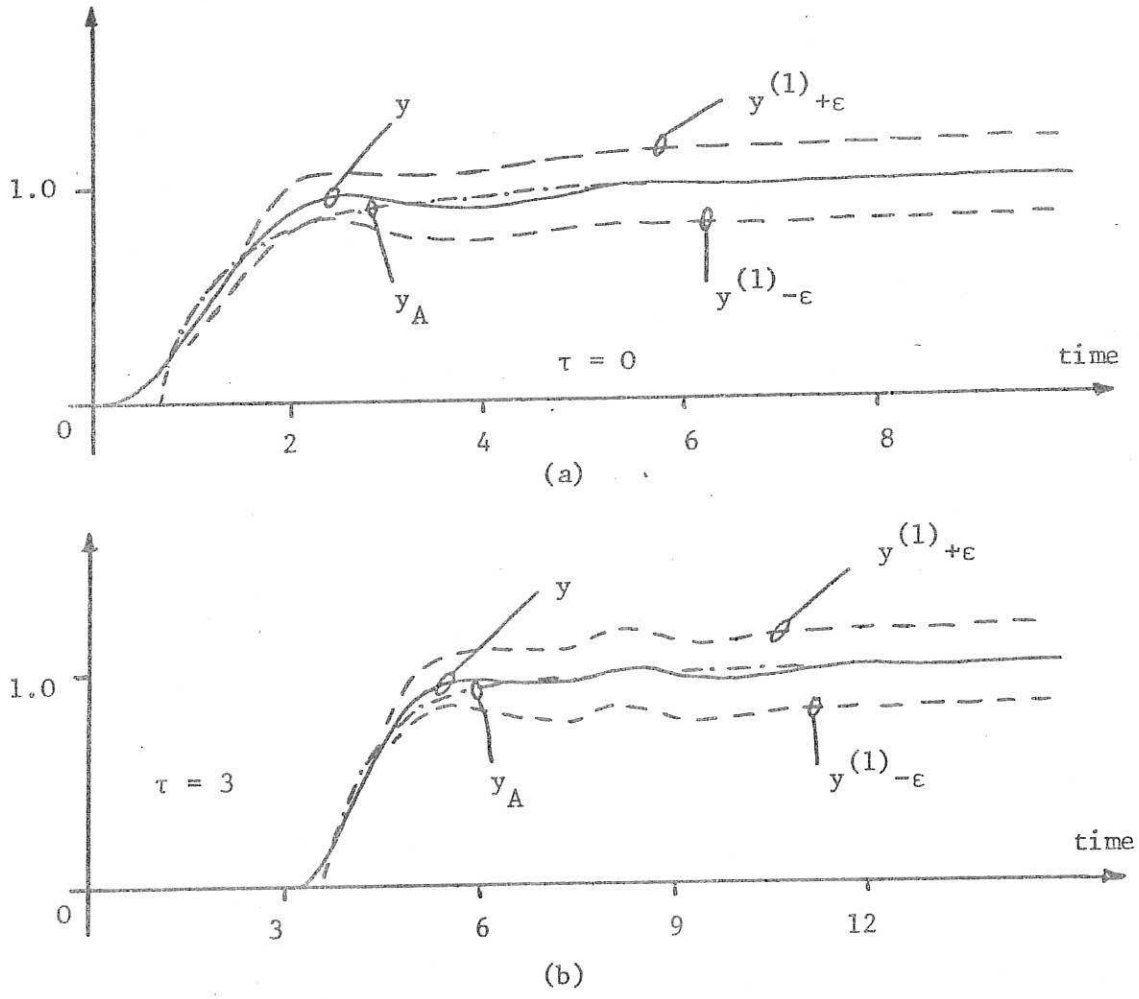
y
$y^{(1)}_{+\varepsilon}$
1.0
y_A
$y^{(1)}_{-\varepsilon}$
τ = 0
time
0
2
4
6
8
(a)
$y^{(1)}_{+\varepsilon}$
y
1.0
τ = 3
y_A
$y^{(1)}_{-\varepsilon}$
time
0
3
6
9
12
(b)

Fig. 7.17

8. EXAMPLE 4

Consider a plant with transfer function

$$G(s) = \frac{3}{3s^5 + 16s^4 + 31s^3 + 26s^2 + 9s + 3} \qquad (8.1)$$

with step response Y shown in Fig. 8.1. Using the technique of Section 4.2, the delay-lag model of the form

$$G_A(s) = \frac{e^{-1.2s}}{1 + 3.6s} \qquad (8.2)$$

was fitted, with step response Y_A again shown in Fig. 8.1 and the error E(t) shown in Fig. 8.2. The total variation $N_\infty(E)$ was found to be 1.73. Using the frequency domain technique and a P+I controller $K(s) = k_1 + s^{-1}k_2$ with $k_2 \neq 0$, $F(s) = 1$ and $\Delta(s) = N_\infty(E)$, the required inequality,

$$\left|1 + (G_A(s)K(s))^{-1}\right| > \left|G_A^{-1}(s)\right| \Delta(s) = \left|G_A^{-1}(s)\right| N_\infty(E) \qquad (8.3)$$

cannot be satisfied as $G_A(o) = 1$ and $N_\infty(E) = 1.73$. We conclude from this analysis that the delay-lag model of (8.2) is not accurate enough to provide a basis for the design of integral controllers using the frequency domain technique and the error bound $\Delta(s) = N_\infty(E)$. Clearly, to use integral actions using the same model we either need to find a better $\Delta(s)$ or use the time-domain technique.

Using the time-domain method with $k_1 = 0.25$ and $k_2 = 0.12$, the function $W_A(t)$ was computed to be as in Fig. 8.3 and graphical analysis of this function leads to the conclusion that $N_\infty(W_A) = 0.75 < 1$, hence verifying the stability prediction. The error bounds $y^{(1)} \pm \varepsilon$ together with y and y_A are illustrated in Fig. 8.4. From this figure it is clear that the error bounds are too large (with a maximum of 80% error) and a more accurate model G_A is required for the system of (8.1) if performance predictions are to be useful.

Using the technique of section 4.3, the second-order model of the form

$$G_A(s) = \frac{0.1225}{s^2 + 0.222 + 0.1225} \qquad (8.3)$$

was fitted to the system of (8.1). The step responses Y and Y_A are shown in Fig. 8.5 and the error E(t) shown in Fig. 8.6. The total variation $N_\omega(E)$ was found to be 0.92. Using the same controller as before (i.e. $K(s) = 0.25 + s^{-1}0.12$), the inverse Nyquist plot of $G_AKF = G_AK$ with superimposed confidence circles shown in Fig. 8.7 indicates that the (-1,0) point does not be in or on the confidence band. Stability of real plant is hence guaranteed provided that the controllability and observability condition is satisfied and this is so for the above plant.

Finally, the closed-loop responses of the real and the approximate feedback schemes are shown in Fig. 8.8.

The function $W_A(t)$ for the above example is shown in Fig. 8.9 and it was found that $N_\infty(W_A) = 0.44 < 1$, hence verifying the stability predictions for the real plant. The correction term $\eta(t)$ is shown in Fig. 8.10 and the errorbound $\varepsilon(t)$ is shown in Fig. 8.11. The bounds $y^{(1)} \pm \varepsilon$, together with y and y_A, are illustrated in Fig. 8.12.

8.1 Summary and Discussion

We make the following observation from the above example.

(1) When the total variation $N_\infty(E)$ is greater than the steady-state value of the real plant, the chosen model is not accurate enought to provide a basis for the design of integral controllers using the frequency-domain method with $\Delta(s) = N_\infty(E)$.

(2) For non-monotonic stable systems, the first-order or first-order with delay model may not be accurate enough to achieve a successful design for the real system and higher order models must be used.

(3) The delay-lag model for the system of (8.1), (non-monotonic) verifies the stability prediction for the controller $K(s) = 0.25 + s^{-1}0.12$

using the time-domain method. However, it gives large performance error bounds, (maximum of 80% error), which are not regarded as acceptable.

(4) The second-order model verifies the stability predictions for the controller $K(s) = 0.25 + s^{-1}0.12$ using both the time-domain and the frequency-domain techniques. The performance error bounds obtained are small with a maximum error of 10% only.

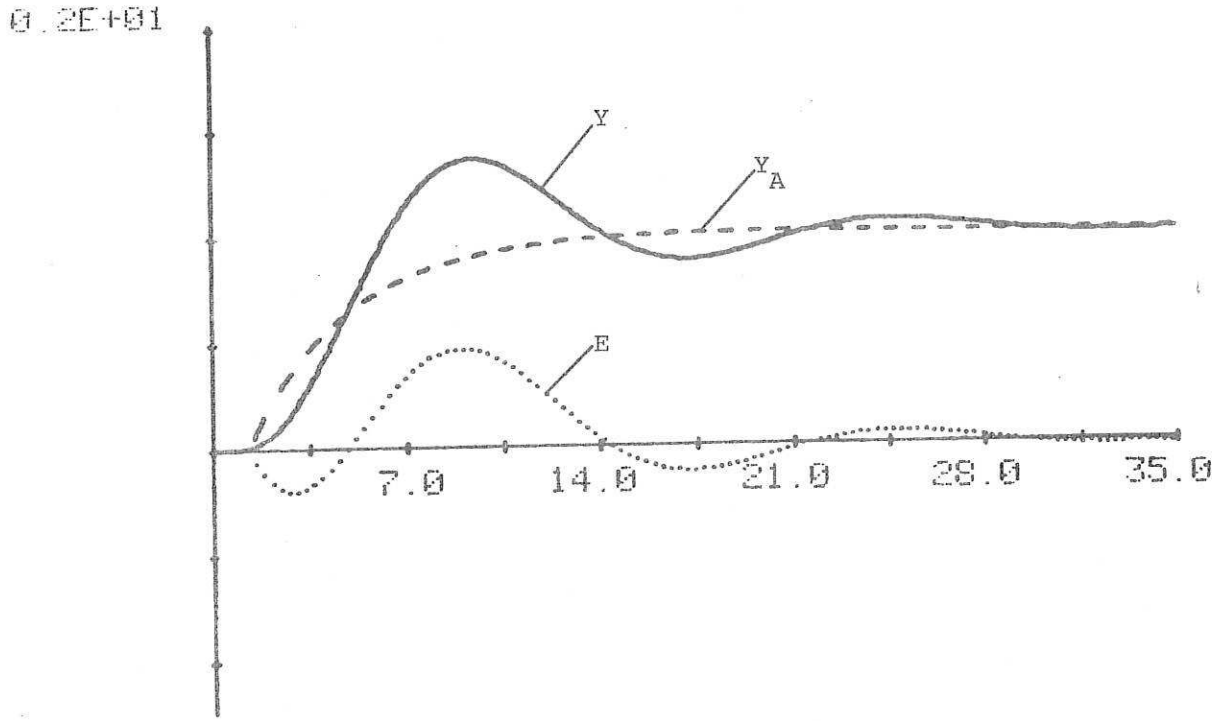

Fig. 8.1

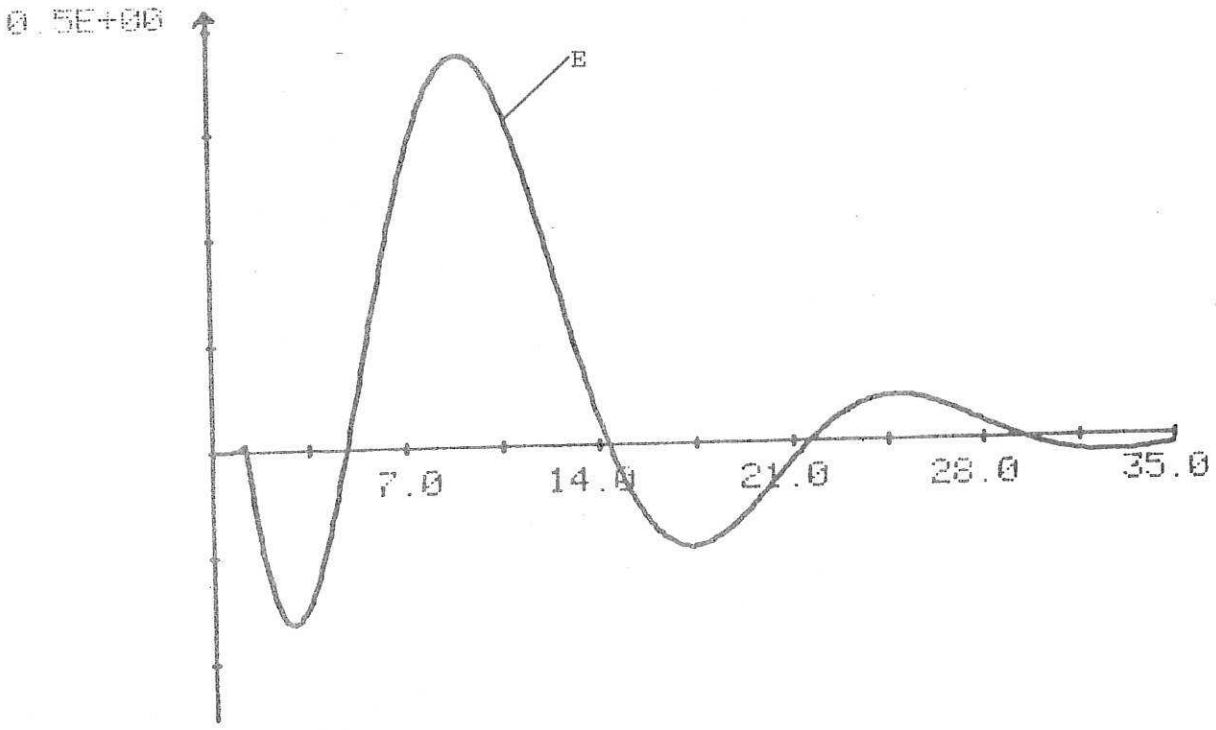

Fig. 8.2

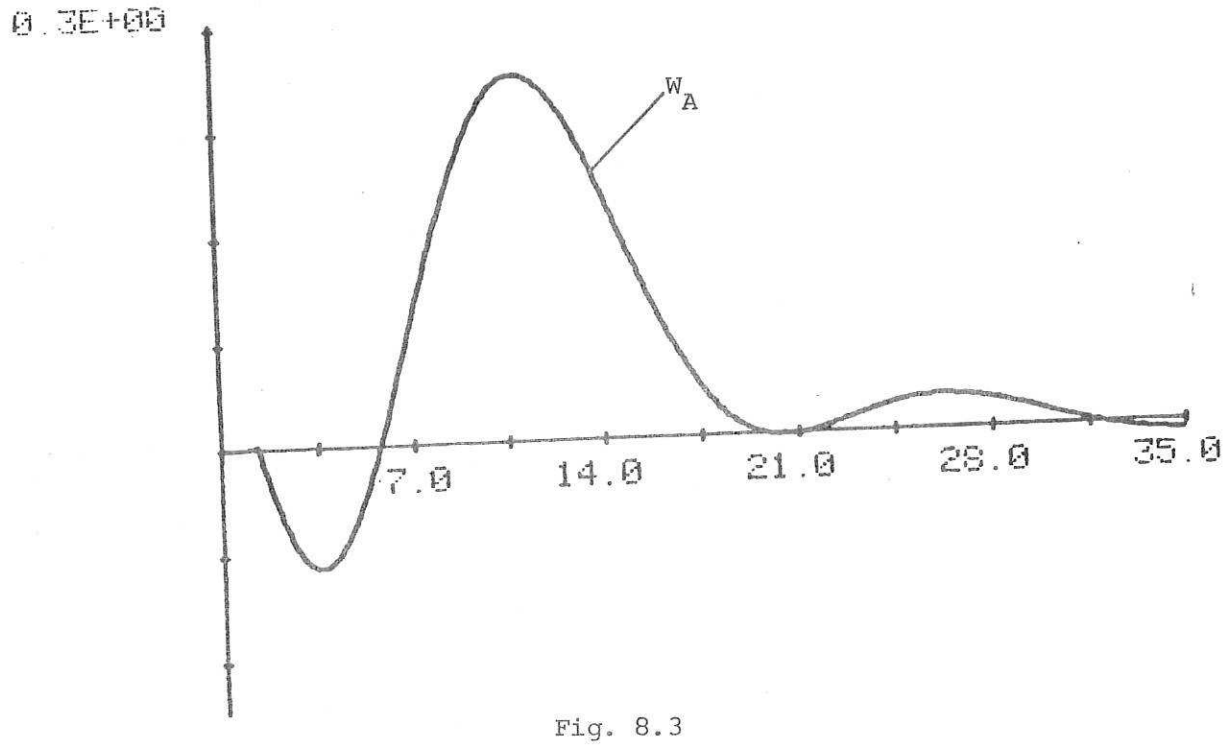
0.3E+00
W_A
7.0
14.0
21.0
28.0
35.0

Fig. 8.3

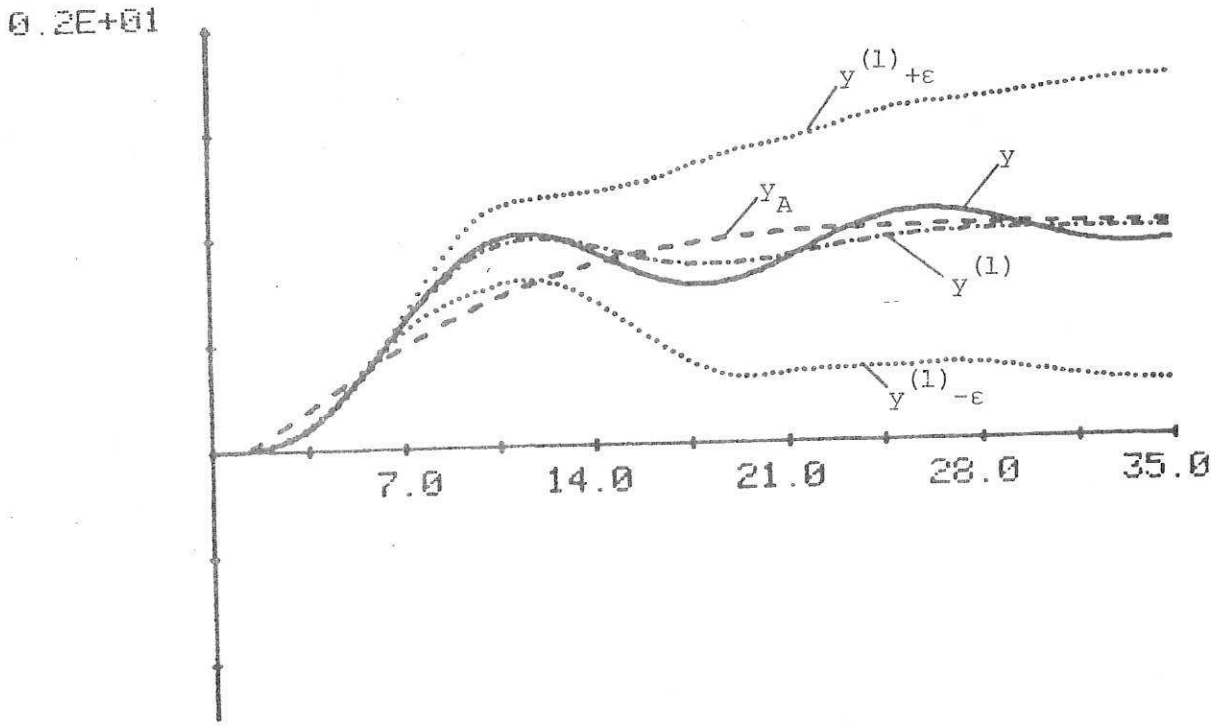
0.2E+01
$y^{(1)}+\varepsilon$
y
y_A
$y^{(1)}$
$y^{(1)}-\varepsilon$
7.0
14.0
21.0
28.0
35.0

Fig. 8.4

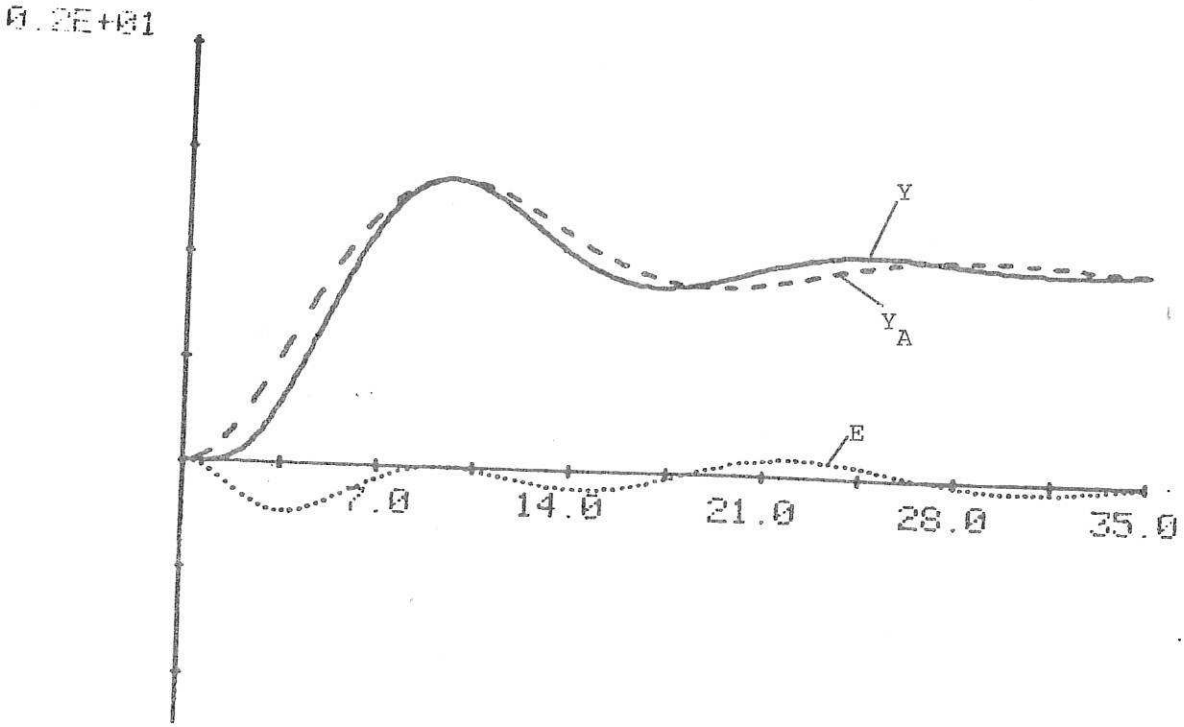

Fig. 8.5

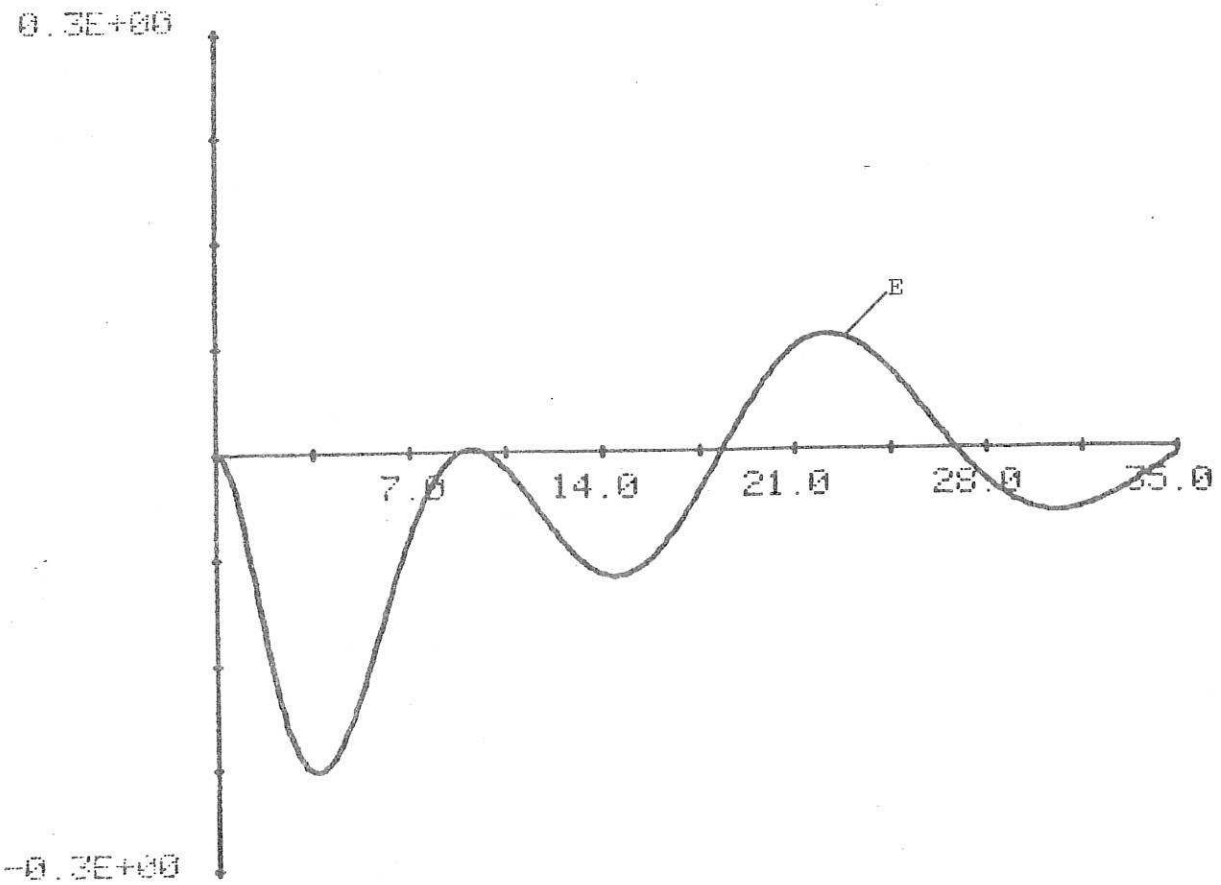

Fig. 8.6

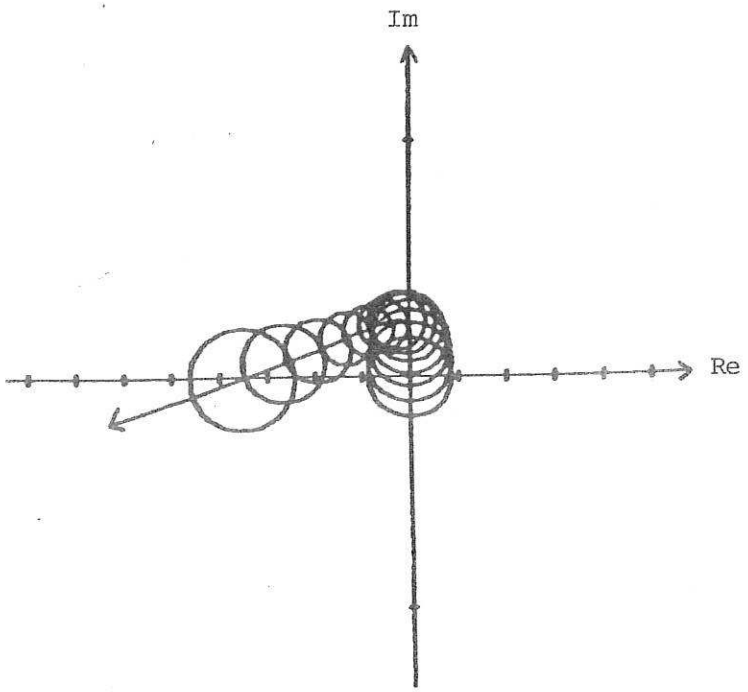

Fig. 8.7

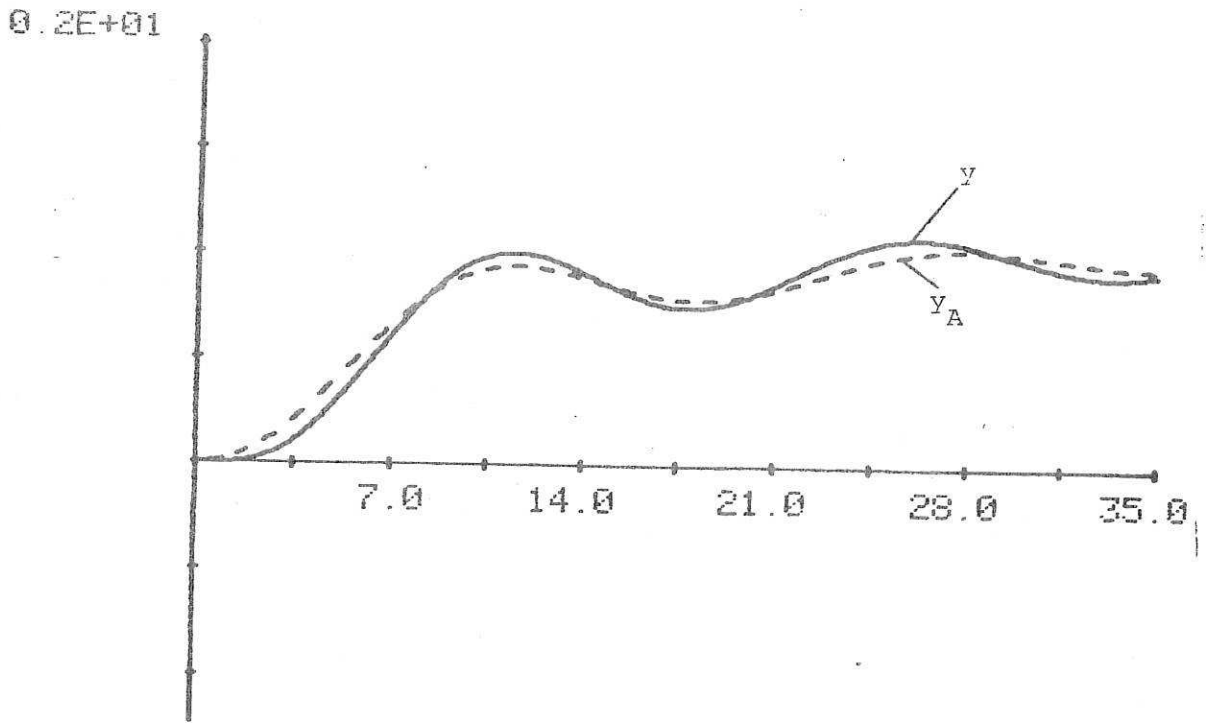

Fig. 8.8

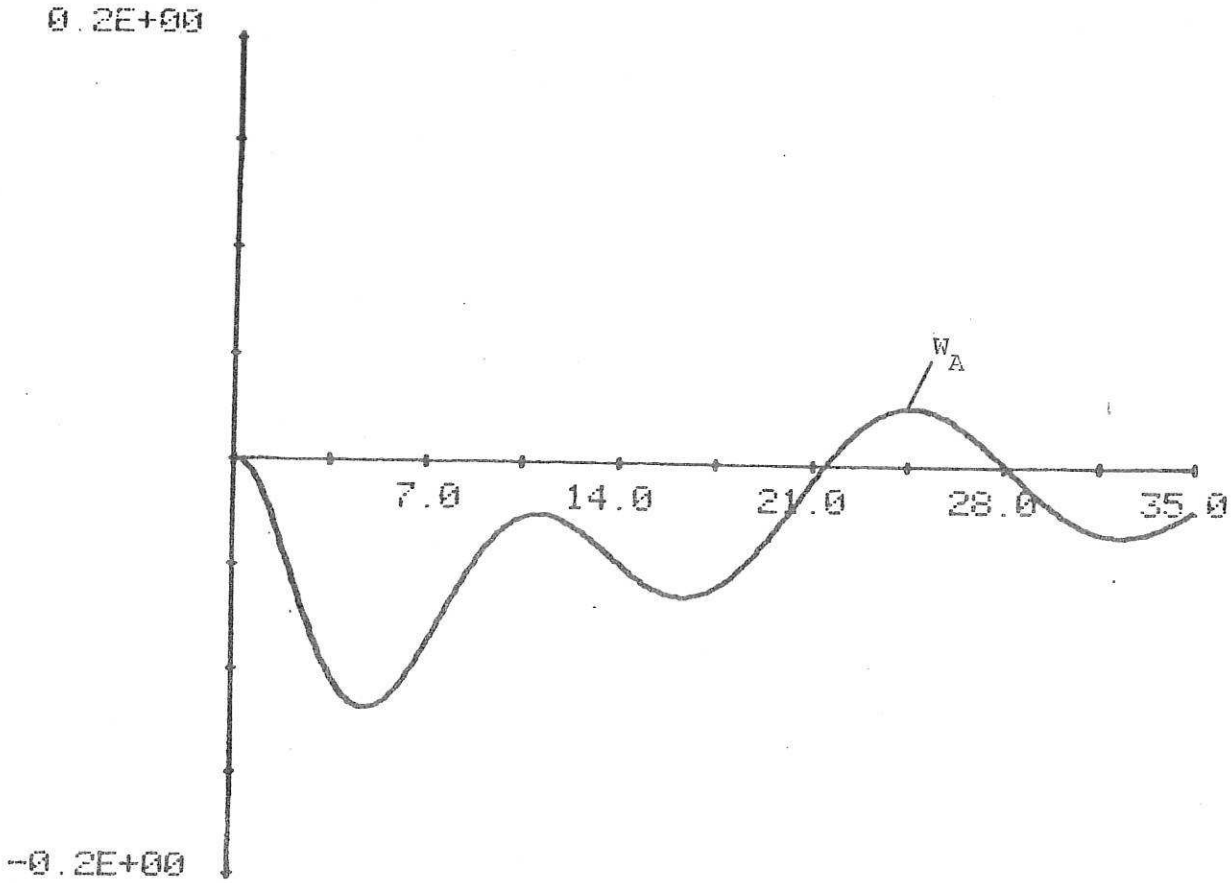

Fig. 8.9

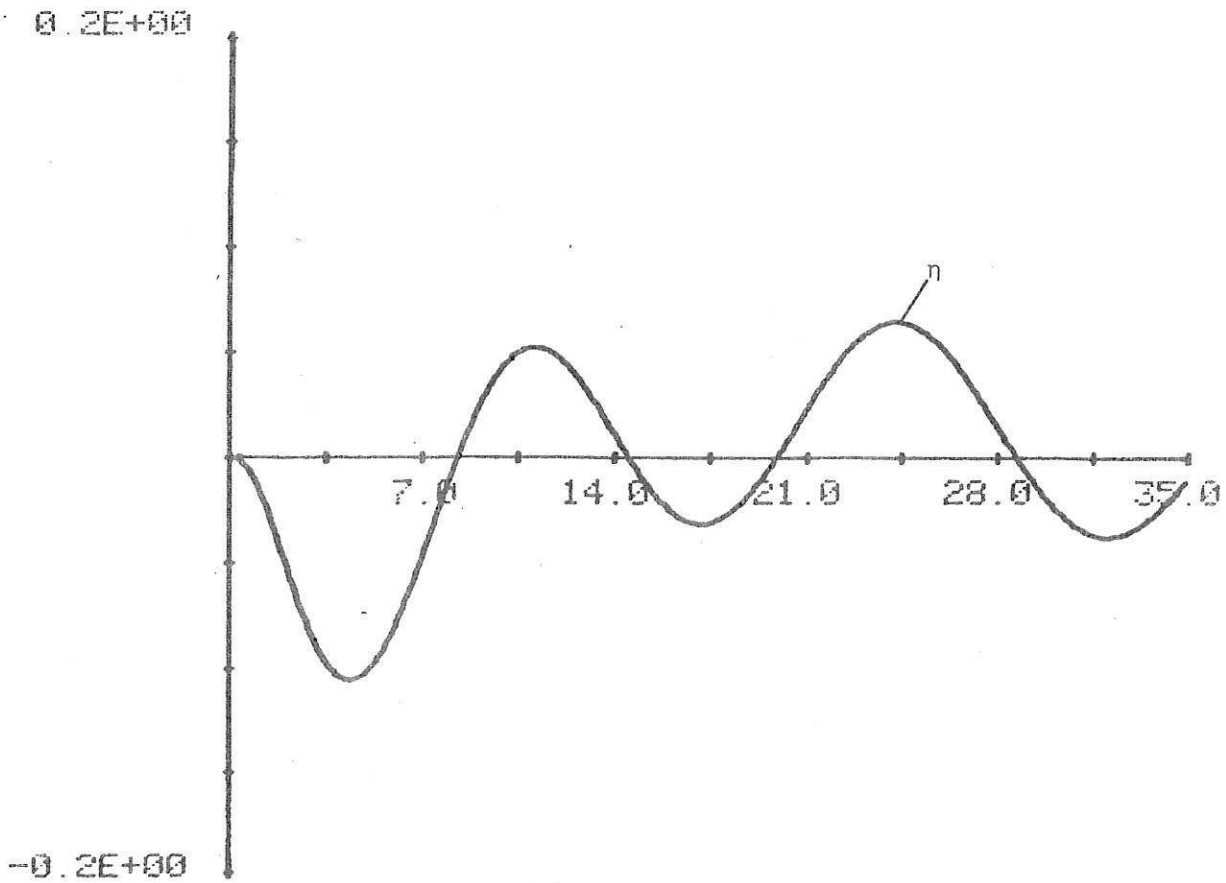

Fig. 8.10

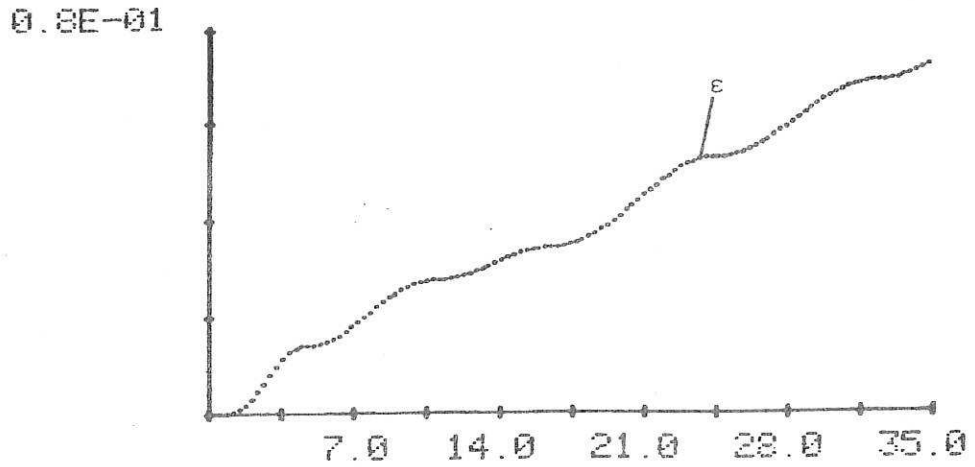

Fig. 8.11

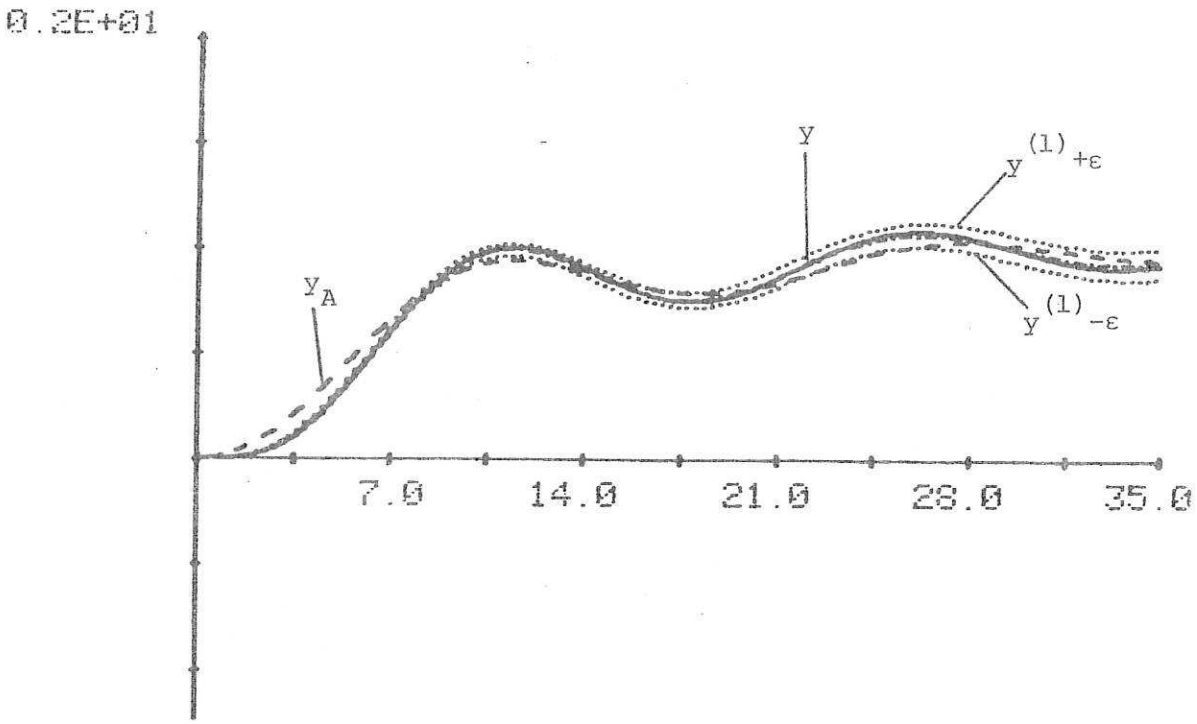

Fig. 8.12

9. EXAMPLE 5

Consider a process with transfer function

$$G(s) = \frac{1}{(s+1)^9} \tag{9.1}$$

with step response Y illustrated in Fig. 9.1. The first-order model of the form

$$G_A(s) = \frac{1}{1 + 9.5s} \tag{9.2}$$

was fitted, with step response Y_A again illustrated in Fig. 9.1 and the error $E(t) = Y - Y_A$ shown in Fig.9.2. The total variations $N_\infty(E)$ was found to be 1.02. Since $N_\infty(E)$ is greater than the steady-state value of plant, the above model is not accurate enough to provide a basis for the design of integral controllers using the standard frequency-domain technique with $\Delta(s) = N_\infty(E)$. Using (2.12), i.e.

$$\Delta(s) = \min\ (N_\infty(E),\ E(\infty) + |s|\ N_\infty(Z),\ |s|^{-1} N_\infty(\dot{E})) \tag{9.3}$$

a better bound on

$|G(s) - G_A(s)|$ can be obtained and this is illustrated in Fig. 9.3. Using (9.3) and the controller

$$K(s) = 0.3 + 0.09\ s^{-1} \tag{9.4}$$

clearly satisfies equantion (2.5) and

the inverse Nyquist plot of $G_A KF = G_A K$ with superimposed confidence circles shown in Fig. 9.4 indicates that the (-1,o) point does not lie in or on the confidence band. Closed-loop stability of the real plant is hence guaranteed as the controllability and observability condition is satisfied. The closed-loop responses of the real and the approximate feedback schemes are shown in Fig. 9.5.

The function $W_A(t)$ for the above example is shown in Fig. 9.6 and it was found that $N_\infty(W_A) = 0.57 < 1$, hence verifying the stability predictions for the real plant. The correction term $\eta(t)$ is shown in Fig. 9.7

and the errorbound $\varepsilon(t)$ is shown in Fig. 9.8. The bounds $y^{(1)} \pm \varepsilon$, together with the responses y and y_A are illustrated in Fig. 9.9.

The delay-lag model of the form

$$G_A(s) = \frac{e^{-4.0s}}{1 + 5.5s} \tag{9.5}$$

was fitted to the systems of (9.1), with step responses Y and Y_A illustrated in Fig. 9.10 and the error E(t) illustrated in Fig. 9.11. The total variation $N_\infty(E)$ was found to be 0.56. Using the time-domain technique and the same controller as before (i.e. equation (9.4)), it was found that $N_\infty(W_A) = 0.3$ (see Fig. 9.12). The correction term $\eta(t)$ is shown in Fig. 9.13 and the errorbound $\varepsilon(t)$ is shown in Fig. 9.14. The bounds $y^{(1)} \pm \varepsilon$, rogether with y and y_A, are illustrated in Fig. 9.15

Using the improved frequency-domains technique. (i.e. $\Delta(s) = \min (N_\infty(\dot{E}), E(\infty) + |s|N_\infty(Z), |s|^{-1} N_\infty(\dot{E}))$ and for higher gain controller

$$K(s) = 1.0 + s^{-1}\, 0.3 \tag{9.6}$$

the inverse Nyquist plot of $G_A K$ with superimposed confidence circles shown in Fig. 9.16 indicates that the (-1,o) point does lie in the confidence band, hence the theory cannot predict the stability of the real systems. The closed-loop responses of the real and the approximate standard feedback schemes are shown in Fig. 9.17. From Fig. 9.17 we noticed that the real system is, in fact, unstable for the controller (9.6). However using the same controller and the Smith predictor scheme, the inverse Nyquist plot of $G_{AS}K$ (where $G_{AS} = \frac{1}{1+5.5s}$) with superimposed confidence circles shown in Fig. 9.18 indicates that the (-1,o) point does not lie in or on the confidence band. Stability of the real system using the Smith predictor scheme is hence guaranteed with the closed-loop responses of the real and the approximate systems as shown in Fig. 9.19.

9.1 Summary and Discussion

The above example has demonstrated the following results

(1) We note that, by using the first-order model for the system of (9.1), the total variation $N_\infty(E)$ is 1.0 2, which is greater than the steady-state value of the real plant and hence the first-order model is not accurate enough for the design of integral controllers using the frequency-domain technique with $\Delta(s) = N_\infty(E)$.

(2) By using the improved frequency-domain technique the first-order model verifies the stability prediction for the controller $K(s) = 0.3 + 0.09\ s^{-1}$. The performance error bounds obtained are acceptable with a maximum of 20% error. This error can be reduced to 7% by using the delay-lag model of (9.5).

(3) We cannot predict the stability or instability of the real systems using the delay-lag model and the controller $K(s) = 1.0 + s^{-1}0.3$ for the standard feedback scheme but stability can be predicted using this control in a Smith predictor scheme.

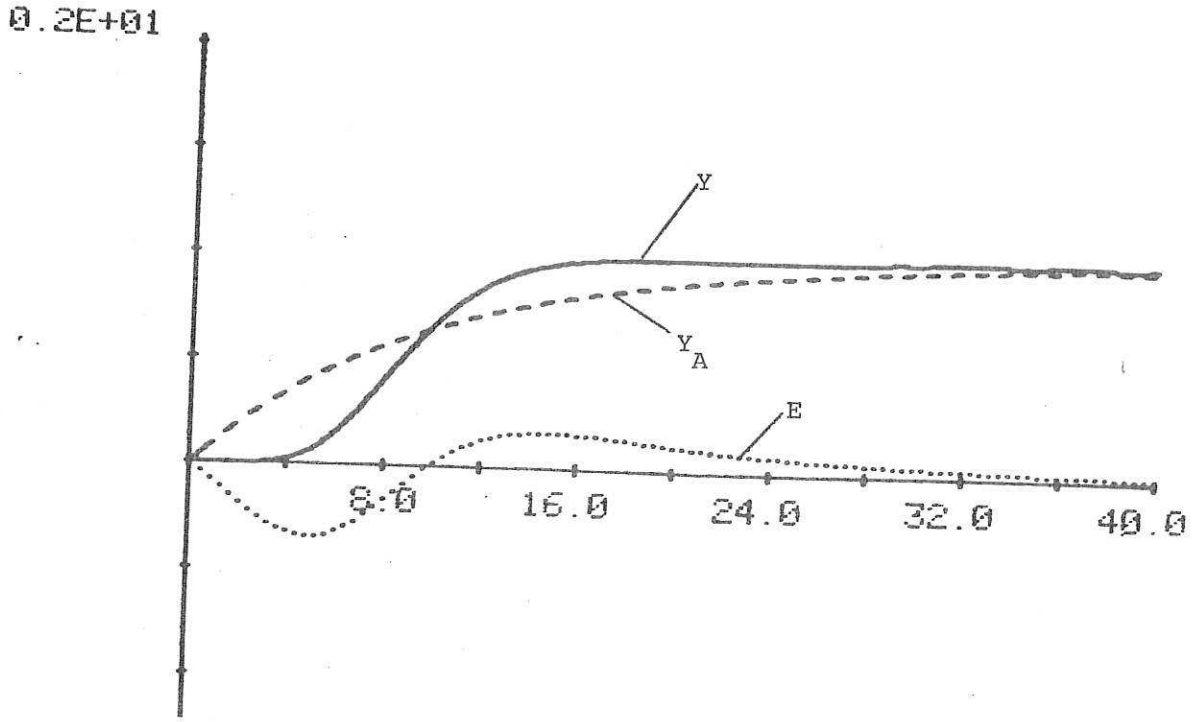

Fig. 9.1

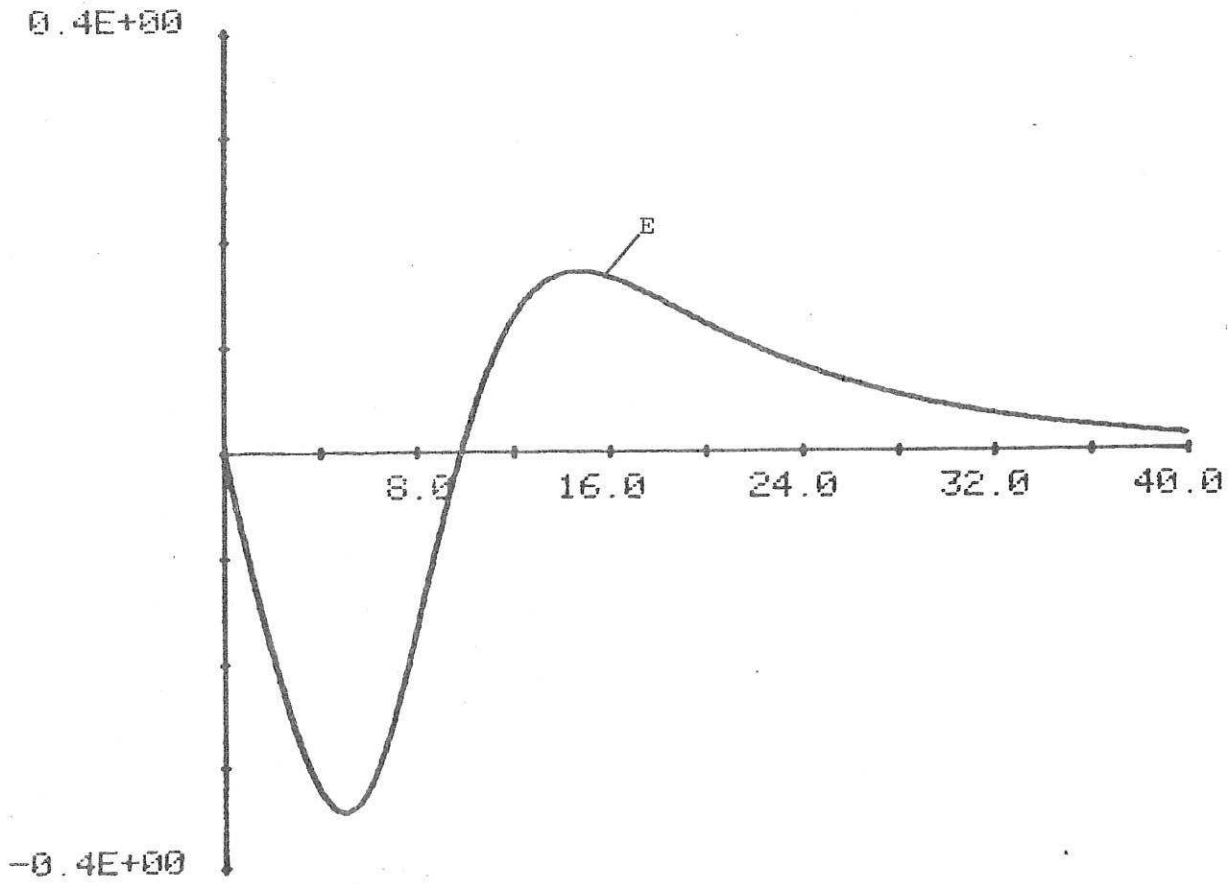

Fig. 9.2

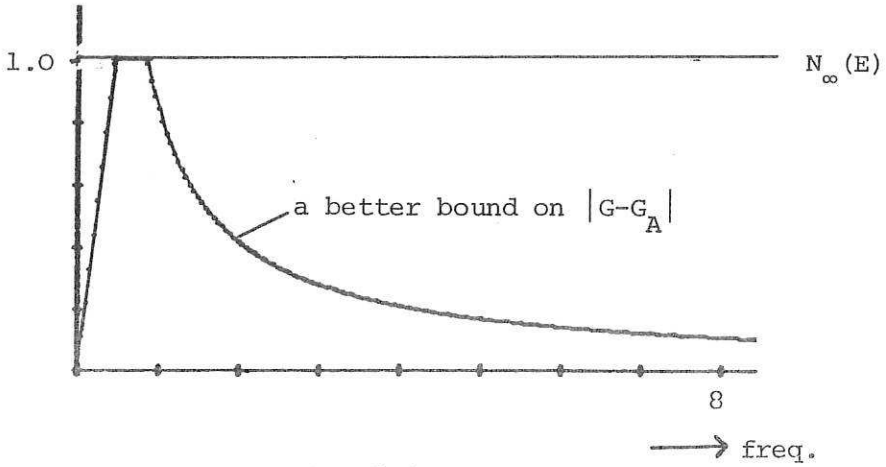

Fig. 9.3

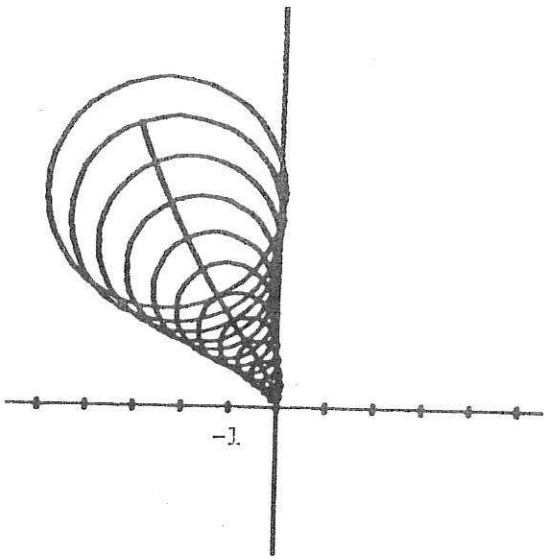

Fig. 9.4

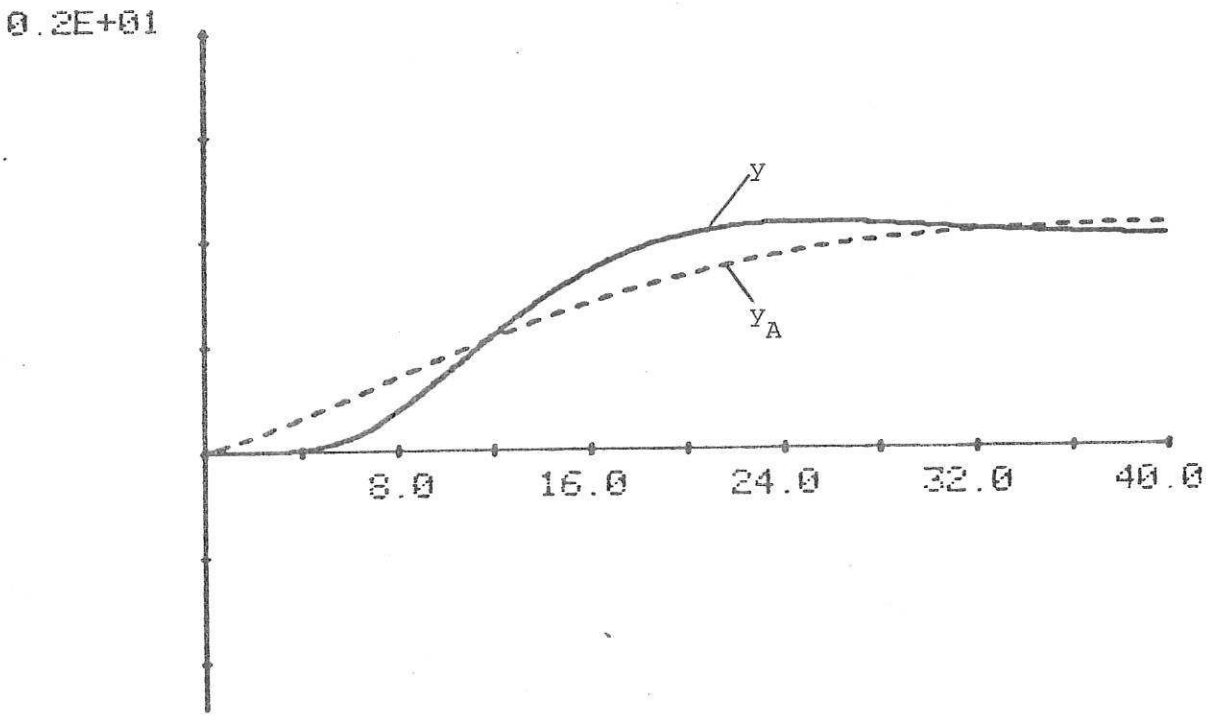

Fig. 9.5

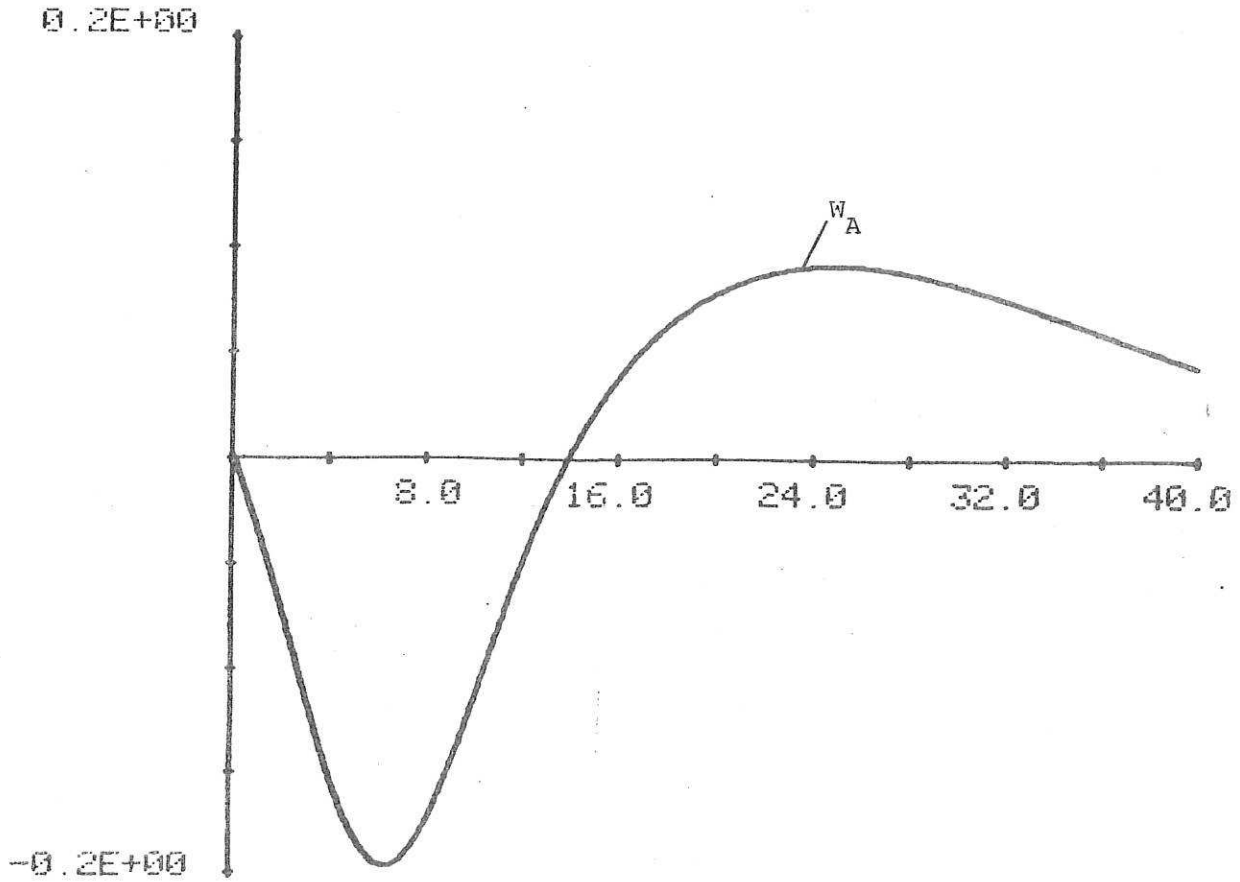
0.2E+00
W_A
8.0
16.0
24.0
32.0
40.0
-0.2E+00

Fig. 9.6

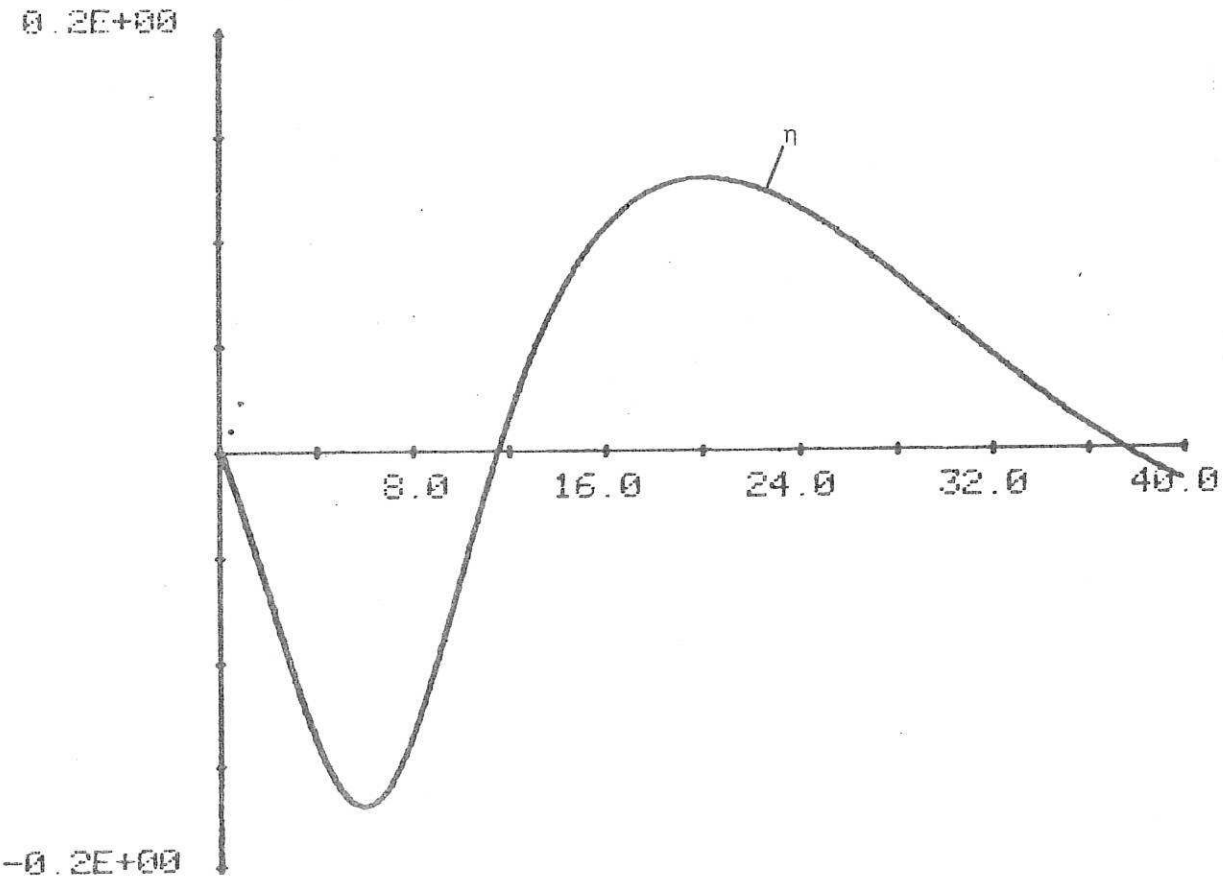
0.2E+00
η
8.0
16.0
24.0
32.0
40.0
-0.2E+00

Fig. 9.7

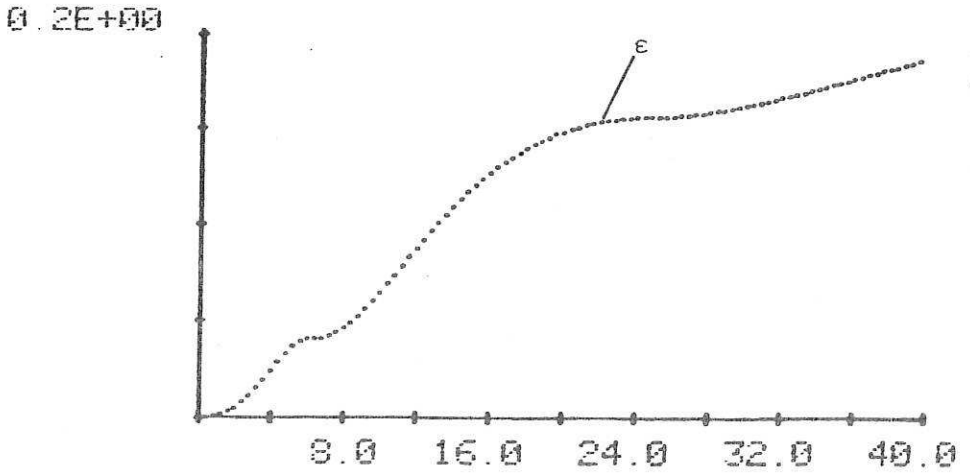
0.2E+00
ε
8.0
16.0
24.0
32.0
40.0

Fig. 9.8

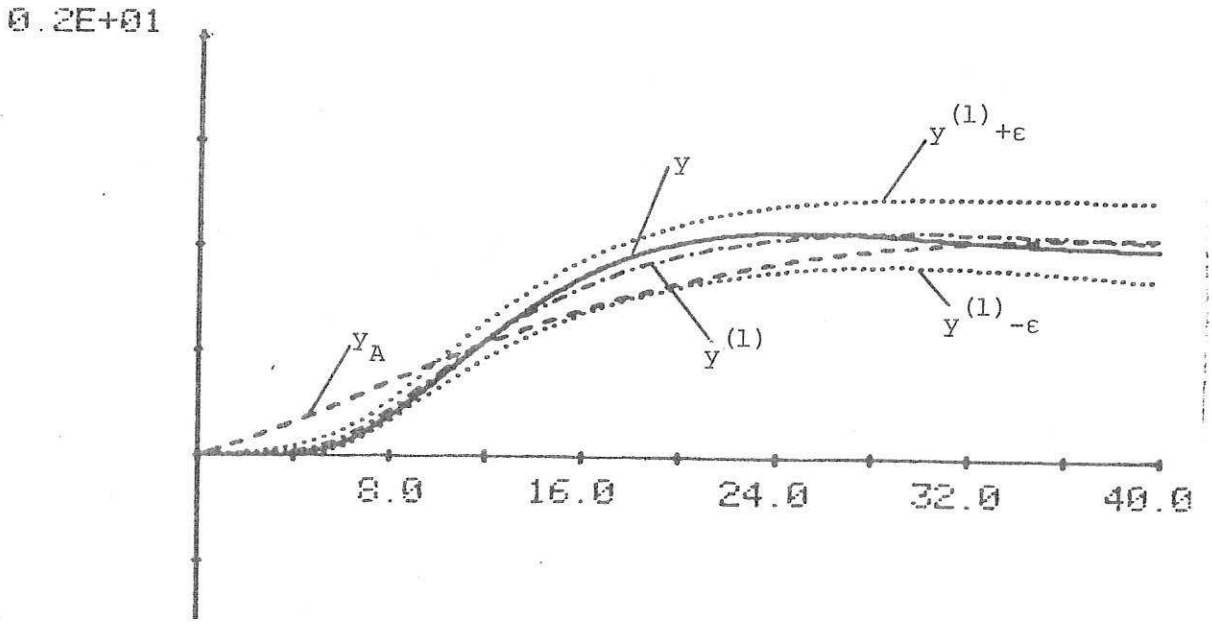
0.2E+01
y(1)+ε
y
y(1)
y(1)-ε
yA
8.0
16.0
24.0
32.0
40.0

Fig. 9.9

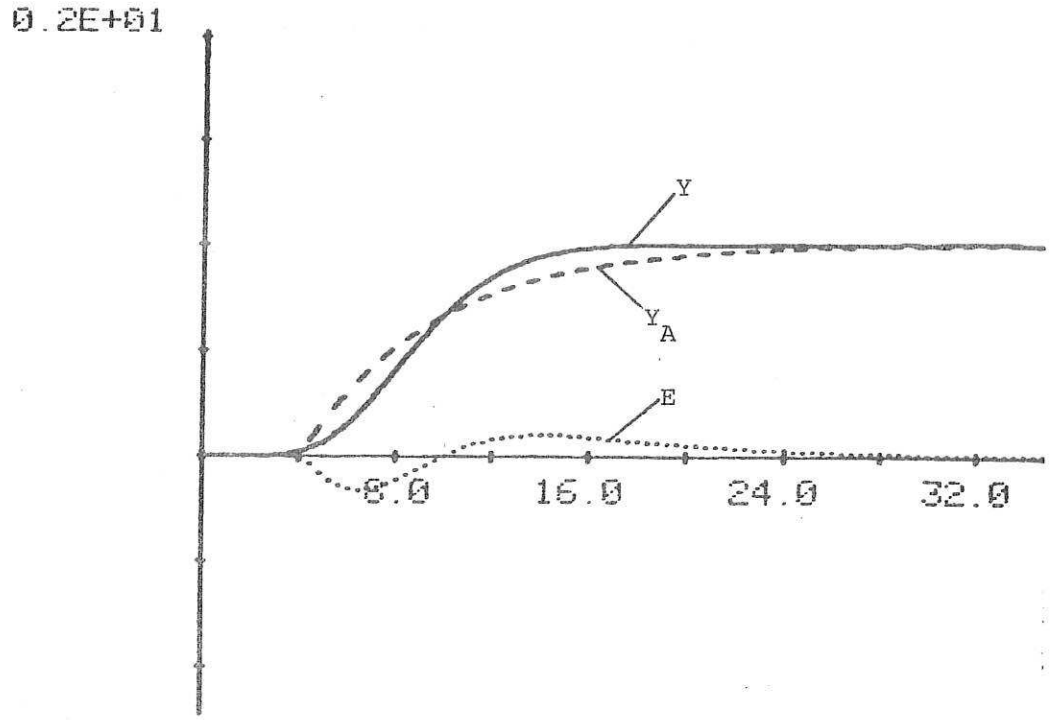

Fig. 9.10

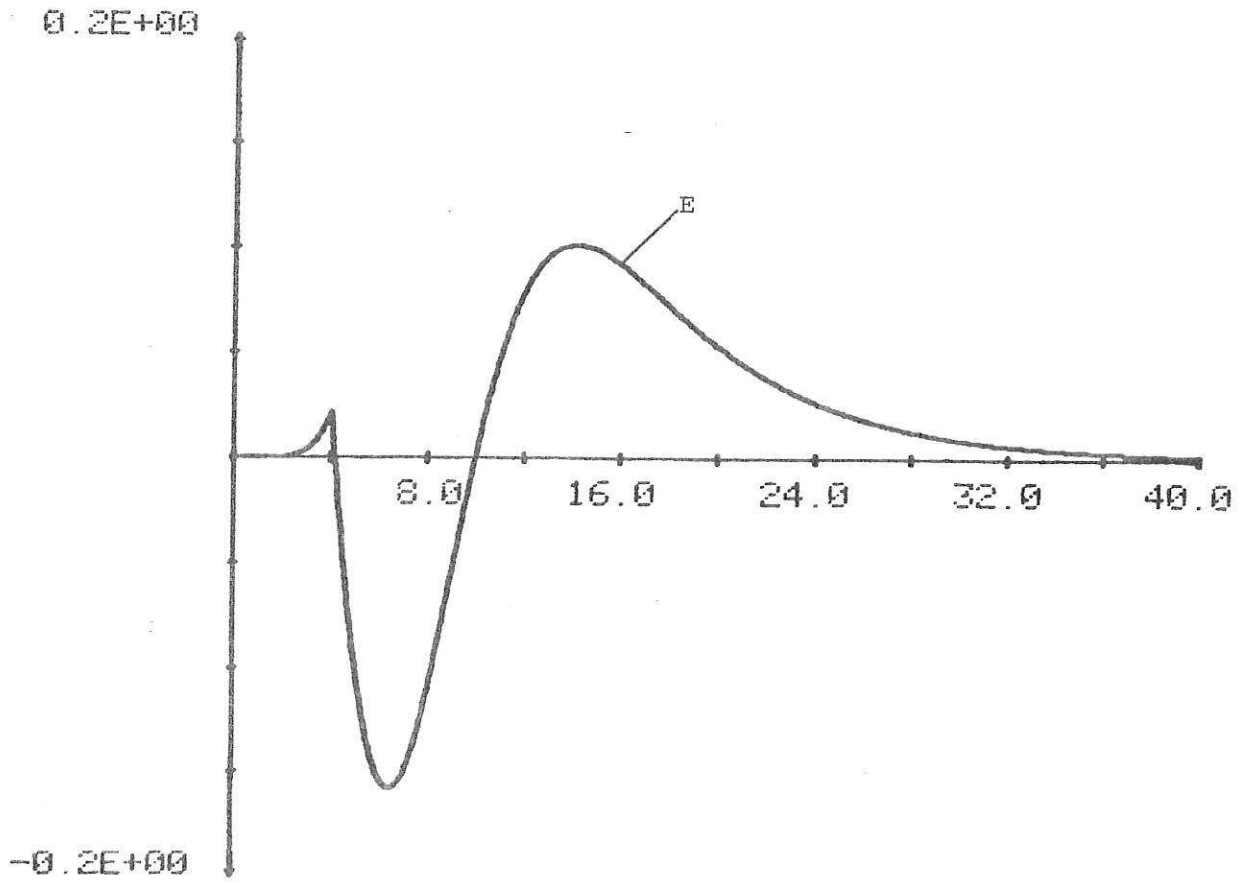

Fig. 9.11

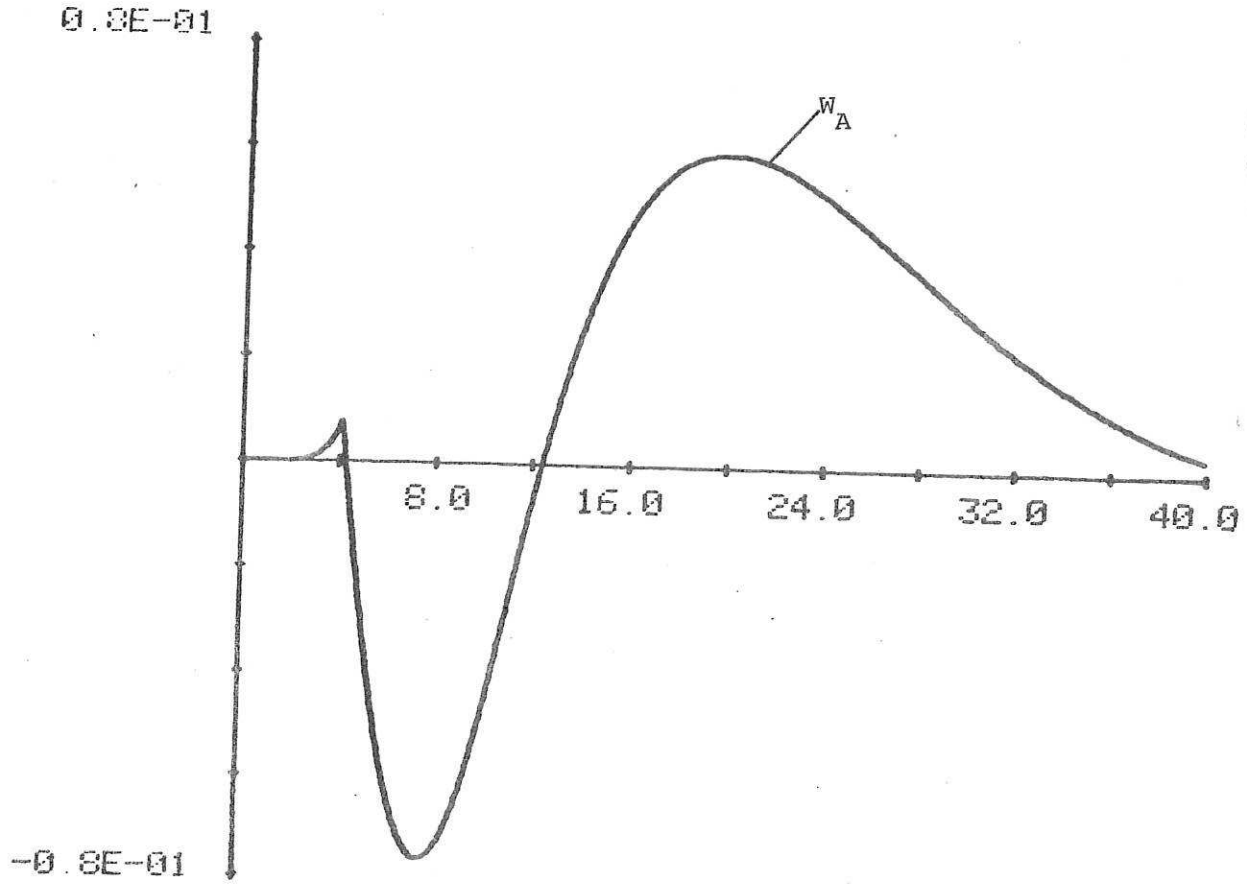

Fig. 9.12

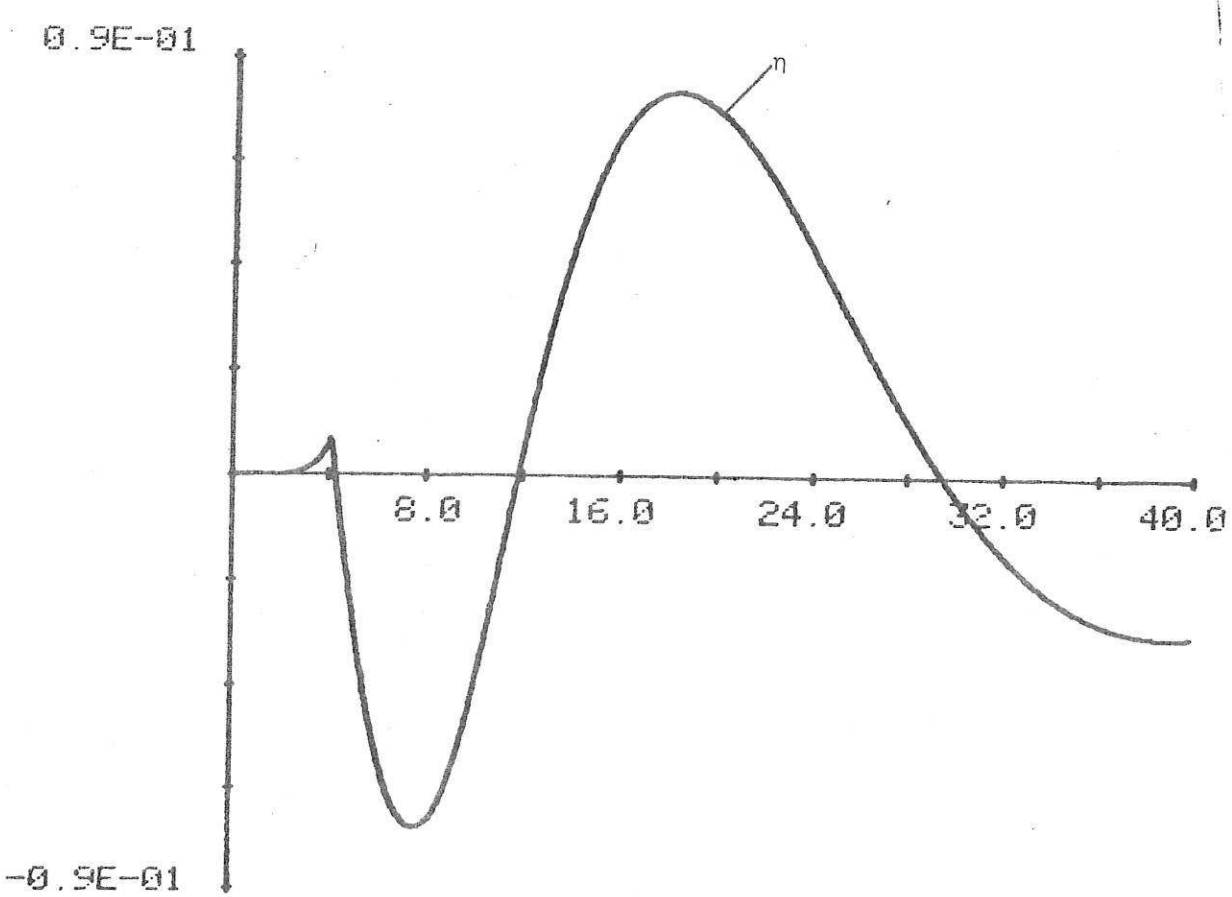

Fig. 9.13

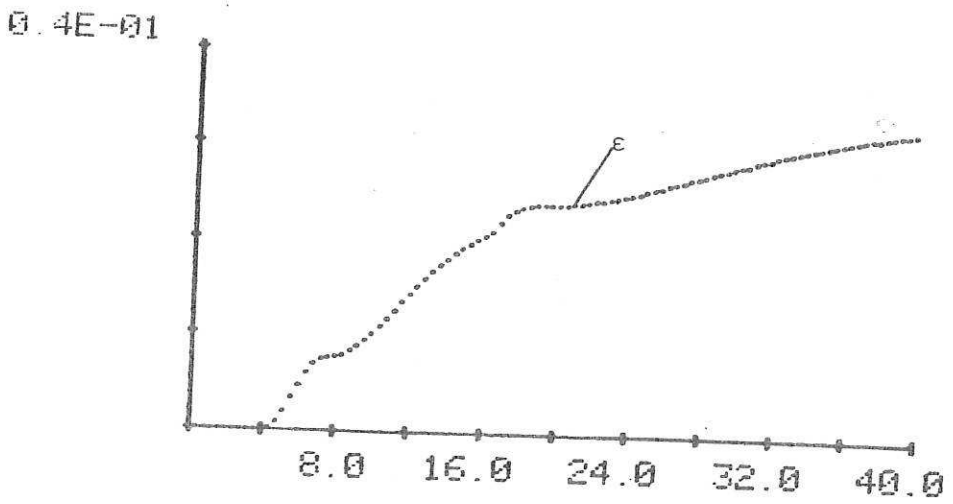

Fig. 9.14

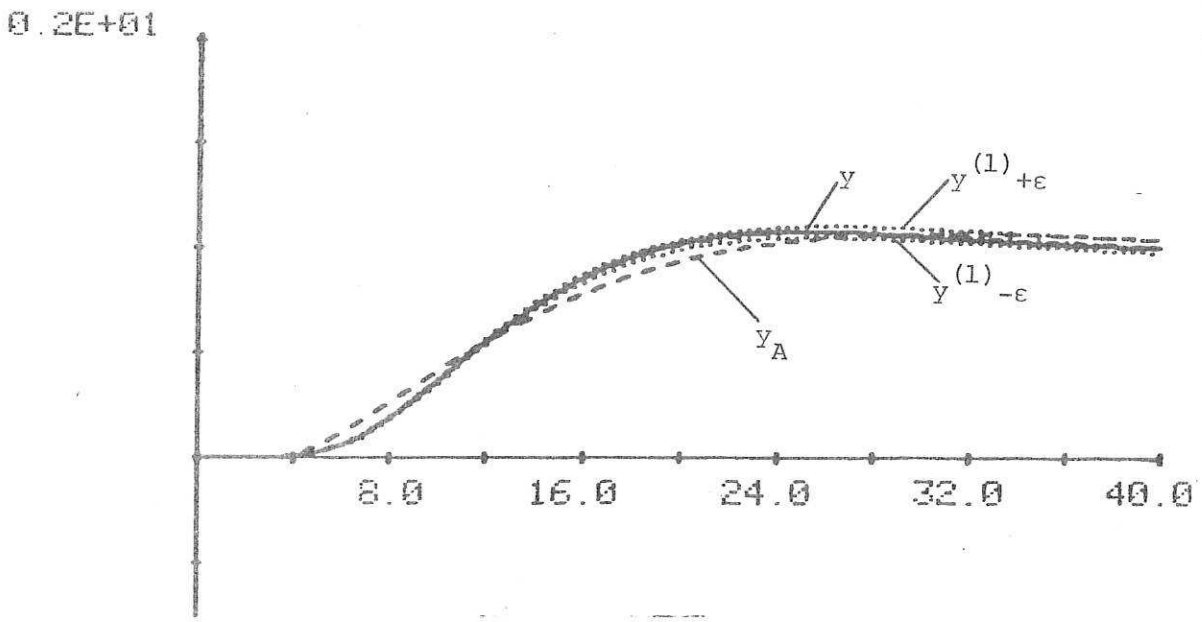

Fig. 9.15

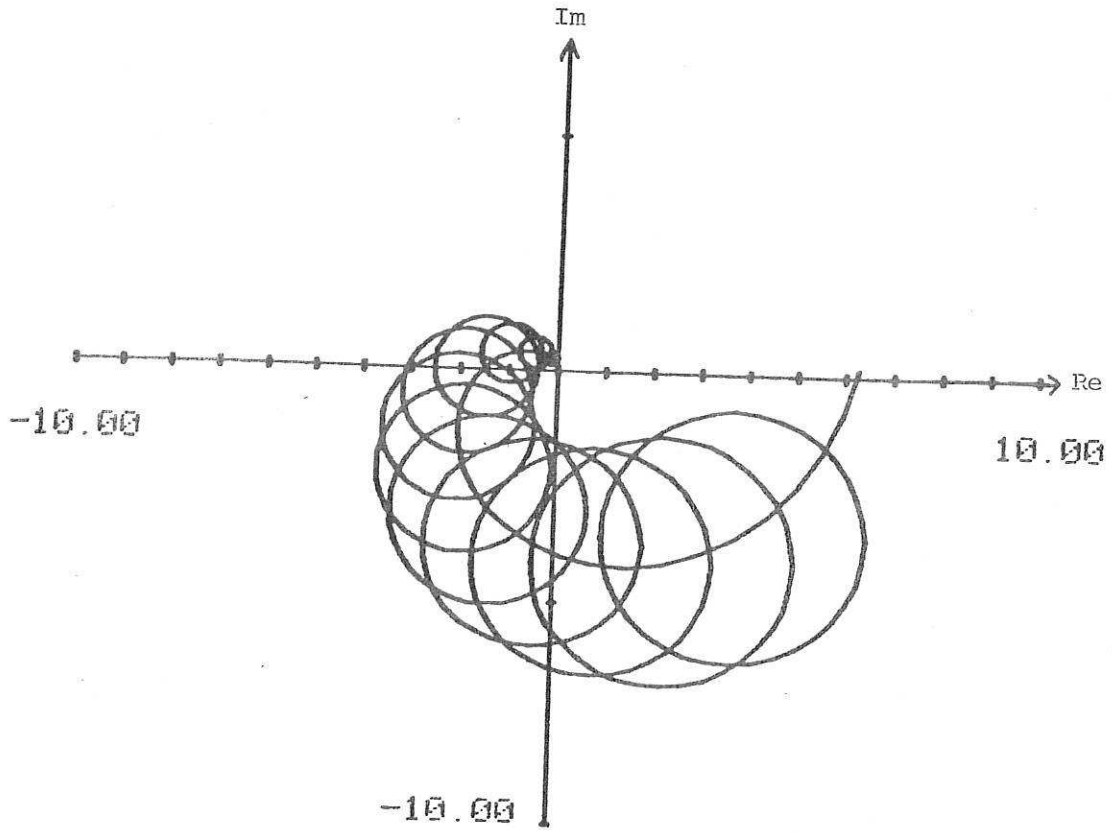

Fig. 9.16

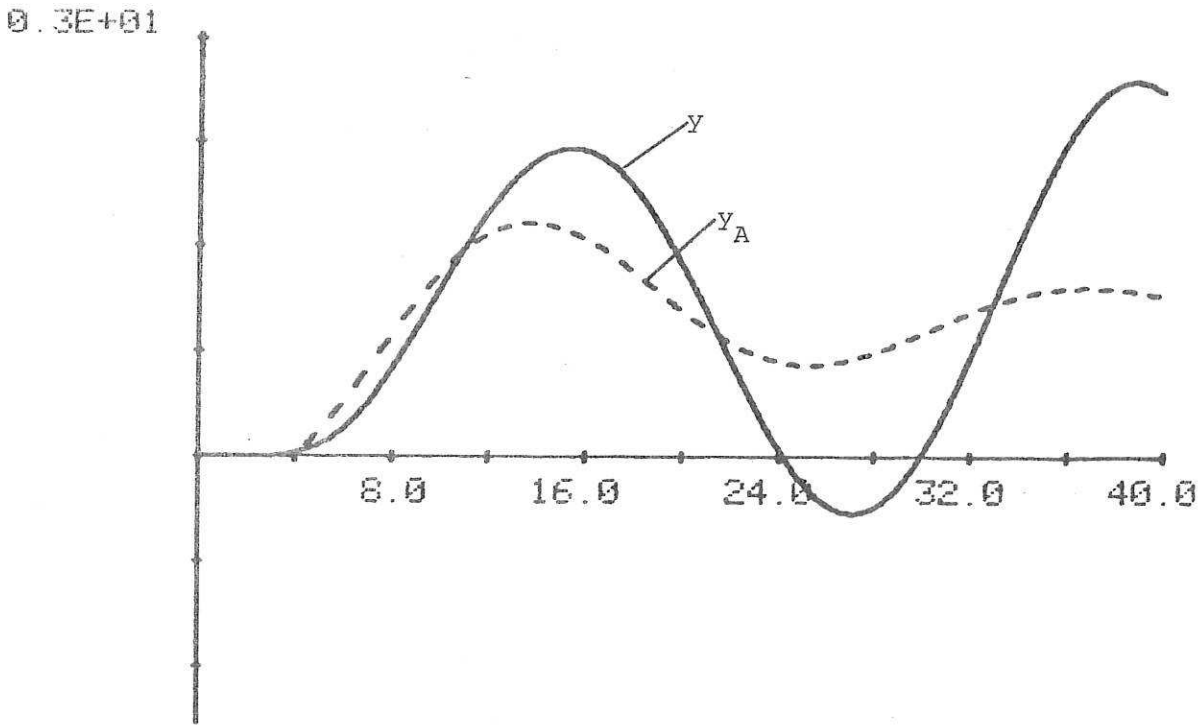

Fig. 9,17

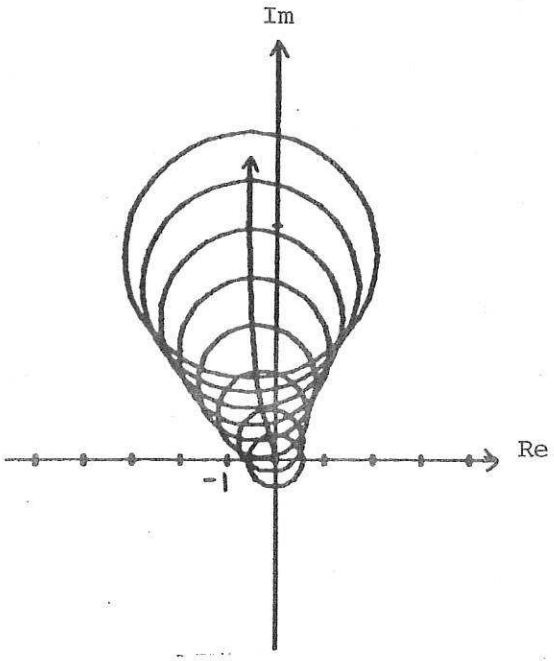

Fig. 9.18

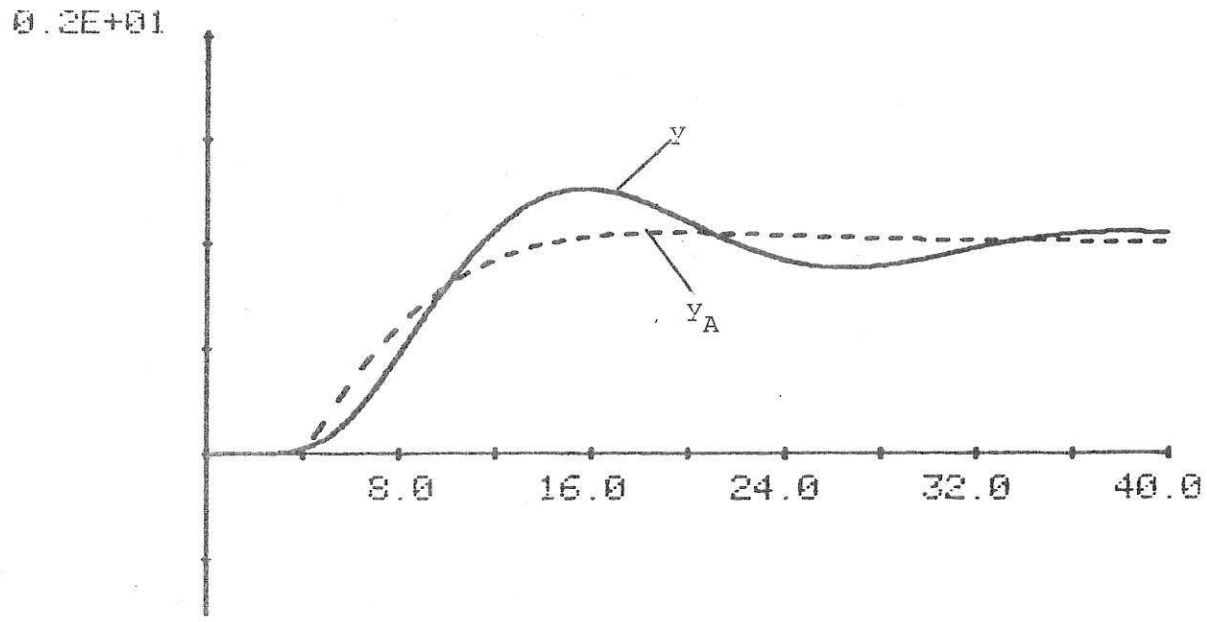

Fig. 9.19

10. CONCLUSION

The problem of designing a controller for an unknown plant using simple model so that the closed loop stability, asymptotic tracking of step input occurs, and also other desirable properties of the controlled system result such as fast response, $\leq$ 10% overshoot occurs, is considered in this report. The design method uses both, the time-domain and the frequency-domain techniques of Owens and Chotai (1983). The stability criterion given using the frequency-domain technique has the same structure as the INA with the Gershgorin band replaced by the 'Confidence band'. The time-domain technique can predict the stability and also can assess the degradation in input and output transient perfornamce of the actual system. In this report we have illustrated simple procedures for choosing the parameters in the first and second order differential-delay plant models using techniques involving only simple graphical operations on the step response Y(t) of the real system to a unit step from zero initial conditions. We have studied a number of single-input/single-output systems and made the following observation.

(1) By using very simple models such as first and second order differential-delay plant models, it appears that a highly satisfactory design can be achieved for most monotonic and for large numbers of non-monotonic stable plants.

(2) The constant measure of modelling error $N_\infty(E)$ used in this report is conservative. However, conservatism in $N_\infty(E)$ is no problem, if we take G_A as a design variable. The numerical study has demonstrated that conservatism in the total variation $N_\infty(E)$ decreases as the complexity of the model increases.

(3) The study has indicated that in most cases the predicted stability region using simple models is a substantial part of the actual stability region and frequentlyincludes the standard design conditions such as Ziegler-Nichols tuning points and standard closed-loop damping

conditions. We also note that the predicted stability regions increase as the complexity of the model increases and coincide with the actual stability region when $G = G_A$.

(4) In some cases, the performance error bounds obtained for a given model and controller may be large and unacceptable for the design purpose, in this case, either the controller gains must be reduced if possible or the designer must use a better model.

(5) When the total variation $N_\infty(E)$ is greater than the steady-state value of the actual plant, the chosen model is not accurate enough to provide a basis for the design of integral controllers using the frequency-domain method with $\Delta(s) = N_\infty(E)$. In this case, to use integral action we must either find a better $\Delta(s)$, use the time-domain technique or find a better model so that $N_\infty(E)$ is less than the steady-state value of the real plant.

(6) The study has shown that the time-domain method is better than the frequency-domain method in the sense that it permits higher gains to be used for a given model.

(7) For a differential-delay model, the Smith predictor scheme gives much better performance than a standard feedback scheme and increases the stability margin in the sense that it permits higher control gains to be used.

ACKNOWLEDGEMENTS

This work is supported by SERC under grant GR/B/23250.

11. REFERENCES

[1] Owens, D.H., Chotai, A.: 'Robust controller design for linear dynamic systems using approximate models', Proc. IEE, Pt.D., 130, pp. 45-56, 1983.

[2] Rosenbrock H.H.: 'Computer-aided-design of control systems', Academic Press, London, 1974.

[3] Owens, D.H.: 'Feedbakc and multivariable systems', Peter Peregrinus, Stevenage, 1978.

[4] Patel, R.V., Munro, N.: 'Multivariable systems theory and design', Pergamon, Oxford, 1982.

[5] MacFarlane, A.G.J.: 'Frequency response methods control systems' (IEEE Press, 1979).

[6] D.H. Owens, A. Chotai: 'Precompensation, approximation and an INA design technique based on plant step data only', Proc. IEE, under consideration.

[7] Marshall, J.E.: 'Control of time-delay systems', Peter Peregrinus, 1979.

[8] Owens, D.H. and Raya, A.: 'Control Theory and Applications, Pt. D.' IEE Proc., 192, (6), 298, 1982.

[9] Chotai, A., Owens, D.H., Raya, A., Wang, H.M.: 'Design of Smith control schemes for time-delay systems based on plant step data', Int. J. Control, 1984, to appear.

[10] Marshall, J.E. and Salehi, S.V.: 'Control Theory and Application, Pt.D' IEE Proc., 129, (5), 177, 1982.

APPENDIX A

Standard Damping Conditions for the Example 1

The closed-loop characteristic equation for the example 1 using P+I controller is given by

$$s^4+3s^3 + 3s^2 + (k_1+1)s + k_2 = 0 \qquad (A1)$$

For the standard damping

$$s = \omega(-1 + i) \text{ and } |s| = \omega\sqrt{2} \quad \omega > 0 \qquad (A2)$$

Substituting (A2) in (A1) and equating real and imaginar parts, we obtain

$$-4\omega^4 + 6\omega^3 - (k_1+1)\omega + k_2 = 0 \qquad (A3)$$

and

$$6\omega^3 - 6\omega^2 + \omega(k_1+1) = 0 \qquad (A4)$$

From (A4)

$$\omega = 0.5 \pm (0.25 - (k_1 + 1)/6)^{\frac{1}{2}} \qquad (A5)$$

For real $\omega > 0$, we require

$$k_1 \leq \tfrac{1}{2} \qquad (A6)$$

From (A3)

$$k_2 = 4\omega^4 - 6\omega^3 + (k_1+1)\omega \qquad (A7)$$

where ω is given by (A5) and k_1 satisfy (A6). For any chosen value of k_1 in $-1 \leq k_1 \leq 0.5$, there are two corresponding values of k_2 and this is illustrated in Fig. 5.7.

APPENDIX B

Ziegler-Nichols control conditions:

Assume that the controller can be expressed by

$$K(s) = K_p\left[1 + 1/(T_I S) + T_D s\right]$$

Let $T_I = \infty$, $T_D = 0$ (assume only proportional control) and determine the stable limit of the control systems by changing K_p. Let the value of K_p at the stable limit be K_{pu} and the period of sustaining oscillation be P_u. Ziegler-Nichols obtained the following formulas to derive the values

for K_p, T_I and T_D.

(a) For only proportional control ($T_I = \infty$, $T_D = 0$)

$$K_p = 0.5K_{pu}$$

(b) For proportional + integral control ($T_D = 0$)

$$K_p = 0.45\ K_{pu},\ T_I = 0.83\ p_u$$

(c) For proportional + integral + differential control

$$K_p = 0.6\ K_{pu},\ T_I = 0.5\ p_u,\ T_D = 0.125\ p_u.$$